

Dissertation zur Erlangung des Doktorgrades
der Fakultät für Chemie und Pharmazie
der Ludwig-Maximilians-Universität München



Cyclin-dependent kinase 5 in endothelial cell migration:
Elucidating regulatory mechanisms upstream of Cdk5
and evaluating novel Cdk inhibitors as anti-angiogenic drugs

Sabine Bianca Monika Weitensteiner
aus Tirschenreuth
2011

Erklärung

Diese Dissertation wurde im Sinne von § 13 Abs. 3 bzw. 4 der Promotionsordnung vom 29. Januar 1998 (in der Fassung der sechsten Änderungssatzung vom 16. August 2010) von Herrn Prof. Dr. Stefan Zahler am Lehrstuhl für Pharmazeutische Biologie betreut.

Ehrenwörtliche Versicherung

Diese Dissertation wurde selbstständig und ohne unerlaubte Hilfe erarbeitet.

München, den 22. September 2011

.....

Sabine Bianca Monika Weitensteiner

Dissertation eingereicht am:

22. September 2011

1. Gutachter:

Prof. Dr. Stefan Zahler

2. Gutachter:

Prof. Dr. Angelika M. Vollmar

Mündliche Prüfung am:

25. Oktober 2011

meiner Familie

CONTENTS

1	INTRODUCTION.....	1
1.1	Angiogenesis and cancer	2
1.1.1	The angiogenic cascade	2
1.2	Function and regulation of Cdks.....	3
1.3	Cdk5 as a unique Cdk in charge of cellular migration.....	5
1.3.1	Functions of Cdk5	5
1.3.2	Regulation of Cdk5.....	5
1.4	Cyclin dependent kinase inhibitors	7
1.4.1	Roscovitine	8
1.5	Aim of the study	8
2	MATERIALS AND METHODS.....	11
2.1	Materials	12
2.1.1	Biochemicals, inhibitors, dyes and cell culture reagents.....	12
2.1.2	Inhibitors	14
2.1.3	LGR compounds	15
2.2	Cell culture.....	16
2.2.1	Cell culture solutions and reagents.....	16
2.2.2	Endothelial cells	16
2.2.2.1	HMEC-1 (Human microvascular endothelial cells).....	17
2.2.2.2	HUVECs (Human umbilical vein endothelial cells).....	17
2.2.3	Passaging	17
2.2.4	Freezing and thawing.....	18
2.3	Western blot analysis	18
2.3.1	Preparation of protein samples.....	18
2.3.2	Membrane fractionation.....	19
2.3.3	Immunoprecipitation.....	20
2.3.4	Cdk5 kinase assay.....	22

2.3.5	Protein Quantification	24
2.3.5.1	Bicinchoninic Acid (BCA) Assay	24
2.3.5.2	Bradford Assay	24
2.3.6	SDS-PAGE	24
2.3.7	Trans electroblotting	25
2.3.8	Protein detection	26
2.3.8.1	Enhanced chemiluminescence (ECL).....	26
2.3.8.2	Infrared imaging	27
2.3.9	Quantification of band intensity	27
2.4	Protein identification from SDS-PAGE gels	28
2.4.1	Coomassie staining	28
2.4.2	In-gel tryptic digestion	28
2.4.3	LC-ESI-MS/MS analysis.....	28
2.4.4	Protein identification.....	29
2.5	Quantitative real time RT-PCR	30
2.5.1	Isolation of mRNA	30
2.5.2	Reverse transcription	30
2.5.3	Quantitative real time PCR.....	30
2.6	Transfection of cells	31
2.6.1	Transfection with siRNA	31
2.6.2	Transfection of plasmids	32
2.7	Flow Cytometry (FACS)	32
2.8	Immunocytochemistry and immunohistochemistry	33
2.8.1	Immunocytochemistry	33
2.8.1.1	Immunocytochemistry and confocal microscopy.....	33
2.8.1.2	Quantification of lamellipodia.....	34
2.8.2	Immunohistochemistry	34

2.8.2.1	Sections of p35 knockout and wild type mice	34
2.8.2.2	Hematoxylin-eosin staining	35
2.8.2.3	Microvessel density of perfusion-fixed and HE stained sections.....	35
2.8.2.4	Sections of the HUH7 xenograft tumors	35
2.8.2.5	CD31 immunohistochemistry staining	36
2.8.2.6	Microvessel density of the CD31 stained tumor sections.....	36
2.9	Angiogenesis assays	37
2.9.1	Cell proliferation assay (crystal violet staining assay).....	37
2.9.2	CellTiter-Blue™ cell viability assay	37
2.9.3	Scratch assay (wound healing assay)	38
2.9.4	Tube formation assay.....	38
2.9.5	Chemotaxis assay.....	38
2.9.6	Chorioallantoic membrane (CAM) assay	39
2.10	In vivo tumor model.....	40
2.10.1	Animals and cell line	40
2.10.2	Tumor cell implantation	40
2.10.3	Intraperitoneal application of LGR 1407	40
2.10.4	Isolation of tumors.....	41
2.11	Statistical Analysis	41
3	RESULTS	43
3.1	Cdk5 regulation in endothelial cell migration	44
3.1.1	Cdk5 expression level in endothelial cell migration.....	44
3.1.2	Cdk5 phosphorylation at tyrosine 15 is not crucial for endothelial cell migration	45
3.1.3	p35 and p39 are not the central Cdk5 activators in endothelial cell migration	48

3.1.3.1	Neuronal Cdk5 activator p35 is expressed at a low level in endothelial cells.....	48
3.1.3.2	Cdk5 is translocated to the membrane during endothelial cell spreading	48
3.1.3.3	The pro-angiogenic factor VEGF does not affect p35 protein levels in endothelial cells.....	49
3.1.3.4	p35 levels in endothelial cells are regulated by proteasomal degradation but not by calpain.....	50
3.1.3.5	siRNA-mediated downregulation of p35 does not influence endothelial cell migration.....	53
3.1.3.6	p35 knockout mice do not show visible defects in their vascular phenotype	55
3.1.3.7	TNF does not affect p35 levels in endothelial cells	57
3.1.4	Cdk5 kinase activity in endothelial cells.....	58
3.1.4.1	Cdk5 immunoprecipitation.....	59
3.1.4.2	p35 immunoprecipitation	59
3.1.4.3	Cdk5 overexpression	60
3.1.4.4	Evaluation of different Cdk5 antibodies with recombinant Cdk5/p35.....	61
3.1.5	A proteomics approach to reveal novel Cdk5 interacting proteins	62
3.2	Novel Cdk inhibitors with increased Cdk5 selectivity show anti-angiogenic effects <i>in vitro</i> and <i>in vivo</i>	65
3.2.1	The LGR compounds do not show acute toxicity on endothelial cells.....	65
3.2.2	The LGR compounds inhibit endothelial cell proliferation	66
3.2.3	LGR 1404, 1406, 1407 and 1492 significantly reduce endothelial cell migration at a concentration of 10 μ M	67
3.2.4	LGR 1404, 1406, 1407 and 1492 concentration-dependently inhibit tube formation.....	69
3.2.5	Overall motility of HUVECs in a chemotactic gradient is affected by LGR 1404, 1406 and 1407	70

3.2.6	LGR 1404, 1406 and 1407 completely inhibit vessel formation in the CAM assay.....	72
3.2.7	Kinase profile of LGR 1406 and 1407 shows preferential inhibition of Cdk5 and Cdk2	72
3.2.8	LGR 1404, 1406 and 1407 reduce lamellipodia formation and Rac1 localization to lamellipodia, indicating a Cdk5-dependent mode of action.....	74
3.2.9	LGR 1407 significantly inhibits tumor growth and vascularization in a hepatoma xenograft mouse model	75
4	DISCUSSION.....	79
4.1	Elucidation of novel endothelial signaling pathways as the basis for future anti-angiogenic therapy.....	80
4.2	Cdk5 regulation in endothelial cell migration exerts non-canonical characteristics	80
4.2.1	Cdk5 phosphorylation on tyrosine 15 is dispensable in endothelial cell migration	80
4.2.2	p35 and p39 are not central for Cdk5 regulation in endothelial cell migration	81
4.2.3	p35 is not increased in Cdk5-dependent endothelial inflammatory reaction	83
4.2.4	Evaluation of Cdk5 activity in endothelial cells	84
4.2.5	A proteomics approach provides novel insights into endothelial Cdk5 signaling.....	85
4.3	Novel LGR inhibitors are potent anti-angiogenic compounds and validate Cdk5 as a target.....	87
4.3.1	<i>In vitro</i> potency of LGR compounds is confirmed in the CAM assay <i>in vivo</i>	87
4.3.2	Kinase data and Cdk5-dependent mode of action of LGR 1404, 1406 and 1407.....	88
4.3.3	Structure and anti-angiogenic potency of the LGR	88

4.3.4	Novel Cdk5 inhibitors validate Cdk5 as an anti-angiogenic target <i>in vitro</i> and in the LGR 1407 tumor xenograft	89
4.4	Conclusion and future aspects	90
4.4.1	Cdk5 upstream regulation in endothelial cells	90
4.4.2	Cdk inhibitors with higher potency and selectivity to Cdk5.....	90
5	SUMMARY.....	91
6	REFERENCES	95
7	APPENDIX.....	107
7.1	Publications.....	108
7.1.1	Original publications.....	108
7.1.2	Poster presentations	108
7.2	Curriculum Vitae.....	109
7.3	Acknowledgements	110

1 INTRODUCTION

1.1 Angiogenesis and cancer

Angiogenesis, the sprouting of new vessels from the existing vasculature, mainly takes place during embryonic development and growth. In the adult it is restricted to distinct physiological processes, e.g. wound healing and pregnancy, by a balance of pro- and anti-angiogenic factors.¹ Unregulated angiogenesis is one of the hallmarks of cancer.² Tumor growth is highly dependent on proper supply with oxygen and nutrients and removal of metabolic waste. Induction of angiogenesis is therefore paramount for tumor survival and proliferation, and tumor size remains limited unless the tumor switches to an angiogenic phenotype.³ The tumor activates the “angiogenic switch” by shifting the balance from anti-angiogenic to pro-angiogenic signaling in order to sustain its growth.⁴ The intent to stop tumor growth and finally starve out the tumor by disruption of tumor derived pro-angiogenic signaling has led to anti-angiogenic drugs for anticancer therapy. Agents interrupting vascular endothelial growth factor (VEGF) induced angiogenesis have already been introduced into tumor therapy and can indeed stop tumor growth. The VEGF-neutralizing antibody bevacizumab (Avastin) and the multi-targeted growth factor tyrosine kinase inhibitors sunitinib (Sutent), sorafenib (Nexavar), pazopanib (Votrient) and vandetanib (Caprelsa⁵, formerly Zactima) have been approved for certain metastatic cancer types as monotherapy or in combination with chemotherapy.⁶

However, in clinical use it has become apparent that anti-angiogenic tumor therapy is more challenging than expected: Many tumors are refractory to VEGF-blockade, or become resistant during treatment. This evasive resistance⁷ can be caused by a shift to alternative angiogenic signaling pathways due to a pre-existing multiplicity of redundant pro-angiogenic signals. Therefore novel targets in angiogenesis need to be identified and characterized as a basis for future therapeutic concepts. If and how anti-angiogenic therapy itself may contribute to increased metastasis is subject to investigation.^{8,9}

1.1.1 The angiogenic cascade

The vessel wall of non-growing capillaries consists of a lining of endothelial cells tightly interconnected by junction molecules like VE-cadherin and claudin, a basement membrane and surrounding pericytes. When the quiescent vessels are activated by angiogenic factors which are released from nearby hypoxic (tumor) tissue a series of events occurs, as summarized in Figure 1:

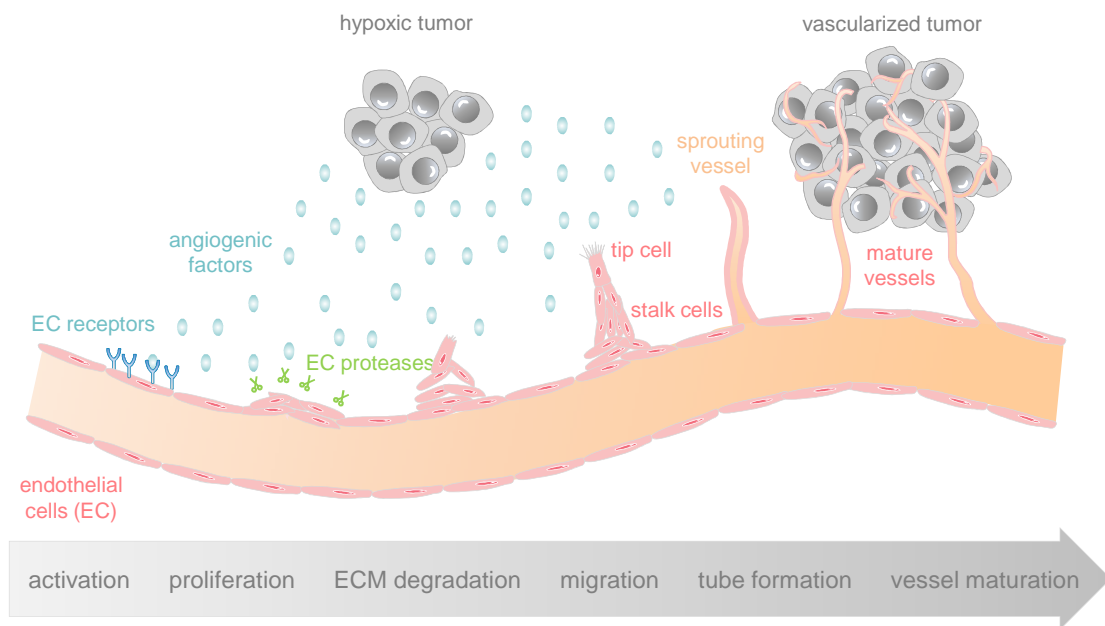


Figure 1 The angiogenic cascade. Pro-angiogenic factors like vascular endothelial growth factor (VEGF) or basic fibroblast growth factor (bFGF) bind to the corresponding receptors on endothelial cells and stimulate degradation of extracellular matrix (ECM) by secretion of digestive enzymes and initiate proliferation of endothelial cells. Newly formed endothelial cell sprouts further proliferate and migrate towards the tumor, navigating along the gradient of angiogenic cues. In order to coordinate endothelial cell movement, a tip cell is selected equipped with filopodia to sense guidance cues while the subsiding stalk cells proliferate and eventually form the lumen.¹⁰ Finally, the endothelial cells organize into hollow tubes and create a novel basement membrane. At the end, tight junctions and firm contacts to the ECM are formed and pericytes and smooth muscle cells are recruited to the mature vessel wall.^{3, 6, 11}

1.2 Function and regulation of Cdks

Cyclin-dependent kinases (Cdks) are a family of small serine/threonine kinases which are only active when they are bound to their regulatory subunits, the cyclins. The presence or absence of the activating cyclin is therefore crucial for Cdk kinase activity. At least 29 proteins have been designated as cyclins, sharing a conserved “cyclin box”. For some classes of cyclins the Cdk binding partner has not yet been identified.¹²

The best-characterized members of the Cdk family are involved in cell cycle control: the mitotic Cdk Cdk1, and the interphase Cdks Cdk2, Cdk4 and Cdk6. They pair with A-, B-, D- and E-type cyclins, whose expression fluctuates during the cell cycle (which explains the term “cyclins”) and this way regulates Cdk activity.¹³ Cdk3 is only little-studied and is also implicated in cell cycle control.¹⁴ Cdk7, Cdk8, Cdk9, Cdk10, Cdk11, Cdk12 and Cdk13 regulate transcription and splicing. They are activated by Cyclin H (Cdk7), C (Cdk8), T and K (Cdk9), and cyclins from the L-type (Cdk10-Cdk13).^{12, 15-24}

In a second function, Cdk7 regulates the activity of the cell cycle Cdks: It is part of the Cdk-activating kinase (CAK) complex together with Cyclin H and the stabilizing protein Mat1²⁵ (see Figure 2), and phosphorylates the cell-cycle Cdks in the T-loop for full activation.²⁶ Cdk kinase activity can further be modulated by inhibitory phosphorylations or endogenous Cdk inhibitors (CKIs), as displayed in Figure 2.

CKIs regulate the activity of the cell cycle Cdks by direct interaction. The CKIs of the INK4 family, p16^{INK4A}, p15^{INK4B}, p18^{INK4C} and p19^{INK4D}, specifically bind the monomeric Cdk and thereby prevent activation via cyclins, whereas p21^{Cip1}, p27^{Kip1} and p57^{Kip2} directly inhibit the Cdk-cyclin complex.¹²

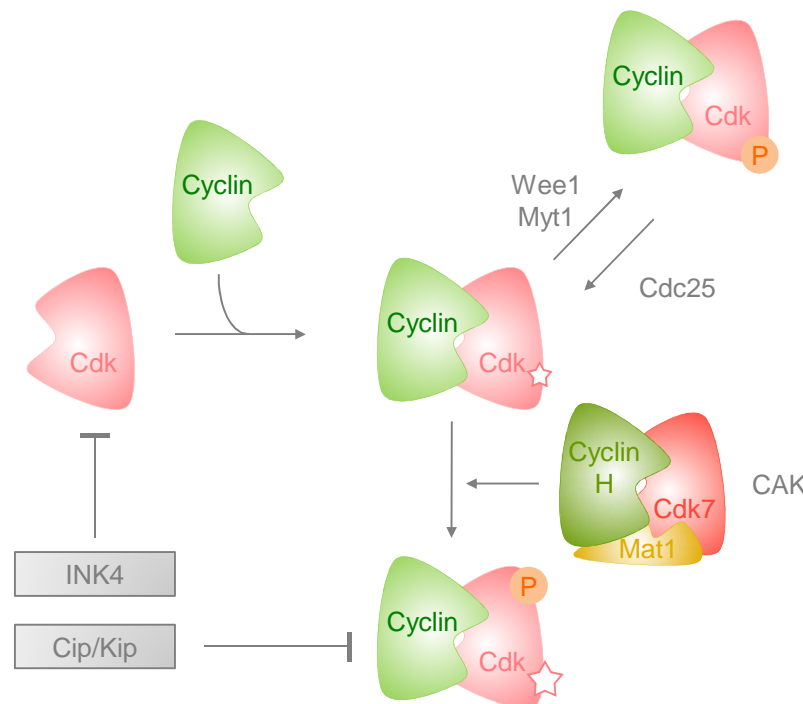


Figure 2 Regulation of cell cycle Cdks. Cdks are only active when bound to their cyclin activators. The Cdk-cyclin complexes can be additionally modulated by phosphorylation: Phosphorylation by Cdk activating kinase (CAK) in the T-loop of the Cdk enhances kinase activity of the complex. By contrast, phosphorylation of a conserved threonine or tyrosine residue by Wee1 or Myt1 negatively regulates kinase activity. The Cdc25 phosphatases abrogate this inhibitory phosphorylation. Cdk inhibitors from the INK4 or Cip/Kip family block kinase activity by either stabilizing the monomeric Cdk or by binding to the cyclin-Cdk complex. (P: Phosphorylation, ☆: Kinase activity; adapted from Malumbres & Barbacid¹²)

1.3 Cdk5 as a unique Cdk in charge of cellular migration

1.3.1 Functions of Cdk5

Cdk5 has been discovered as a neuronal cdc2-like kinase (nclk) in 1992.²⁷ Cdk5 is a proline-directed serine/threonine kinase that phosphorylates serine or threonine residues directly upstream of a proline, with a preference for a basic residue in the +3 position and the consensus sequence (S/T)PX(K/H/R).²⁸ Despite its high sequence homology with the mitotic Cdk1 (cdc2), Cdk5 is not involved in cell cycle control and unique among the Cdks in its regulation and function. Cdk5 deficient mice die perinatally due to severe defects in neuronal layering, as Cdk5 is crucial for the cytoarchitecture of the CNS.²⁹ On the cellular level, Cdk5 is well-described in neurons as the key hub in the dynamic network of trafficking and transport, integrating signals in cytoskeletal dynamics during neuronal migration, in synaptic plasticity and synaptic vesicle endo- and exocytosis, cell adhesion and axon guidance, neuromuscular development and pain signaling.^{30, 31} Deregulated Cdk5 activity in neurons is a major feature of Alzheimer's disease resulting in the aggregation of neurofibrillary tangles comprised of Cdk5-hyperphosphorylated tau.³² Although Cdk5 expression and activity is highest in the central nervous system²⁷, Cdk5 is as well expressed in various tissues, and an increasing body of research uncovers extraneuronal functions of Cdk5, where it is involved in the regulation of migration, cell death and survival, glucose metabolism and inflammation.^{33, 34}

1.3.2 Regulation of Cdk5

Monomeric Cdk5 requires the association with a regulatory subunit for activation; the known Cdk5 activators p35 and p39 however are no cyclins. It has been shown that Cyclin D, E and G bind to but do not activate Cdk5.³⁵⁻³⁸ The expression and cleavage of p35 and p39 essentially determines Cdk5 activity and localization, as displayed in Figure 3 for p35.³⁹

Neuronal growth factor (NGF)⁴⁰, tumor necrosis factor-alpha (TNF- α)^{41, 42} and interferon-gamma (INF- γ)⁴³ increase transcription and expression of p35 via extracellular signal regulated kinase (ERK) / early growth response-1 (Egr-1) mediated pathways.

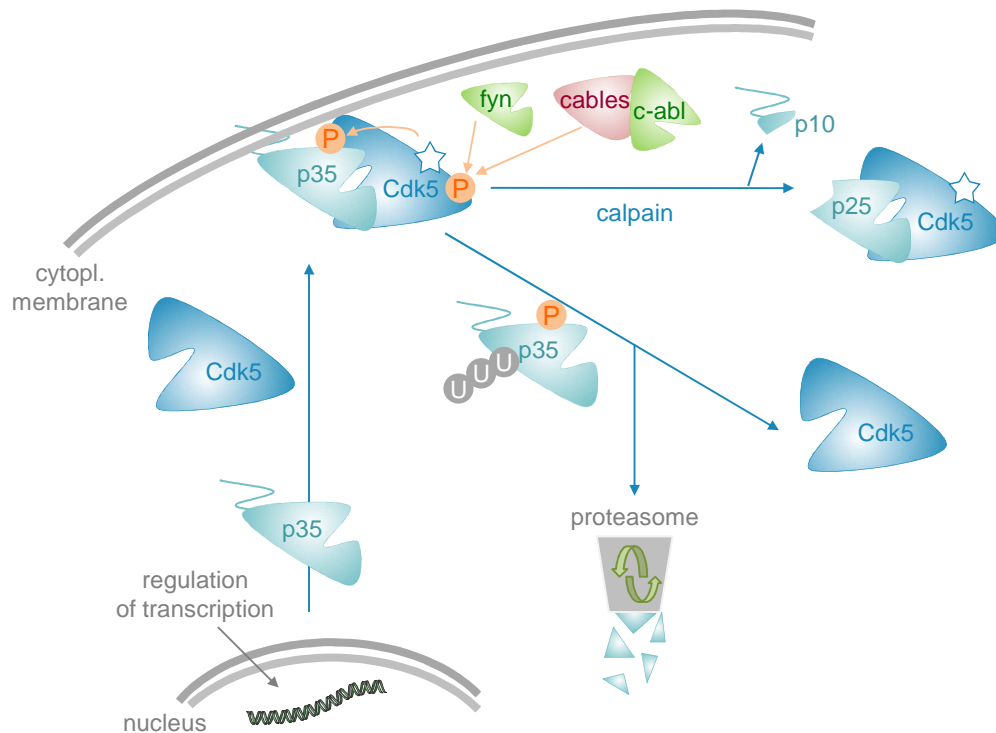


Figure 3 Regulation of Cdk5. p35 activates Cdk5 and recruits the p35/Cdk5 complex to the membrane, as p35 carries a myristoylation.^{32, 44} The short-lived p35 is rapidly degraded by the ubiquitin-proteasome pathway after phosphorylation by Cdk5.⁴⁵ The tyrosine kinases c-abl (via the adaptor protein cables)⁴⁶ and fyn⁴⁷ activate Cdk5 by phosphorylation of tyrosine 15. Neurotoxic events activate calpain which cleaves p35 into p25^{48, 49} and liberates the p25/Cdk5 complex from the membrane. p25 is more stable than p35 and dislocates Cdk5 activity to the cytoplasm, which leads to tau hyperphosphorylation³² (P: Phosphorylation, U: Ubiquitination, ☆: Kinase activity; adapted from Dhavan & Tsai³⁹).

p39, which exhibits similar characteristics, is less explored: p39 carries a myristoylation⁴⁴ and is either degraded by the proteasome or cleaved by calpain into p29⁵⁰. p35/Cdk5 and p39/Cdk5 show similar substrate specificity⁵¹, although they seem to have physiologically distinct functions. The expression patterns of p35 and p39 in the developing brain differ⁵², they locate Cdk5 activity to different subcellular regions⁴⁴ and p39 can compensate only for some but not all functions of p35 in p35 knockout mice.⁵³ Cdk5 activation by p35 and p39 has mainly been explored in neurons but p35-dependent Cdk5 activity was detected in several non-neuronal tissues as well.⁵⁴⁻⁵⁸ Recently, Cyclin I was described as an alternative activator of Cdk5 in podocytes.⁵⁹ In addition, Cdk5 regulation is unique in the family of cyclin-dependent kinases in two further aspects: 1) The endogenous Cdk inhibitors (CKIs) are not involved in Cdk5 regulation and modulation. Yet, Cdk5 can phosphorylate and stabilize p27^{Kip1}, which is crucial for migration.^{60, 61} 2) Modulation of Cdk5 activity by phosphorylation fundamentally differs from the cell cycle Cdk5. In contrast to the cell cycle Cdk5,

phosphorylation by CAK in the T-loop seems dispensable for Cdk5 full activation. CAK can phosphorylate Cdk5 on serine 159, but the function of this phosphorylation is disputed.⁶²⁻⁶⁵ Activity of mitotic Cdks is inhibited by phosphorylation of conserved threonine or tyrosine residues (T14 and Y15 in Cdk2) by Wee1 or Myt1 (see Figure 2). Cdk5 is phosphorylated on T14 *in vitro* and this inhibits kinase activity.⁶⁶ Cdk5 is not inhibited by Wee1⁶⁴, but can be phosphorylated at tyrosine 15 by fyn and c-abl.^{47 46} In contrast to the mitotic Cdks, this phosphorylation stimulates Cdk5 activity.

1.4 Cyclin-dependent kinase inhibitors

Tumor cells characteristically display limitless replicative potential which is caused by alterations in cell-cycle control systems.² Cdks as prominent regulators of the cell cycle exhibit deregulated activity in tumors, resulting from overexpression and mutations in cell cycle cyclins and Cdks, as well as from a loss of their endogenous inhibitors, the CKIs.^{67, 68} To target Cdks is therefore a promising strategy in anticancer therapy and several approaches are imaginable to alter Cdk activity – either by direct inhibition of the catalytic Cdk subunit, or by indirectly modulating regulatory pathways that govern Cdk activity, for example binding of cyclins, phosphorylation of the Cdk subunit or interaction with the CKIs. Most small molecule Cdk inhibitors interact with the ATP-binding site of the kinase subunit, which is fundamental for kinase activity. The ATP-binding site is well conserved among the Cdks which is why adequate Cdk selectivity of inhibitors remains a big challenge.⁶⁹ If selective or broad-spectrum Cdk inhibitors are more effective remains under discussion. Established Cdk modulators such as flavopiridol (Alvocidib) and roscovitine (CYC202, seliciclib) inhibit a relatively wide range of Cdks. Second generation Cdk inhibitors are under preclinical and clinical investigation at present. They can be subdivided in three classes: 1) Broad spectrum Cdk inhibitors that target both cell cycle and transcriptional Cdks, 2) Selective inhibitors of Cdk2 or Cdk4/6 or 3) Compounds with combined activity against Cdks and additional kinases with a benefit for anticancer therapy, for example receptor tyrosine kinases or Aurora kinases. The most promising strategy for successful therapy with selective or combined Cdk inhibitors is very likely depending on the genetic alterations present in the tumor.⁷⁰

1.4.1 Roscovitine

(*R*)-roscovitine or CYC-202/seliciclib – in the following referred to as roscovitine – belongs to the class of 2,6,9-trisubstituted purines and is one of the best-studied Cdk inhibitors.⁷¹

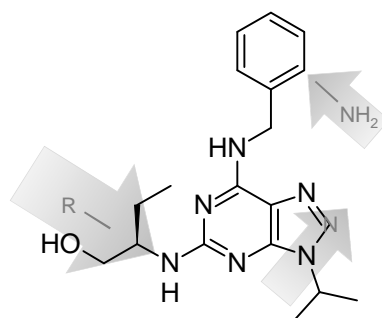


Figure 4 Structure of (*R*)-roscovitine. The arrows indicate how the structure was modified for the tested Cdk inhibitors.

It is developed by Cyclacel Pharmaceuticals⁷² and currently tested in several Phase I and Phase II clinical trials for tumor treatment.⁷³ Roscovitine inhibits mainly Cdk1, Cdk2, Cdk5, Cdk7 and Cdk9 and exerts anti-mitotic and pro-apoptotic effects in a wide range of tumor cells.⁷⁴ Cell-cycle independent actions of roscovitine mainly derive from Cdk5 inhibition and include anti-angiogenic⁷⁵ and anti-inflammatory⁷⁶ effects, inhibition of cell migration and motility^{77, 78} and modulation of glucose metabolism.⁷⁹

The roscovitine derivatives evaluated for their anti-angiogenic potential were kindly provided by V. Krystof and R. Jorda (Palacký University & Institute of Experimental Botany, Olomouc, Czech Republic) and the structures are displayed in the Materials and Methods section (Figure 5).

1.5 Aim of the study

As explained in the previous paragraphs, Cyclin-dependent kinases (Cdks) and their activators, the cyclins, control the transitions of the cell cycle, which is deregulated in many tumor types.⁶⁷ Cdk inhibitors like roscovitine or flavopiridol are currently tested in clinical trials as anti-proliferative anticancer drugs.

Anti-angiogenic actions of these Cdk inhibitors have been observed *in vitro* and *in vivo*.⁸⁰⁻⁸² Recently, it has been demonstrated that the anti-angiogenic effect of the Cdk inhibitor roscovitine most likely results from impaired endothelial cell migration. The effect on migration was traced down to Cdk5 inhibition which led to Rac1 inactivation

and lamellipodia disruption.⁷⁵ A promising novel strategy in anti-angiogenic therapy may therefore be Cdk5 inhibition. Up to date, improved Cdk inhibitors have mainly been developed in order to block cancer cell proliferation but have not systematically been optimized and evaluated for anti-angiogenic action by Cdk5 inhibition.

In contrast to the mitotic Cdks, Cdk5 is a cell-cycle independent Cdk that is known to control migration of post-mitotic neurons during CNS development.

With regard to its regulation, Cdk5 is as well unique among the Cdks: First, Cdk5 activity and subcellular localization is directed by non-cyclin proteins (p35 and p39). Second, phosphorylation of a conserved tyrosine 15 decreases activity of mitotic Cdks but stimulates Cdk5 activity and third, endogenous Cdk inhibiting proteins (CKIs), which control cell cycle Cdks, do not influence Cdk5 activity. Activation of Cdk5 in non-neuronal cells, as investigated so far, parallels the neuronal Cdk5 activation pathways, however distinct mechanisms have been reported as well.⁵⁴ The mechanisms which are responsible for the activation of Cdk5 during endothelial cell migration have not yet been explored.

Aims of the study were therefore:

- 1. to elucidate the characteristics of Cdk5 regulation during endothelial cell migration by investigating the role of the neuronal activators p35/p25 and p39/p29 and the tyrosine 15 phosphorylation.***
- 2. to evaluate the anti-angiogenic potency of novel roscovitine-derived Cdk inhibitors in vitro and in vivo, thereby paying particular consideration on their potency to inhibit Cdk5.***

2 MATERIALS AND METHODS

2.1 Materials

2.1.1 Biochemicals, inhibitors, dyes and cell culture reagents

Table 1 Biochemicals, inhibitors, dyes and cell culture reagents

Reagent	Producer
Accustain [®] paraformaldehyde	Sigma-Aldrich, Taufkirchen, Germany
Amphotericin B	PAA Laboratories, Pasching, Austria
BC Assay reagent	Interdim, Montulocon, France
Bovine Serum Albumin (BSA)	Sigma-Aldrich, Taufkirchen, Germany
Roti [®] -Quant Bradford Reagent	Carl Roth, Karlsruhe, Germany
Cdk5/p35, active	Millipore, Billerica, MA, USA,
Collagen G	Biochrom AG, Berlin, Germany
Collagenase A	Biochrom AG, Berlin, Germany
Complete [®] mini EDTA free	Roche diagnostics, Penzberg, Germany
Coomassie brilliant blue G250	Carl Roth, Karlsruhe, Germany
DMEM medium	PAA Laboratories, Pasching, Austria
DMSO	AppliChem, Darmstadt, Germany
Endothelial Cell Growth Medium (ECGM) with Supplement Mix #C-39215	PromoCell, Heidelberg, Germany
FCS gold	PAA Laboratories, Pasching, Austria
FluorSave [™] Reagent mounting medium	Merck, Darmstadt, Germany
M199 Medium	PAA Laboratories, Pasching, Austria
NaF	Merck, Darmstadt, Germany
Na ₃ VO ₄	ICN Biomedicals, Aurora, OH, USA
Page Ruler [™] Prestained Protein Ladder	Fermentas, St. Leon-Rot, Germany
Penicillin/Streptomycin	PAA Laboratories, Pasching, Austria
PMSF	Sigma-Aldrich, Taufkirchen, Germany
TNF- α human recombinant	PeproTech GmbH, Hamburg, Germany
Triton X-100	Merck, Darmstadt, Germany
Tween [®] 20	BDH Prolabo, Ismaning, Germany
VEGF 165 human recombinant	PeproTech GmbH, Hamburg, Germany

Table 2 Technical equipment

Name	Device	Producer
AB7300 RT-PCR	Real-time PCR system	Applied Biosystems, Foster City, CA, USA
Axioskop	Upright microscope	Zeiss, Jena, Germany
Culture flasks, plates, dishes	Disposable cell culture material	TPP, Trasadingen, Switzerland
Curix 60	Tabletop film processor	Agfa, Cologne, Germany
FACSCalibur	Flow cytometer	Becton Dickinson, Heidelberg, Germany
LSM 510 Meta	Confocal laser scanning microscope	Zeiss, Jena, Germany
Mikro 22R	Table centrifuge	Hettich, Tuttlingen, Germany
Nanodrop [®] ND-1000	Spectrophotometer	Peqlab, Wilmington, DE, USA
Nucleofector II	Electroporation device	Lonza GmbH, Cologne, Germany
Odyssey 2.1	Infrared Imaging System	LI-COR Biosciences, Lincoln, NE, USA
Olympus BX41	Clinical microscope	Olympus, Hamburg, Germany
Polytron PT1200	Ultrax homogenizer	Kinematica AG, Lucerne, Switzerland
SpectraFluor Plus [™]	Microplate multifunction reader	Tecan, Männedorf, Austria
Sunrise [™]	Microplate absorbance reader	Tecan, Männedorf, Austria
Vi-Cell [™] XR	Cell viability analyzer	Beckman Coulter, Fullerton, CA, USA

Table 3 Commonly used buffers

PBS (pH 7.4)		PBS+Mg²⁺/Ca²⁺	
NaCl	132.2 mM	NaCl	137 mM
Na ₂ HPO ₄	10.4 mM	KCl	2.68 mM
KH ₂ PO ₄	3.2 mM	Na ₂ HPO ₄	8.10 mM
H ₂ O		KH ₂ PO ₄	1.47 mM
		MgCl ₂	0.25 mM
		H ₂ O	

2.1.2 Inhibitors

The following inhibitors were used for experiments:

Table 4 Inhibitors

Compound		Producer
A-705253.13 ⁸³	calpain inhibitor	Abbott Bioresearch Corp. Worcester, MA, USA
Imatinib (STI571)	c-abl inhibitor	Selleck Chemicals, Houston, TX, USA
SU6656 ⁸⁴	src family kinase inhibitor	Sigma-Aldrich, Taufkirchen, Germany
(<i>R</i>)-roscovitine	Cdk inhibitor	Sigma-Aldrich, Taufkirchen, Germany

2.1.3 LGR compounds

Novel roscovitine derivatives were synthesized and kindly provided by V. Krystof and R. Jorda (Palacký University & Institute of Experimental Botany, Olomouc, Czech Republic).

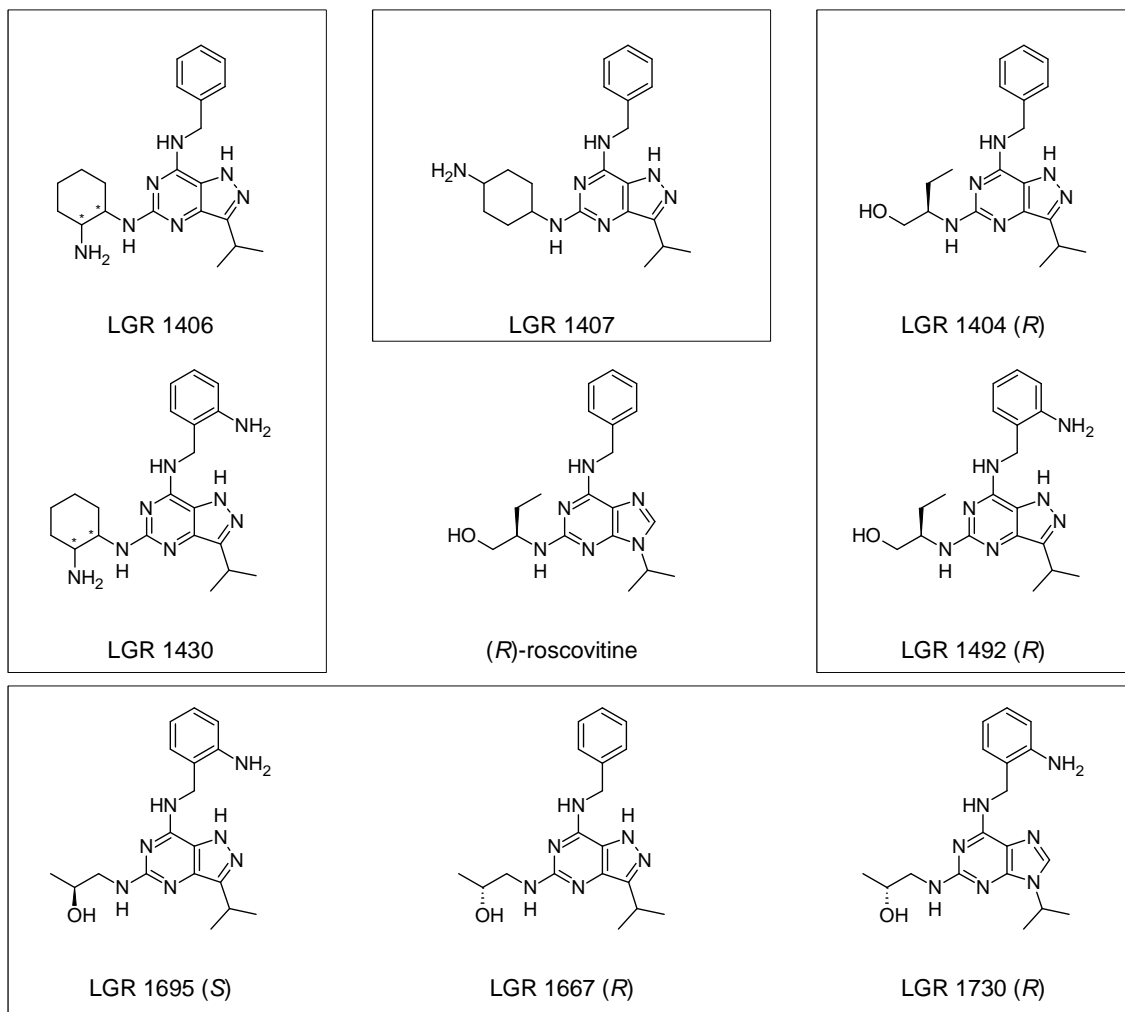


Figure 5 Chemical Structures of the tested LGR compounds in comparison to (*R*)-roscovitine. The LGR compounds have been modified in comparison to (*R*)-roscovitine in one or more of the following aspects: 1. The purine scaffold has been changed to pyrazolo[4,3-*d*]pyrimidine (LGR 1404, 1406, 1407, 1430, 1492, 1667, 1695), with LGR 1404 being a bioisoster of (*R*)-roscovitine. 2. In the aminobenzyl group, an additional *ortho* amino function is present (LGR 1430, 1492, 1695, 1730). 3. The residue at purine C2 or pyrazolo[4,3-*d*]pyrimidine C5 respectively, differs from (*R*)-roscovitine either in structure and/or stereochemistry. Defined configurations are shown in the chemical structures. LGR 1407 contains no stereocenter. LGR 1406 and LGR 1430 are an equal mixture of 4 stereoisomers: the *trans* enantiomers (*R,S*) and (*S,R*); and the *cis* enantiomers (*R,R*) and (*S,S*).

2.2 Cell culture

2.2.1 Cell culture solutions and reagents

The following solutions were used for isolation and cultivation of endothelial cells:

Table 5 Cell culture solutions

Growth medium		Stopping medium	
ECGM	500 ml	M 199	500 ml
Supplement Mix #C-39215	23.5 ml	FCS	50 ml
FCS gold	50 ml		
Penicillin/Streptomycin	5 ml		
Amphotericin B	5 ml		
Freezing medium		Trypsin/EDTA (T/E)	
FCS gold	10 %	Trypsin	0.05 %
DMSO	10 %	EDTA	0.20 %
Growth medium		PBS	
Collagen G			
Collagen G	0.001 %		
PBS			

Before use, FCS gold was heat inactivated. First, FCS gold was partially thawed at room temperature for 30 min, then completely thawed at 37°C. Heat inactivation was carried out at 56°C for 30 min. FCS aliquots were stored at -20°C

2.2.2 Endothelial cells

Endothelial cells (ECs) were cultured under constant humidity at 37°C with 5 % CO₂ in an incubator (Heraeus, Hanau, Germany). Cells were routinely tested for mycoplasma contamination with the Venor[®]GeM PCR detection kit (Minerva Biolabs, Berlin, Germany). All cell culture flasks, Petri dishes and multiwell plates were coated with Collagen G for 30 min in the incubator prior to plating the cells.

2.2.2.1 HMEC-1 (Human microvascular endothelial cells)

The cell line CDC/EU.HMEC-1 was kindly provided by the Centers for Disease Control and Prevention (Atlanta, GA, USA). The immortalized HMEC-1 cell line was created by transfection of human dermal microvascular endothelial cells with a plasmid coding for the transforming SV40 large T-antigen. HMEC-1 were shown to retain endothelial morphologic, phenotypic, and functional characteristics.^{85, 86} HMEC-1 were used for endothelial cell proliferation experiments, siRNA transfection and immunoprecipitations for kinase assay and LC-ESI-MS/MS.

2.2.2.2 HUVECs (Human umbilical vein endothelial cells)

Human umbilical cords were kindly provided by Klinikum München Pasing, Frauenklinik München West/Krüsman Klinik, Rotkreuzklinikum München, and WolfartKlinik Gräfelfing. After childbirth, umbilical cords were placed in PBS+Ca²⁺/Mg²⁺ containing penicillin (100 U/ml) and streptomycin (100 µg/ml), and stored at 4°C. Cells were freshly isolated every week. The umbilical vein was washed with PBS+Ca²⁺/Mg²⁺, filled with 0.1 g/l collagenase A, and incubated for 45 min at 37°C. To isolate endothelial cells, the vein was flushed with stopping medium and the cell suspension was centrifuged (1,000 rpm, 5 min). Afterwards, cells were resuspended in growth medium and plated in a 25 cm² flask (passage #0). After reaching confluency, cells were trypsinized and plated in a 75 cm² flask. Unless otherwise indicated, experiments were performed using cells at passage #3. HUVECs were used for all other experiments except endothelial cell proliferation experiments, siRNA transfection and immunoprecipitations for LC-ESI-MS/MS.

2.2.3 Passaging

After reaching confluency, cells were either sub-cultured 1:3 in 75 cm² culture flasks or seeded either in multiwell-plates or dishes for experiments. For passaging, medium was removed and cells were washed twice with PBS before incubation with T/E for 1-2 min at 37°C. Thereafter, cells were gradually detached and the digestion was terminated using stopping medium. After centrifugation (1,000 rpm, 5 min), the pellet was resuspended in growth medium and cells were plated.

2.2.4 Freezing and thawing

For freezing, confluent HMEC-1 from a 150 cm² flask were trypsinized, centrifuged in stopping medium (1,000 rpm, 5 min) and resuspended to 2×10^6 cells/ml in ice-cold freezing medium. 1.5 ml aliquots were frozen in cryovials. After storage at -80°C for 24 h, aliquots were moved to liquid nitrogen for long term storage.

For thawing, a cryovial was warmed to 37°C and the content was immediately dissolved in pre-warmed stopping medium. In order to remove DMSO, cells were centrifuged (1,000 rpm, 5 min), resuspended in growth medium and transferred to a 75 cm² culture flask.

2.3 Western blot analysis

2.3.1 Preparation of protein samples

Endothelial cells were treated as indicated, washed once with ice-cold PBS and subsequently lysed in RIPA lysis buffer or in modified RIPA lysis buffer for phosphoproteins. Immediately, cells were frozen at -80°C. Afterwards, cells were scraped off and transferred to Eppendorf tubes (Peske, Aindling-Arnhofen, Germany) before centrifugation (14,000 rpm, 10 min, 4°C). Tissue samples as positive controls were homogenized in lysis buffer with a POLYTRON PT 1200 C homogenizer (Kinematica AG, Lucerne, Switzerland), frozen at -80°C and centrifuged twice (14,000 rpm, 10 min, 4°C). Protein concentration was determined in the supernatant using either the BCA or the Bradford assay. Afterwards, Laemmli sample buffer (3x) was added and samples were heated at 95°C for 5 min. Samples were kept at -20°C until Western blot analysis.

Table 6 Buffers for protein sample preparation

RIPA buffer		Lysis buffer for phosphoproteins	
Tris/HCl (pH 7.4)	50 mM	Tris/HCl (pH 7.4)	50 mM
NaCl	150 mM	NaCl	150 mM
Nonidet NP 40	1%	Nonidet NP 40	1%
Deoxycholic acid	0.25%	Deoxycholic acid	0.25%
SDS	0.10%	SDS	0.10%
H ₂ O		Na ₃ VO ₄	0.3 mM
Complete [®] mini EDTAfree	4.0 mM	NaF	1.0 mM
PMSF	1.0 mM	β-Glycerophosphate	3.0 mM
Na ₃ VO ₄	1.0 mM	Pyrophosphate	10 mM
NaF	1.0 mM	H ₂ O	
		Complete [®] mini EDTAfree	4.0 mM
		PMSF	1.0 mM
		H ₂ O ₂	600 μM
5x SDS-sample buffer		3x Laemmli buffer	
Tris/HCl (pH 6.8)	3.125 M	Tris/HCl (pH 6.8)	187.5 mM
Glycerol	10 ml	SDS	6%
SDS	5%	Glycerol	30%
DTT	2%	Bromphenol blue	0.025%
Pryonin Y	0.025%	H ₂ O	
H ₂ O		β-Mercaptoethanol	12.5%

2.3.2 Membrane fractionation

HUVEC lysates were separated into a soluble (cytosolic) and a particulate (membranous) fraction, as described previously by Li H *et al.*⁸⁷ HUVECs were treated as indicated, washed twice with ice-cold PBS+Ca²⁺/Mg²⁺, and homogenized in lysis buffer. Protein quantification with Bradford Assay was used to obtain equal protein amount in the samples. Lysates were centrifuged at 100,000 g and 4°C for 45 min. The supernatant (cytosolic fraction) was collected and boiled with 5x SDS sample buffer (5 min, 95°C). The pellet was washed in lysis buffer containing 1.0 M NaCl and centrifuged at 100,000 g and 4°C for 20 min. The supernatant was discarded and the pellet was solubilized with lysis buffer containing 20 mM CHAPS at 4°C for 30 min.

After centrifugation at 100,000 g and 4°C for 45 min, the supernatant was kept as membranous fraction and boiled with 5x SDS sample buffer (5 min, 95°C). The cytosolic and membranous fractions were used for Western blotting.

Table 7 Buffer for membrane fractionation

**Membrane fractionation
lysis buffer**

Tris/HCl (pH 7.5)	50 mM
EDTA	0.5 mM
EGTA	0.5 mM
Glycerol	10 %
Glutathion	7 mM
DTT	2 mM
PMSF	1 mM
Complete [®] mini EDTAfree	4 mM
H ₂ O	

2.3.3 Immunoprecipitation

Immunoprecipitation for Kinase Assay

Immunoprecipitations were used in order to obtain active Cdk5 complexes for Cdk5 kinase assay. Cells or tissue samples were lysed (see 2.3.1) in the indicated lysis buffer (Table 6 and Table 8) and kept on ice for 30 min. Thereafter, the samples were centrifuged and protein concentrations were determined in the supernatants. Cell lysates were incubated with 2 µg of the indicated antibodies over night at 4°C under gentle agitation. Thereafter, Protein A (for rabbit IgG) or Protein G (for mouse IgG) Agarose beads (Sigma-Aldrich, Taufkirchen, Germany) were washed with lysis buffer and 50 µl bead suspension (25 µl packed beads) was added to each sample. After 3 h of incubation at 4°C, the beads were spun down and an aliquot of the supernatant was collected as binding control and boiled with Laemmli sample buffer (3x) for 5 min at 95°C. Subsequently, two washing steps with lysis buffer and two washing steps with kinase buffer were performed, and 50 µl kinase buffer (Table 9) were added to the bead pellet. The beads were resuspended in the kinase buffer before taking a 10 µl aliquot of the beads as binding control and boiling the aliquot with Laemmli sample buffer (3x) for 5 min at 95°C. The rest of the beads was used for Cdk5 kinase assay.

For the HA-immunoprecipitation of the Cdk5-HA transfected cells, the Pierce Mammalian HA-Tag IP/Co-IP Kit (Thermo Fisher Scientific, Rockford, IL, USA) was used according to the manufacturer's instructions. The kinase assay reaction was carried out directly on the beads.

Immunoprecipitation for the detection of novel Cdk5-interacting proteins by LC-ESI-MS/MS

HMEC-1 were treated as indicated, lysed in the Lysis buffer for phosphoproteins (Table 6) and immunoprecipitation with Cdk5 mouse monoclonal antibody was performed as described in the paragraph above. After three washing steps with lysis buffer, the beads were spun down, 25 μ l Laemmli sample buffer (3x) were added and the samples were boiled for 5 min at 95°C and stored at -20°C until gel electrophoresis and subsequent analysis.

Table 8 Lysis buffers for Cdk5 immunoprecipitation/kinase assay

Kinase assay lysis buffer 1 (Miyamoto et al. ⁴⁷)		Homogenization buffer (Menn et al. ⁸⁸)	
HEPES (pH 7.5)	50 mM	MOPS (pH 7.2)	25 mM
NaCl	150 mM	MgCl ₂	15 mM
EDTA	1 mM	EGTA	15 mM
DTT	1 mM	DTT	2 mM
MgCl ₂	20 mM	Na ₃ VO ₄	1 mM
Nonidet NP 40	0.5 %	NaF	1 mM
PMSF	1 mM	β -Glycerophosphate	60 mM
Na ₃ VO ₄	1 mM	p-Nitrophenylphosphate	10 mM
NaF	10 mM	Disodiumphenylphosphate	1 mM
Leupeptin	1 μ g/ml	Leupeptin	10 μ g/ml
H ₂ O		Aprotinin	10 μ g/ml
		Soybean trypsin inhibitor	10 μ g/ml
		Benzamidine	100 μ M
		H ₂ O	

MPER lysis buffer with inhibitors

mammalian protein extraction reagent (MPER), supplied in the HA Co-IP Kit

PMSF	1 mM
Na ₃ VO ₄	1 mM
NaF	1 mM
Complete [®] mini EDTAfree	4 mM

2.3.4 Cdk5 kinase assay

Cdk5 for the kinase assay was immunoprecipitated from cell lysates as described in 2.3.3. Kinase assay mix containing the indicated kinase buffer (Table 9), 2 μ M ATP, 10 μ Ci ³²P- γ -ATP (Hartmann Analytic, Braunschweig, Germany) and 2.5 μ g Histone H1 (Type III from calf thymus, Sigma-Aldrich, Taufkirchen, Germany) as a substrate was added to the beads and the enzyme reaction was carried out at 30°C for 20 min. The reaction was then terminated by adding 3x Laemmli Sample Buffer and boiling the samples for 5 min at 95°C. Aliquots of the samples were loaded onto a 15 % SDS-PAGE gel and electrophoresis was run at 100 V for 21 min and at 200 V for 60 min. For autoradiography, an X-ray film (Super RX, Fuji, Düsseldorf, Germany) was placed on the gel for 8 to 48h at -80°C. After exposure, the film was developed with a Curix 60 Developing system (Agfa-Gevaert AG, Cologne, Germany).

Table 9 Kinase buffers used for Cdk5 kinase assay

Kinase buffer 1 (modified from Tsai et al. ⁸⁹)		Kinase buffer 2 (Menn et al. ⁸⁸)	
HEPES (pH 7.0)	50 mM	Tris-HCl (pH 7.2)	25 mM
MgCl ₂	20 mM	MgCl ₂	10 mM
EDTA	0.1 mM	EGTA	1 mM
DTT	1 mM	DTT	1 mM
NaF	10 mM	Heparin	50µg/ml
Na ₃ VO ₄	1 mM	Na ₃ VO ₄	1 mM
PMSF	1 mM	NaF	1 mM
Leupeptin	1µg/ml	β-Glycerophosphate	60 mM
H ₂ O		p-Nitrophenylphosphate	10 mM
		Disodiumphenylphosphate	1 mM
		Leupeptin	10 µg/ml
		Aprotinin	10 µg/ml
		Soybean trypsin inhibitor	10 µg/ml
		Benzamidine	100 µM
		H ₂ O	

Kinase Buffer 3 (EDTA free)(Tsai et al.⁸⁹)

HEPES (pH 7.0)	50 mM
MgCl ₂	10 mM
DTT	1 mM
NaF	1 mM
Na ₃ VO ₄	1 mM
PMSF	1 mM
β-Glycerophosphate	3 mM
Complete [®] mini EDTAfree	4 mM
H ₂ O	

2.3.5 Protein Quantification

In order to employ equal amounts of protein in all samples for Western blot analysis, protein concentrations were determined using either the Bicinchoninic Acid (BCA) Assay or Bradford Assay. After measurement, protein concentration was adjusted by adding Laemmli sample buffer (1x).

2.3.5.1 Bicinchoninic Acid (BCA) Assay

Bicinchoninic Acid (BCA) Protein Assay was performed as described previously.⁹⁰ 10 µl protein samples were incubated with 200 µl BC Assay reagent (BC Assay reagents, Interdim, Montulocon, France) for 30 min at 37°C. Absorbance was measured at 550 nm (Tecan Sunrise Absorbance reader, TECAN, Crailsheim, Germany). Protein standards were obtained by diluting a 2 mg/ml stock solution of bovine serum albumin (BSA, Sigma-Aldrich, Taufkirchen, Germany). Linear regression was used to determine the actual protein concentration of each sample.

2.3.5.2 Bradford Assay

Bradford Assay was performed as described previously.⁹¹ 10 µl protein samples were incubated with 190 µl Bradford solution (Roti[®]-Quant Bradford Reagent, Carl Roth, Karlsruhe, Germany; 1:5 dilution in water) for 5 min. Thereafter, absorbance was measured at 592 nm (Tecan Sunrise Absorbance reader, TECAN, Crailsheim, Germany). Protein standards were obtained as described above for the BCA Assay.

2.3.6 SDS-PAGE

Proteins were separated by discontinuous SDS-polyacrylamide gel electrophoresis (SDS-PAGE) according to Laemmli *et al.*⁹² Equal amounts of protein were loaded on discontinuous polyacrylamide gels, consisting of a separation and a stacking gel, and separated using the Mini-PROTEAN 3 electrophoresis module (Bio-Rad, Munich, Germany). The concentration of Rotiphorese[™] Gel 30 (acrylamide) in the separating gel was adjusted for an optimal separation of the proteins depending on their molecular weights. Electrophoresis was carried out at 100 V for 21 min for protein stacking and at 200 V for 45 min for protein separation. The molecular weight of proteins was determined by comparison with a prestained protein ladder (PageRuler[™], Fermentas, St. Leon-Rot, Germany).

Table 10 Acrylamide gel concentration and SDS-PAGE buffers

Separation gel 12%/15%		Stacking gel	
Rotiphorese™ Gel 30	40%/50%	Rotiphorese™ Gel 30	17%
Tris (pH 8.8)	375 mM	Tris (pH 6.8)	125 mM
SDS	0.1%	SDS	0.1%
TEMED	0.1%	TEMED	0.2%
APS	0.05%	APS	0.1%
H ₂ O		H ₂ O	
Electrophoresis buffer			
Tris	4.9 mM		
Glycine	38 mM		
SDS	0.1%		
H ₂ O			

2.3.7 Tank electroblotting

After protein separation, proteins were transferred to a nitrocellulose membrane (Hybond-ECL™, Amersham Bioscience, Freiburg, Germany) by tank electroblotting.^{93,}

⁹⁴ A blotting sandwich was prepared in a box filled with 1x tank buffer as follows:

cathode – pad – blotting paper –
 separating gel (from SDS-PAGE) – nitrocellulose membrane –
 blotting paper – pad – anode.

The membrane was equilibrated with 1x tank buffer for 15 minutes prior to running the tank blot. Sandwiches were mounted in the Mini Trans-Blot® system (Bio-Rad, Munich, Germany), ice-cold 1x tank buffer was filled into the chamber and a cooling pack inserted to avoid excessive heat. Transfers were carried out at 4°C, 100 V for 90 min.

Table 11 Tank blotting buffer

5x Tank buffer		1x Tank buffer	
Tris base	240 mM	5x Tank buffer	20 %
Glycine	195 mM	Methanol	20 %
H ₂ O		H ₂ O	

2.3.8 Protein detection

Prior to immunodetection, unspecific protein binding sites were blocked by incubating the membrane in 5 % non-fat dry milk powder (Blotto, Carl Roth, Karlsruhe, Germany) in PBS for 2 h at room temperature. Subsequently, the membrane was incubated with the respective primary antibody at 4°C overnight. After four washing steps with PBS containing 0.1 % Tween[®]20 (PBS-T), the membrane was incubated with the secondary antibody for 2 h at room temperature, followed by four additional washing steps with PBS-T. All steps regarding the incubation of the membrane were performed under gentle agitation. In order to visualize the proteins, two different methods have been used depending on the labels of the secondary antibodies: enhanced chemiluminescence or infrared imaging.

2.3.8.1 Enhanced chemiluminescence (ECL)

Membranes were incubated with HRP-conjugated secondary antibodies (Table 14). For detection, luminol (5-Amino-2,3-dihydro-1,4-phthalazinedione) was used as a substrate. The membrane was incubated with ECL solution for 1 minute protected from light. The appearing luminescence was detected by exposure of the membrane to an X-ray film (Super RX, Fuji, Düsseldorf, Germany), which was developed with a Curix 60 Developing system (Agfa-Gevaert AG, Cologne, Germany).

Table 12 ECL solution

ECL	
Tris (pH 8.5)	100 mM
luminol	2.5 mM
p-Coumaric acid	1 mM
H ₂ O ₂	17 µM
H ₂ O	

2.3.8.2 Infrared imaging

Secondary antibodies coupled to IRDye™ 800 or Alexa Fluor® 680 with emission at 800 and 700 nm, respectively, were used (Table 14). Incubation and the following washing steps were carried out protected from light. Protein bands of interest were detected using the Odyssey imaging system (LI-COR Biosciences, Lincoln, NE).

Table 13 Primary antibodies for Western blot immunodetection

Antigen	Source	Dilution	In	Provider
β-actin (C4)	mouse monocl.	1:1,000	Blotto 5%	Millipore
Cdk5 (DC34)	rabbit polycl.	1:1,000	Blotto 1%	Invitrogen
Cdk5 (C-8)	rabbit polycl.	1:1,000	Blotto 1%	Santa Cruz
phos.-Cdk5Y15	rabbit monocl.	1:1,000	BSA 5%	Epitomics
p35/p25 (C64B10)	rabbit monocl.	1:250	BSA 5%	Cell Signaling
p35/p25 (C-19)	rabbit polycl.	1:500	Blotto 1%	Santa Cruz
HA.11 (16B12)	mouse monocl.	1:1,000	Blotto 1%	Covance

Table 14 Secondary antibodies for Western blot immunodetection

Antibody	Dilution	In	Provider
Goat anti-mouse IgG1: HRP	1:1,000	Blotto 1%	Biozol
Goat anti-rabbit HRP	1:1,000	Blotto 1%	Dianova
Goat anti-rabbit HRP	1:1,000	Blotto 1%	Biorad
Alexa Fluor® 680 Goat anti-mouse IgG	1:20,000	Blotto 1%	Molecular Probes
Alexa Fluor® 680 Goat anti-rabbit IgG	1:20,000	Blotto 1%	Molecular Probes
IRDye™ 800CW Goat anti-mouse IgG	1:20,000	Blotto 1%	LI-COR Biosciences

2.3.9 Quantification of band intensity

Intensity of Western blot bands detected with enhanced chemiluminescence was measured densitometrically with ImageJ Gel analyzer (Version 1.43q; NIH, Bethesda, MD, USA).

Quantification of bands obtained with infrared imaging was carried out with the Quant Data function of the Odyssey software.

2.4 Protein identification from SDS-PAGE gels

2.4.1 Coomassie staining

Table 15 Solutions for Coomassie staining

Coomassie staining solution		Destaining solution	
Coomassie blue G250	0.3 %	Ethanol	33.3 %
Ethanol	45 %	Acetic acid	10 %
Acetic acid	10 %	H ₂ O	
H ₂ O			

The SDS-PAGE gel was incubated under gentle agitation in Coomassie staining solution for 1 h. The staining solution was removed and the gel was washed in destaining solution for several times until the bands became clearly visible. After a last washing step in water the gel was kept at 4°C until protein analysis.

2.4.2 In-gel tryptic digestion

The gel band was cut and destained twice with a 1/1 mixture of acetonitrile (ACN) / 20 mM ammonium bicarbonate (NH₄HCO₃) pH 8.5 at 37°C for 30 min. The gel slice was dried at room temperature, rehydrated with the addition of 25 mM NH₄HCO₃ and then reduced with 10 mM dithiothreitol (DTT) for 30 min at 56°C in darkness. After removing the supernatant, 55 mM iodoacetamide (IAA) in 25mM NH₄HCO₃ was added. The reaction of carboxyamidomethylation proceeded for 30 min at RT in darkness. For the enzymatic digestion, the gel slice was incubated overnight at 37°C with 200 ng trypsin in 20 mM NH₄HCO₃ pH 8.5. To quench the enzymatic reaction 1 % aqueous acetic acid was added. After the digestion, peptides were extracted by incubating the slice with 2 % aqueous formic acid (HCOOH) / ACN (1/1) at RT for 20 min and then sonicating for 5 min. The extraction procedure was repeated twice. Supernatants were pooled and then dried using a Savant Speedvac Plus SC210A apparatus (Thermo Scientific, San José CA, USA).

2.4.3 LC-ESI-MS/MS analysis

The extracted peptides were dissolved in 0.1 % HCOOH aqueous solution and separated with a nano-LC system (Eksigent, Dublin, CA, USA), consisting of

autosampler and 2D-nano HPLC devices, coupled to the LTQ-Orbitrap XL mass spectrometer (Thermo Scientific, Bremen, Germany) equipped with a nano ESI source. The sample was loaded onto a RP-C18 micro column (10 mm x 100 μ m i.d.) trapping column (Agilent technologies, Santa Clara, CA, USA) and washed for 10 min with 0.1 % HCOOH at 3 μ l/min. The peptides were separated on a nano column (75 μ m i.d. x 15 cm, capillary column (New Objectives, USA) packed in-house with 3 μ m C18 coated particles). For the liquid chromatography, 0.1 % HCOOH aqueous buffer (solvent A) and ACN / 0.1% HCOOH (95/5, v/v) organic buffer (solvent B) were used. The peptides were eluted with a linear gradient of solvent B from 2 to 10 % in 5 min and from 10 to 40 % in 98 min at flow rate of 200 nl/min. The eluted peptides were on-line analyzed in ESI-MS and -MSMS positive mode. The mass spectrometer was set so that one full scan was acquired in the Orbitrap parallel to the MSMS scans in the LTQ linear ion trap. The resolving power of the Orbitrap mass analyzer was set at resolution 60000 (FMHW, m/z 400). The fragmentation spectra (MSMS mode) were acquired in data dependent mode, five most intensive signal ions (m/z) per scan were selected for fragmentation with repeat duration time 30 s and exclusion duration time 60 s, isolation width (m/z) 2 amu, activation time 30 ms, activation Q 0.250, normalized collision energy (V) 35. The chromatographic separation and the spectra acquisition were performed in automatic mode, controlled and monitored by Xcalibur software (version 2.0.7, Thermo Scientific, San José CA, USA).

2.4.4 Protein identification

Prior the submission to protein database (DB) search the MSMS spectra were converted in mzData format using a conversion tool embedded in Bioworks software (version 3.1, Thermo Scientific, San José CA, USA). The protein database searches were performed using the Mascot search engine (www.matrixscience.com). The tandem spectra were searched against the protein database SwissProt 15.3 (uniprot 29.05.09), choosing for taxonomy specimen *homo sapiens*. The peptide and the fragment mass accuracies were set to 20 ppm and 0.6 Da, respectively. Full tryptic peptides including one missed cleavage side were accepted. Carboxyamidomethylation at cysteine was set as a static modification. Methionine oxidation was set as variable modifications. The Mascot database search of the data sets was performed with a confidential index over 95 %.

2.5 Quantitative real time RT-PCR

2.5.1 Isolation of mRNA

Total RNA was extracted from cell and tissue samples using the RNeasy mini Kit (Qiagen GmbH, Hilden, Germany) according to the instruction manual. QuiaShredder columns (Qiagen GmbH, Hilden, Germany) were used for sample homogenization. DNA-digestion was performed during the isolation procedure with the RNase Free DNase Set (Qiagen, Hilden, Germany).

2.5.2 Reverse transcription

Reverse transcription was performed with the High Capacity cDNA Reverse Transcription Kit (Applied Biosystems, Foster City, DA, USA) according to the users' manual. Reverse transcription was carried out in a Primus 25 advanced[®] thermocycler (PepLab Biotechnologie GmbH, Erlangen, Germany), using the cycling protocol displayed in Table 16. cDNA was aliquoted and stored at -20°C until used for real time RT-PCR.

Table 16 Reverse transcription

Temperature	Time
25°C	10 min
37°C	2 h
85°C	5 min

2.5.3 Quantitative real time PCR

Quantitative real-time PCR was performed on AB 7300 RealTime PCR system, using TaqMan[®] Gene Expression Mastermix (Applied Biosystems, Foster City, CA, USA). The thermal cycling conditions are shown in Table 17. GAPDH primers shown in Table 18 were designed using the Primer Express[®] 2.0 software program (Applied Biosystems). For p35 and p39, pre-mixed TaqMan[®] Gene Expression Assays were used (See Table 19). PCR on GAPDH was used as reference, and serial dilution of cDNA served as standard curves. Fluorescence-development was analyzed using the AB 7300 system software, and calculation of relative mRNA amount was done according to Pfaffl et al.⁹⁵

Table 17 Real Time RT-PCR thermal cycling conditions

Temperature	Time	Step
95°C	10 min	Amplitaq [®] Gold enzyme activation
95°C	15 sec	denature
60°C	1 min	anneal / extend

PCR (40 cycles)

Table 18 GAPDH Primers and Probe**GAPDH**

forward	human	5'-GGGAAGGTGAAGGTCGGAGT-3'
reverse	human	5'-TCCACTTTACCAGAGTTAAAAGCAG -3'
probe	human	6-Fam-ACCAGGCGCCCAATACGACCAA-Tamra

Table 19 TaqMan[®] Gene Expression Assays

Target	Species	Product Id
p35	human	Hs00243655_s1
p39	human	Hs00269563_s1

2.6 Transfection of cells

For transient transfection with the indicated siRNA and plasmids, HUVECs or HMEC-1 were electroporated using the Nucleofector[®] II device in combination with the HUVEC Nucleofector[®] Kit (both from LONZA Cologne AG, Cologne, Germany).

2.6.1 Transfection with siRNA

In order to downregulate p35, HMEC-1 were transiently transfected with p35 siRNA. A 4-siRNA duplexes bundle from riboxx (Radebeul, Germany) was used. The sequences are shown in Table 20. The duplexes were dissolved in RNase free water to 0.3 µg/l, aliquoted and stored at -80°C. The concentration of siRNA was verified using a NanoDrop (Wilmington, DE, USA). Before transfection, equal parts of the four duplexes were mixed. 1×10^6 HMEC-1 were suspended in HUVEC Nucleofector[®] Solution and added to 1.2 µg of the siRNA mixture. The mixture of cells and siRNA was transferred to a Nucleofector[®] cuvette and transfection was performed (program A-

034). Immediately after electroporation, pre-warmed growth medium was added to the cuvette. Afterwards, cells were seeded into 24-well plates (250,000 cells per well) for scratch assays and into 6-well plates (750,000 cells per well) for real time RT-PCR to ensure successful downregulation.

Table 20 4-siRNA duplexes bundle - sequences

	5'-3'sequence	3'-5'sequence
p35-1	AUUAAUGAGUCAACCAGCCCCC	GGGGGCUGGUUUGACUCAUUAU
p35-2	AUAAACCACACAUACUCACCCCC	GGGGGUGAGUAUGUGUGGUUUAU
p35-3	ACAUJGGUCUUUGUUCUCCCCC	GGGGGAGAACAAGACCAAUGU
p35-4	UUACACAAUACUGAUGACCCCC	GGGGGUCAUCAGUAUUGUGUAA

2.6.2 Transfection of plasmids

To evaluate the effect of a non-phosphorylatable Cdk5 mutant, HUVECs were transfected with pEGFP-CDK5Y15F-C1, which was a gift from P. Zelenka (National Eye Institute, National Institutes of Health, Bethesda, MD, USA).⁹⁶ The respective control plasmid pEGFP-C1 was purchased from Clontech Laboratories, Mountain View, CA, USA.

For the Cdk5 kinase assay with Pierce Mammalian HA-Tag IP/Co-IP Kit, HUVECs were transfected with the following constructs (all purchased from Addgene, Cambridge, MA, USA): Cdk5-HA-pCMV-NeoBam,⁹⁷ (Addgene plasmid 1872) and p35-myc-pCMV (Addgene plasmid 1347), or the respective backbone vectors.

For each transfection, 1×10^6 HUVECs were suspended in HUVEC Nucleofector[®] Solution and added to 3 μg plasmid. For co-transfection, a mixture of 1.5 μg Cdk5 construct and 1.5 μg p35 construct was used. Electroporation was performed in analogy to the siRNA experiments. Subsequently, cells were seeded into 24-well plates (250,000 cells per well) for scratch assays and FACS, or into 60 mm Petri dishes (2×10^6 cells per dish) for immunoprecipitation followed by Cdk5 kinase assay.

2.7 Flow Cytometry (FACS)

Transfection efficiency of the GFP-tagged plasmids was evaluated by flow cytometry. The measurements were performed on a FACSCalibur (Becton Dickinson, Heidelberg, Germany). Cells were illuminated by a blue argon laser (488 nm).

Transfected cells were seeded in duplicates into 24-well plates in parallel to the migration experiments. After finishing the scratch assay, the cells for FACS transfection control were washed with warm PBS, harvested by trypsination and resuspended in PBS. Immediately thereafter, 10,000 cells/sample were measured by flow cytometry.

2.8 Immunocytochemistry and immunohistochemistry

2.8.1 Immunocytochemistry

2.8.1.1 Immunocytochemistry and confocal microscopy

HUVECs were cultured in 8-well μ -slides (ibiTreat, ibidi GmbH, Martinsried, Germany) until reaching confluency. Afterwards, the cell layer was scratched and washed twice with PBS+Ca²⁺/Mg²⁺. The cells were treated as indicated and allowed to migrate for 8 h. The cells were then washed with PBS and fixed with 4 % paraformaldehyde in PBS at room temperature (10 min), followed by permeabilization for 2 min with 0.1 % Triton X-100 in PBS. Cells were washed and unspecific binding was blocked with 0.2 % BSA in PBS for 15 min. Thereafter, cells were incubated with primary antibody in 0.2 % BSA / PBS over night at 4°C. After three washing steps with PBS, the specimen were incubated with the corresponding AlexaFluor[®]-labeled secondary antibodies or rhodamine-phalloidin for f-actin staining in 0.2 % BSA / PBS for 30 min at room temperature. Finally, the slides were again washed three times with PBS (5 min), embedded in FluorSave[™] Reagent mounting medium and covered with 8 mm x 8 mm glass cover slips (custom made by Helmut Saur Laborbedarf, Reutlingen, Germany).

Table 21 Primary and secondary antibodies for immunocytochemistry

Antigen	Source	Dilution	Provider
cortactin	rabbit polyclonal	1:100	Cell Signaling
Rac1	mouse monoclonal	1:100	Upstate

Antibody	Dilution	Provider
Alexa Fluor® 488 Goat anti-rabbit IgG (H+L)	1:400	Molecular Probes
Alexa Fluor® 633 Goat anti-mouse IgG (H+L), highly cross absorbed	1:400	Molecular Probes
rhodamine-phalloidin	1:400	Molecular Probes

A Zeiss LSM 510 META confocal microscope (Zeiss, Oberkochen, Germany) was used for obtaining immunofluorescence images.

2.8.1.2 Quantification of lamellipodia

Confluent layers of HUVECs were scratched and stimulated in 8-well μ -slides as described above. The cells were allowed to migrate for 8 h in the presence or absence of the respective concentration of the compounds, until clear lamellipodia formation was visible in the control. The actin cytoskeleton was then stained with rhodamine-phalloidin and fluorescence images of the scratches were taken in 10x magnification with the Zeiss LSM 510 META. For quantitative evaluation of lamellipodia formation, cells with prominent lamellipodia and ruffles were counted with ImageJ (Cell Counter plug-in by Kurt De Vos) in relation to the total number of cells at the scratch front. The ratio was calculated as number of lamellipodia-positive cells per 100 cells at scratch front.

2.8.2 Immunohistochemistry

2.8.2.1 Sections of p35 knockout and wild type mice

Brain, heart, kidney, liver and lung of four p35 knockout mice and three wild type mice were used (age between 11 and 15 weeks). All organs, which were perfusion-fixed in paraffin, were kindly provided by J. A. Bibb (University of Texas Southwestern Medical Center, Dallas, TX, USA). Generation of the p35 k.o. mice is described in Chae *et al.*⁹⁸ The paraffin-fixed organs were sectioned with a rotation microtome (5 μ m sections).

Table 22 Identification numbers of p35 k.o. and wt mice

p35 knockout mice	wt mice
008 KO	010 wt
890 KO	042 wt
892 KO	891 wt
893 KO	

2.8.2.2 Hematoxylin-eosin staining

Sections were treated twice with xylene and each once with ethanol 100 %, 95 % and 70 % for deparaffinization. Sections were then incubated with Mayer's Hematoxylin Solution (Sigma-Aldrich, Taufkirchen, Germany) for 15 min, watered for 15 min, treated with Accustain[®] Eosin Y Solution Aqueous (Sigma-Aldrich, Taufkirchen, Germany) for 3 min and finally watered for 3 min. Sections were mounted with FlourSave[™] Reagent and covered with 18 mm x 18 mm cover slips (Menzel, Braunschweig, Germany).

2.8.2.3 Microvessel density of perfusion-fixed and HE stained sections

To estimate the number of blood vessels in the brain and liver of p35 knockout and wild type mice, sections of 4 different p35-deficient mice and sections of 3 different wild type mice were used. As the sections were perfusion-fixed, blood vessels could be recognized by their particular lumen in the HE-staining. Four images of each brain section were taken with the clinical microscope Olympus BX41 (Olympus, Hamburg, Germany) with 10x magnification ($A = 0.56819712 \text{ mm}^2$) and four images of each liver section were taken with 40x magnification ($A = 0.03551232 \text{ mm}^2$).

Blood vessels were then identified and counted using ImageJ (Cell Counter plug-in). Every blood vessel needed to be clearly separated from each other and to show a lumen big enough to be identified by human eye. Blood vessels that were truncated were also counted. Blood vessels that showed two or more lumina and were identified as one connected blood vessel, were counted as only one. The microvessel density (MVD) per image was calculated with the formula $MVD = n / A$ with n as the number of vessels, and A as the image area, and averaged for each p35 wt or k.o. mouse.

2.8.2.4 Sections of the HUH7 xenograft tumors

The mice were sacrificed by neck fracture. Tumors were removed and weighed and volume was determined. Afterwards, tumors were fixed with 4 % paraformaldehyde in

PBS for one day and with 1 % paraformaldehyde for additional three days prior to embedding in paraffin. The paraffin-embedded tumors were sectioned with a rotation microtome (5 μ m sections).

2.8.2.5 CD31 immunohistochemistry staining

The slides were treated three times with xylene, twice with ethanol 100 %, twice with ethanol 95 % and twice with distilled water for deparaffinization. For antigen retrieval, sections were incubated with Proteinase K Working Solution (Roche, Indianapolis, IN, USA, see Table 23) at 37°C for 15 min and at room temperature for 10 min, and washed twice with PBS + 0.05 % Tween[®]20. Endogenous peroxidase was blocked by incubation in 7.5 % hydrogen peroxide for 10 minutes. Subsequently, the slides were incubated with Purified Rat Anti-Mouse CD31 antibody (clone MEC 13.3; BD Biosciences, Franklin Lake, NJ, USA) diluted 1:100 in PBS. For antibody detection, Vectastain[®] Universal Elite ABC Kit (Vector Laboratories, Burlingame, CA, USA) was used according to the manual together with ImmPACT[™] AEC Peroxidase Substrate Kit (Vector Laboratories, CA, USA) as a chromogen. Slides were counterstained with hematoxylin for 1 min and washed with distilled water. Finally, the sections were mounted with FlourSave[™] Reagent Mounting Medium and covered with 18 mm x 18 mm cover slips.

Table 23 Proteinase K solutions

TE Buffer		Proteinase K stock solution 12 U/ml	
Tris Base (pH 8)	50 mM	Proteinase K	57.2 μ l
EDTA	1 mM	TE Buffer	971.4 μ l
Tween [®] 20	0.05 %	Glycerol	971.4 μ l
H ₂ O			
Proteinase K working solution 0.6 U/ml			
Proteinase K stock solution	0.4 ml		
TE Buffer	7.6 ml		

2.8.2.6 Microvessel density of the CD31 stained tumor sections

Microvessel density per mm² tumor tissue was determined after CD31 staining of tumor sections. For each tumor, four 10x magnification overview images of well vascularized areas were taken with the Olympus BX41. For each 10x overview, four detail images at

40x magnification ($A = 0.03551232 \text{ mm}^2$) were taken and CD31 positive stained vessels were counted with the ImageJ Cell Counter plug-in. Every blood vessel counted needed to be clearly separated from each other and positively stained for CD31. Blood vessels that were definitely identified as one connected blood vessel were counted as only one. The microvessel density (MVD) per image was calculated with the formula $MVD = n / A$ with n as the number of vessels and A as the image area, and averaged for each tumor.

2.9 Angiogenesis assays

2.9.1 Cell proliferation assay (crystal violet staining assay)

HMEC-1 were seeded into 96-well-plates (1,500 cells / well). After 24 h, the cells were stimulated with the indicated compounds. At the same time point, cells in a reference plate were stained with crystal violet, serving as initial cell number. After 72 hours of stimulation, cells were fixed and stained with crystal-violet solution for 10 minutes, washed with water, and air dried. Crystal violet was eluted with dissolving buffer and absorbance was measured at 550 nm (Tecan Sunrise Absorbance reader, TECAN, Crailsheim, Germany).

Table 24 Solutions for proliferation assay

Crystal violet solution		Dissolving buffer	
crystal violet	0.5 %	sodium citrate 0.1 M	50 %
methanol	20 %	ethanol	50 %
H ₂ O			

2.9.2 CellTiter-Blue™ cell viability assay

HUVECs were seeded in 96-well plates. After reaching confluency, the cells were treated for 16 h with the indicated compounds or left untreated as control. After addition of CellTiter-Blue™ Reagent (Promega Corporation, Madison, WI, USA), cells were incubated for additional 4 h and fluorescence was measured at 560 nm in a plate-reading photometer (SpectraFluor Plus; Tecan, Crailsheim, Germany).

2.9.3 Scratch assay (wound healing assay)

Cdk inhibitors:

HUVECs were seeded into a 24-well plate. After reaching confluency, cells were scratched using a pipette tip. The wounded monolayers were washed twice with PBS+Ca²⁺/Mg²⁺ and growth medium containing the indicated concentration of the compounds was added.

siRNA/plasmids

After transfection, HMEC-1 were seeded into a 24 well plate (250,000 cells per well). 40 h (siRNA) or 24 h (plasmids) after transfection, cells were scratched, washed twice with PBS+Ca²⁺/Mg²⁺ and growth medium was readded.

After 16 h (HUVECs) or 8-12 h (HMEC-1) of migration, cells were washed with PBS+Ca²⁺/Mg²⁺ and fixed with 4 % paraformaldehyde. Images were taken using the TILLvisON system (TILL Photonics GmbH, Gräfelfing, Germany) and a CCD-camera connected to an Axiovert 200 microscope (Zeiss, Oberkochen, Germany). Quantitative image analysis of the cell covered area was done by Wimasis GmbH, Munich.

2.9.4 Tube formation assay

Pre-cooled BD Matrigel™ Matrix Growth Factor Reduced (GFR) (BD Biosciences, Heidelberg, Germany) was filled into the lower compartment of μ -slide Angiogenesis wells (ibidi GmbH, Martinsried, Germany) on ice. For polymerization of the Matrigel™ Matrix, the slides were incubated at 37°C for 30 min. 12,000 HUVECs/well were seeded onto the Matrigel™ and stimulated in quintuplets for 16h. The level of tube formation was determined by light microscopy using the TILLvisON system. Quantitative image analysis of tube length, number of branching points and tubes was done by Wimasis GmbH, Munich.

2.9.5 Chemotaxis assay

The effect of the LGR compounds on endothelial cell chemotaxis was determined using Collagen IV coated μ -slides Chemotaxis (ibidi, Martinsried, Germany).⁹⁹ The slides and the media were equilibrated overnight in the incubator before the experiment. A HUVECs suspension of 5×10^6 cells per ml was seeded into the observation channel of the slides according to the protocol, and the cells were allowed to attach for 4 hours.

Thereafter, the chambers of the chemotaxis slide were completely filled with serum-free medium M 199; and growth medium containing 30 % FCS was added to one chamber in order to generate an FCS-gradient from 0 % to 10 %. 10 μ M of the indicated compounds were added both to the M199 and to the 30 % FCS. Chemotaxis was observed over 20 hours by live-cell imaging with a Zeiss LSM 510 META confocal microscope equipped with a heating stage (EMBLem, Heidelberg, Germany). During observation, cells were incubated with constant humidity at 37°C and with 5 % CO₂. A time series was collected taking 1 picture every 10 minutes. For cell tracking and data analysis, the manual tracking plug-in (Fabrice Cordelieres) and the Chemotaxis and Migration Tool (Version 1.01, ibidi, Martinsried, Germany) for ImageJ were used.

2.9.6 Chorioallantoic membrane (CAM) assay

Preparation of cellulose discs

After preparing the cellulose solution, the mixture was autoclaved, resulting in a homogenized, clear solution. For each disk, 200 μ l of the warm solution were given into the preformed circles of the lid of a 96 well plate and allowed to polymerize under a laminar air flow for 48 h. Finally, the cellulose disks were removed using tweezers and stored in a sterile Petri dish until use.

Table 25 Cellulose solution

Cellulose solution

Hydroxyethyl cellulose (HEC)	2.5 %
PVP 17	2 %
PEG 400	2 %
H ₂ O	

Preparation of the eggs and stimulation

Fertilized white leghorn eggs were incubated for 72 h at 37°C in humidified atmosphere. After transferring the growing embryo into a Petri dish, a second incubation period of 72 h followed. At day 6, two cellulose discs, one with 2.5 ng VEGF / 250 nmol compound and the other with 2.5 ng VEGF / DMSO as control were placed on one CAM. After 24 h of stimulation, the vascular structure in the stimulated areas of the CAM was visualized using a stereomicroscope and a CCD camera (Olympus, Munich, Germany) and pictures were taken.

2.10 In vivo tumor model

The HUH7 xenograft tumor model in SCID mice was performed in cooperation with M. Günther (Pharmaceutical Biotechnology, Department of Pharmacy, Ludwig-Maximilians-Universität, Munich, Germany).

2.10.1 Animals and cell line

Female SCID mice (8-10 weeks) were housed in individually ventilated cages under specific pathogen free conditions with a 12 h day/night cycle and with free access to food and water. All experiments were performed according to German legislation for the protection of animals and approved by the local government authorities.

The HUH7 cell line was kindly provided by M. Günther (Pharmaceutical Biotechnology, Department of Pharmacy, Ludwig-Maximilians-Universität, Munich, Germany) and cultured in DMEM medium (PAA, Pasching, Austria) with 10% FCS gold.

2.10.2 Tumor cell implantation

HUH7 were harvested with T/E at approximately 70 % confluency. 5×10^6 HUH7 cells in 100 μ l PBS were injected subcutaneously with a 25 G needle (Braun, Melsungen, Germany) into the flank of SCID mice. Animals were checked regularly for tumor progression. Tumor volume was determined in situ, using a digital measuring slide (Digi-Met, Preisser, Gammertingen, Germany). Length (a), width (b) and height (c) of the tumor were measured and tumor volume was calculated by the formula $a \cdot b \cdot c \cdot \pi/6$; with $\pi/6$ as the correction factor for tumor shape.

2.10.3 Intraperitoneal application of LGR 1407

The tumors were allowed to become established for 6 days before initiation of treatment. On treatment day 1, mice were randomly assigned to the treatment (n=4) or the control group (n=3). LGR 1407 was dissolved in DMSO (50 mg/ml) and freshly diluted 1:10 with PBS / 40 mM HCl before injection. 30mg/kg/d LGR 1407 solution (treatment) or the respective volume of vehicle only (control) was administered intraperitoneally with a 25 G needle (Braun, Melsungen, Germany). The mice were treated daily from day 1 to day 7.

2.10.4 Isolation of tumors

For investigation of tumor size, mice were sacrificed by neck fracture. Tumors were removed and weight and volume was determined. For immunohistochemistry and determination of microvessel density according to 2.8.2.6, the tumors were fixed and stained according to 2.8.2.

2.11 Statistical Analysis

The number of independently performed experiments is stated in the respective figure legend. One representative image is shown. Bar graph data are mean values \pm SEM. Statistical analysis was performed with the GraphPad Prism software version 3.03 (GraphPad Software, San Diego, CA, USA). Unpaired *t* test was used to compare two groups. To compare three or more groups, one-way ANOVA followed by Dunnett post hoc test was used. Values of $p < 0.05$ were considered statistically significant.

3 RESULTS

3.1 Cdk5 regulation in endothelial cell migration

Our group has previously shown that Cdk5 is a central regulator of endothelial cell migration and a potential target for anti-angiogenic compounds.⁷⁵ Therefore, the first part of the study aimed at the elucidation of the regulation of Cdk5 in endothelial cell migration. To get a uniform activated migratory cell phenotype for Western blot or Real Time RT-PCR, the cells were detached and freshly seeded for spreading, as indicated in the graph labels.

3.1.1 Cdk5 expression level in endothelial cell migration

First, we tested the basal Cdk5 protein expression in comparison to brain tissue. In endothelial cells Cdk5 protein expression was by trend lower than in human cortex tissue, but the difference was not statistically significant (Figure 6)

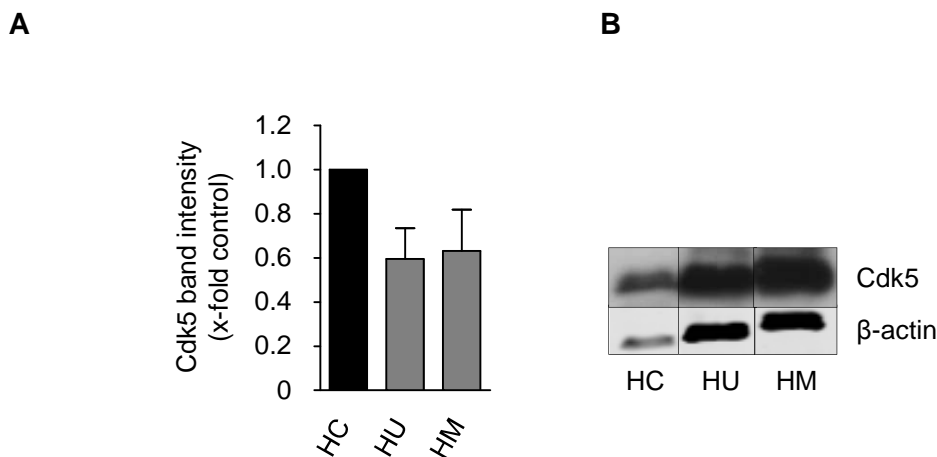
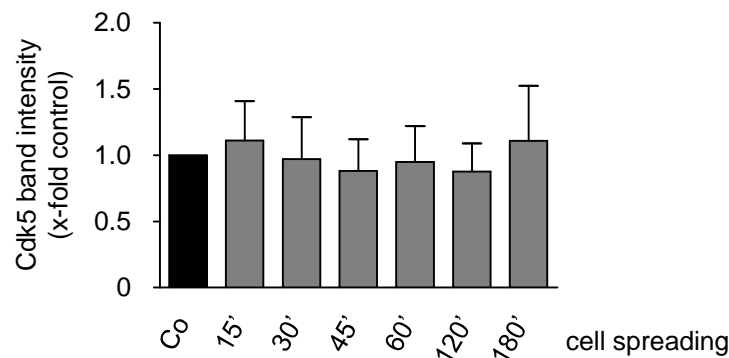


Figure 6 Cdk5 protein expression in endothelial cells in comparison to human cortex. Cdk5 protein amount was analyzed by Western blot in samples of human cortex (HC), confluent HUVECs (HU) and HMEC-1 (HM). β -actin served as a loading control and for normalization of protein amount. Relative quantification (A) and one representative image (B) of three individual blots are shown. Note the much lower protein loading in the HC sample in panel B (n=3, mean \pm SEM, $p > 0.05$, One Way ANOVA, Dunnett).

Cdk5 regulation mainly takes place by transcriptional control of its activators p35 and p39, only to a minor degree by alteration of Cdk5 expression.³⁹ In order to find out if this also accounts for the regulation of Cdk5 in endothelial cell migration, we first analyzed whether the protein levels of Cdk5 are changed during endothelial cell spreading (Figure 7). The amount of Cdk5 protein was not significantly altered in the migration-activated cells in comparison to confluent control.

A



B

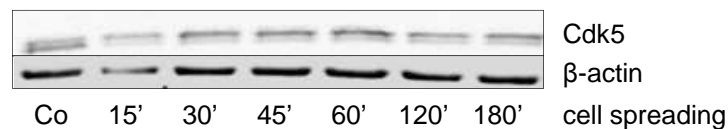


Figure 7 Cdk5 expression in endothelial cells is not changed during spreading. HUVECs were freshly seeded and allowed to spread for the indicated time periods or grown to confluency as control. Cdk5 protein amount was analyzed by Western blot. β -actin served as a loading control and for normalization of protein amount. Relative quantification (A) and one representative image (B) of three individual blots are shown (n=3, mean \pm SEM, $p > 0.05$, One Way ANOVA, Dunnett).

3.1.2 Cdk5 phosphorylation at tyrosine 15 is not crucial for endothelial cell migration

Cdk5 phosphorylation on tyrosine 15 by the non-receptor tyrosine kinases fyn or c-abl enhances Cdk5 activity and stimulates migration in oligodendrocyte precursor cells⁴⁷ and neurite outgrowth in cortical neurons⁴⁶. So we assumed that Cdk5 phosphorylation on tyrosine 15 might also be central for endothelial cell migration. First, we determined if treatment with the fyn inhibitor SU6656 or with the c-abl inhibitor imatinib affected endothelial cell migration. Neither inhibition of fyn nor inhibition of c-abl decreased endothelial cell migration (Figure 8).

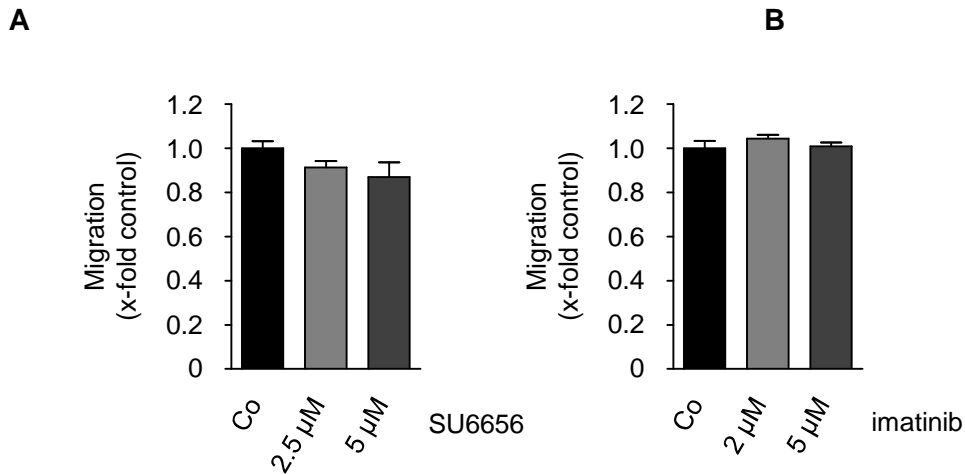
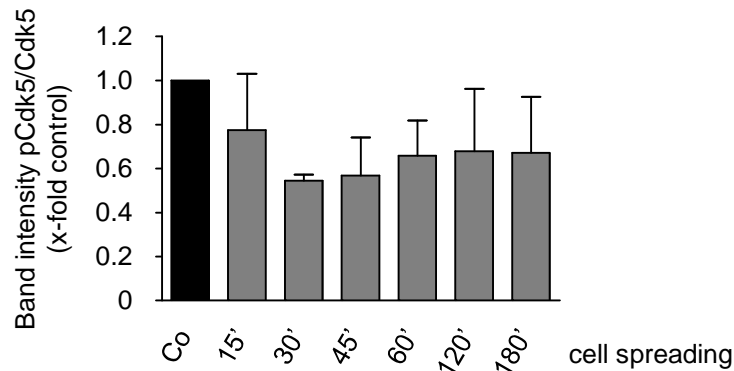


Figure 8 **Neither fyn nor c-abl inhibition affect endothelial cell migration.** Confluent layers of HUVECs were scratched and allowed to migrate for 16 h in the presence or absence of the respective concentration of the inhibitors. The columns indicate the relative area recovered by migrating cells. **A:** Effect of the fyn inhibitor SU6656 **B:** Effect of the c-abl inhibitor imatinib (**A** and **B:** n=3, mean ± SEM, $p > 0.05$, One Way ANOVA, Dunnett).

Phosphorylation of Cdk5 on tyrosine 15 might still be crucial for endothelial cell migration, because during endothelial cell migration other tyrosine kinases are activated which could also phosphorylate Cdk5. Nevertheless, in Western blots we found no increase of Cdk5 phosphorylation level during spreading in comparison to confluent control (Figure 9).

A



B

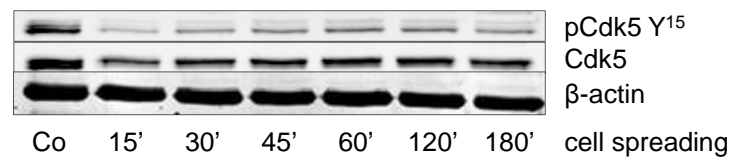


Figure 9 Cdk5 phosphorylation at tyrosine 15 is not increased during spreading. HUVECs were freshly seeded and allowed to spread for the indicated time periods or grown to confluency as control. Phospho-Cdk5 Y¹⁵ and Cdk5 amount were determined by Western blot. The ratio pCdk5/Cdk5, normalized to control (A) and one representative image (B) of three individual blots are shown. (n=3, mean \pm SEM, $p > 0.05$, One Way ANOVA, Dunnett).

Overexpression of a non-phosphorylatable Y15F-Cdk5 in endothelial cells did not lead to a decrease in migration as well (Figure 10). Therefore, Cdk5 tyrosine 15 phosphorylation does not seem to be crucial for endothelial cell migration.

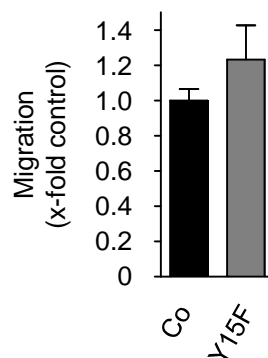


Figure 10 Overexpression of a non-phosphorylatable Cdk5 mutant does not affect endothelial cell migration. HUVECs were transfected with the Y15F-Cdk5-EGFP plasmid or the empty EGFP vector as a control. 24h after transfection, the cells were scratched and allowed to migrate for 16h (n=3, mean \pm SEM, $p > 0.05$, t-test). Transfection efficiency of at least 45% was determined by FACS analysis of GFP positive cells (data not shown).

3.1.3 p35 and p39 are not the central Cdk5 activators in endothelial cell migration

3.1.3.1 Neuronal Cdk5 activator p35 is expressed at a low level in endothelial cells

Cdk5, although in the beginning discovered in neurons, has now been described in various non-neuronal cell types, for example epithelial cells¹⁰⁰, endothelial cells¹⁰¹, podocytes⁵⁴, adipocytes⁵⁵, pancreatic β -cells⁷⁹, and several cancer cells^{56, 57, 102}. For p35, extraneuronal expression has also been reported.⁵⁴⁻⁵⁸

As p35 is described as the central regulator of Cdk5, we first determined whether p35 is present in endothelial cells and compared the amount of p35 mRNA in endothelial cells to that in human cortex tissue. The detected amount of p35 mRNA in endothelial cells was only about 0.3% of that in brain tissue. p35 protein is present in endothelial cells, but to a substantially lesser degree than in brain tissue (Figure 11).

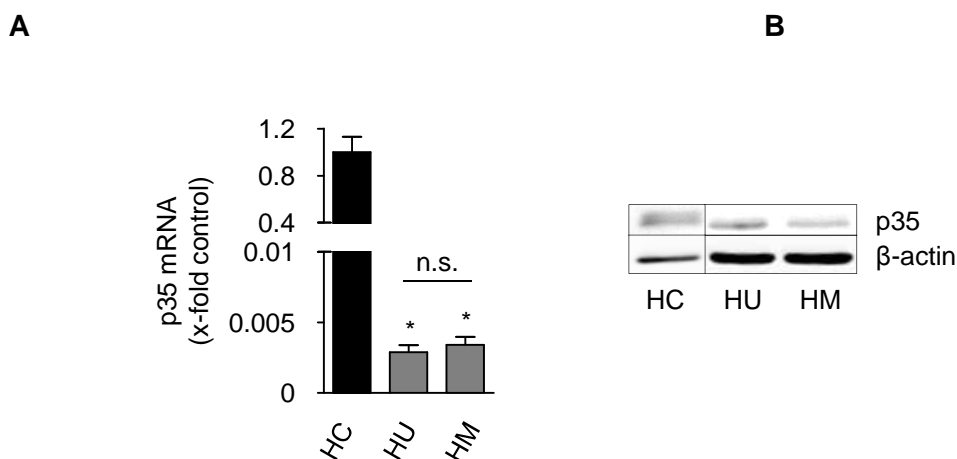


Figure 11 In endothelial cells, p35 is expressed at a very low level in comparison to brain tissue. **A:** mRNA from human cortex (HC), confluent HUVECs (HU) and HMEC-1 (HM) was isolated and the amount of p35 mRNA was determined by Real Time RT-PCR (n=3, mean \pm SEM, * p<0.05, One Way ANOVA, Dunnett). **B:** Western blot of p35 protein levels of human cortex and confluent HUVECs and HMEC-1. Note the much lower protein loading in the HC sample (n=1).

3.1.3.2 Cdk5 is translocated to the membrane during endothelial cell spreading

In neurons, Cdk5 is translocated to the membrane when coupled to its activator p35, which carries a myristoylation motif that anchors it to the plasma membrane.^{32, 44}

In endothelial cells, we found an increased amount of Cdk5 in the membrane fraction after 45 min cell spreading (Figure 12).

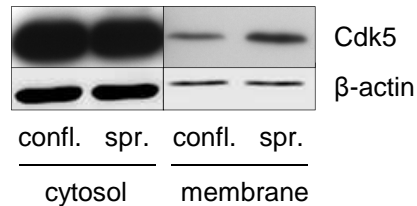


Figure 12 Cdk5 is translocated to the membrane during spreading. Confluent HUVECs or HUVECs which were allowed to spread for 45 min were lysed for membrane fractionation and the amount of Cdk5 in the cytosolic or membranous fraction was determined by Western blot. β -actin served as a loading control (confl. = confluent, spr. = 45 min spreading; n=3).

On the one hand p35 expression is very low in confluent endothelial cells; and on the other hand a translocation of Cdk5 to the membrane takes place during spreading, in a similar manner as described in neuronal cells, where this translocation is p35 dependent. This indicates that p35 expression might be increased during endothelial cell migration.

We found that p35 mRNA levels are elevated in spreading cells in comparison to confluent cells, with peaks at 45 and 240 minutes after plating. The Real time RT-PCR experiments shown in Figure 13 have been performed under my supervision by Suvi Heiskanen for her Master Thesis.

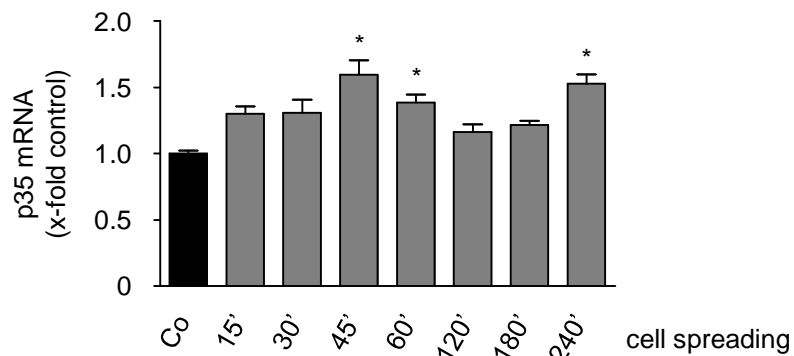


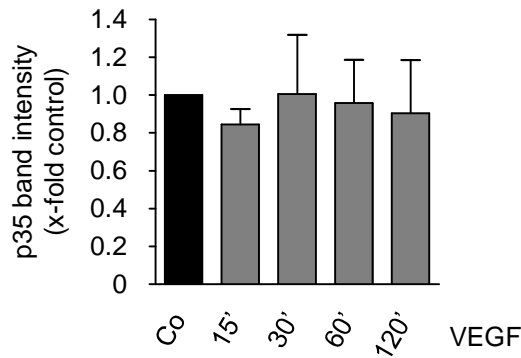
Figure 13 p35 mRNA expression is regulated in spreading cells, with peaks at 45 and 240 min. HUVECs were freshly seeded for the indicated time periods or as control grown to confluency. p35 mRNA amount was analyzed by Real-time RT-PCR (n=3, mean \pm SEM, * p<0.05, One Way ANOVA, Dunnett).

3.1.3.3 The pro-angiogenic factor VEGF does not affect p35 protein levels in endothelial cells

To further investigate the potential role of p35 in endothelial cell migration, we tested the influence of growth factor signaling on the level of p35. p35 expression has been

shown to be under the control of NGF signaling in neurons via an ERK/Egr1 pathway.⁴⁰ Treatment with VEGF did not lead to increased levels of p35 (Figure 14). Treatment with PDGF-B and bFGF did not augment p35 protein levels as well (data not shown).

A



B

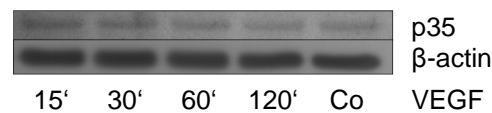


Figure 14 p35 protein level is not increased upon VEGF treatment. HUVECs were serum-starved for 4 h and subsequently treated with 50 ng/ml VEGF for the indicated time periods or left untreated as control. p35 protein amount was determined by Western blot. β -actin served as a loading control and for normalization of protein amount. Relative quantification and one representative image of three individual blots is shown ($n=3$, mean \pm SEM, $p>0.05$, One Way ANOVA, Dunnett).

3.1.3.4 p35 levels in endothelial cells are regulated by proteasomal degradation but not by calpain.

p35 protein level is known to be controlled by two degradation pathways: On the one hand, it can be degraded via the ubiquitin-proteasome pathway after autophosphorylation by p35/Cdk5 in a negative feedback loop.^{45, 103} On the other hand, p35 can be cleaved by calpain into p10 and the more stable Cdk5 activator p25, whose binding leads to a translocation of Cdk5 from the membrane to the cytosol.⁴⁸ We investigated therefore whether p35 levels in endothelial cells are influenced by proteasomal degradation or by calpain activity. Our hypothesis was that the degradation of p35 by the proteasome or calpain might be involved in Cdk5 activation and redistribution within the cell. Further, inhibiting the degradation of the unstable p35 protein might be useful for detection.

Treatment with the proteasome inhibitor MG132 led to an increase of p35 protein levels in HUVECs. Both antibodies used for Western blot are able to detect also the p35 cleavage product p25 besides p35. The two proteins can be distinguished by their molecular weight of 25 kDa or 35 kDa respectively. No 25 kDa band could be detected in control cells or after MG132 treatment, which should result in an increased cleavage of p35 via the calpain pathway, suggesting that p25 is not present in endothelial cells (Figure 15).

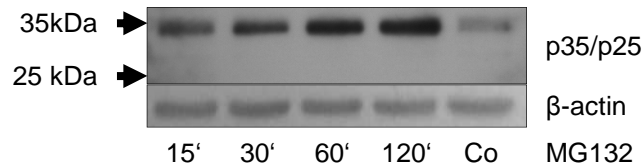
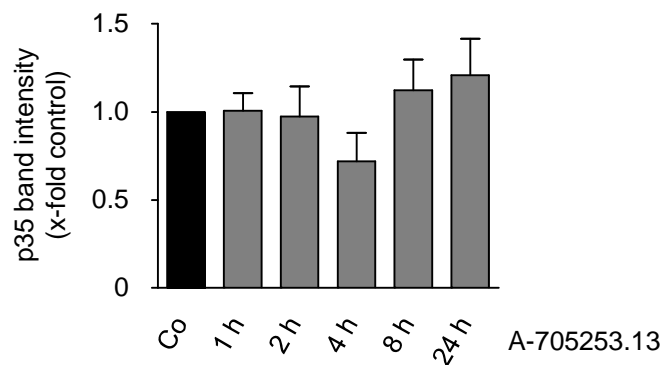


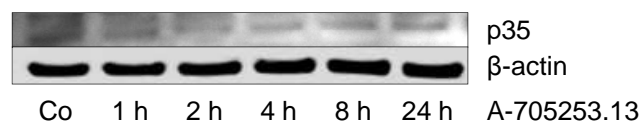
Figure 15 p35 protein level increases upon proteasome inhibition. HUVECs were treated with 10 μ M MG132 for the indicated time periods or left untreated as control. p35 protein amount was determined by Western blot. β -actin served as a loading control. p25 is not detectable (n=3).

In contrast to the effect of proteasome inhibition, treatment of HUVECs with the calpain inhibitor A-705253.13 did not lead to increased p35 protein levels and had no effect on endothelial cell migration (Figure 16).

A



B



C

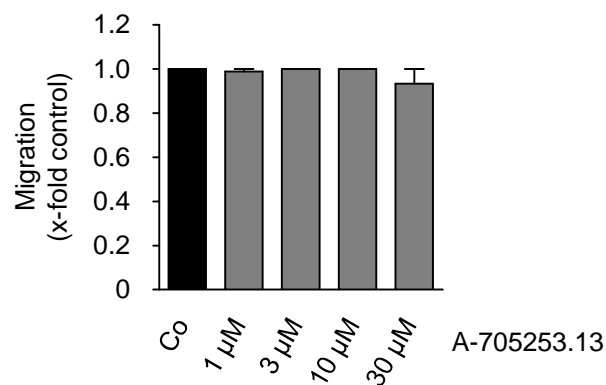


Figure 16 p35 protein levels and migration are not affected upon calpain inhibition in endothelial cells. **A, B:** HUVECs were treated with 10 μ M of the calpain inhibitor A-705253.13 for the indicated time periods or left untreated as control. p35 protein amount was determined by Western blot. β -actin served as a loading control and for normalization of protein amount. Relative quantification (**A**) and one representative image (**B**) of three individual blots are shown. **C:** Confluent layers of HUVECs were scratched and allowed to migrate for 16 h in the presence or absence of the respective concentration of the calpain inhibitor A-705253.13. The columns indicate the relative area re-covered by migrating cells (**A-C**: $n=3$, mean \pm SEM, $p>0.05$, One Way ANOVA, Dunnett).

3.1.3.5 siRNA-mediated downregulation of p35 does not influence endothelial cell migration

Although p35 does not seem to be involved in growth-factor induced signaling in the endothelium, the fact that it is regulated in spreading cells implicates a role in cytoskeletal rearrangement during endothelial cell migration. To finally elucidate the role of p35 in endothelial cell migration, p35 siRNA experiments were performed in HMEC-1. A concentration-dependent decrease in migration after Cdk5 inhibition with roscovitine was confirmed in the microvascular HMEC-1, comparable to the effect in HUVECs (Figure 17).

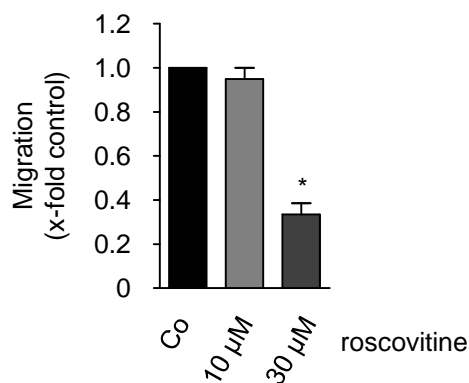


Figure 17 Cdk5 inhibition leads to decreased migration not only in HUVECs but also in HMEC-1. Confluent layers of HMEC-1 were scratched and allowed to migrate for 8-12 h in the presence or absence of the respective concentrations of (*R*)-roscovitine. The columns indicate the relative area re-covered by migrating cells (n=3, mean \pm SEM, * p<0.05, One Way ANOVA, Dunnett).

For the RNAi experiments, p35 downregulation was assured by Real Time RT-PCR. p35 downregulation with siRNA did not lead to a decrease of endothelial cell migration (Figure 18).

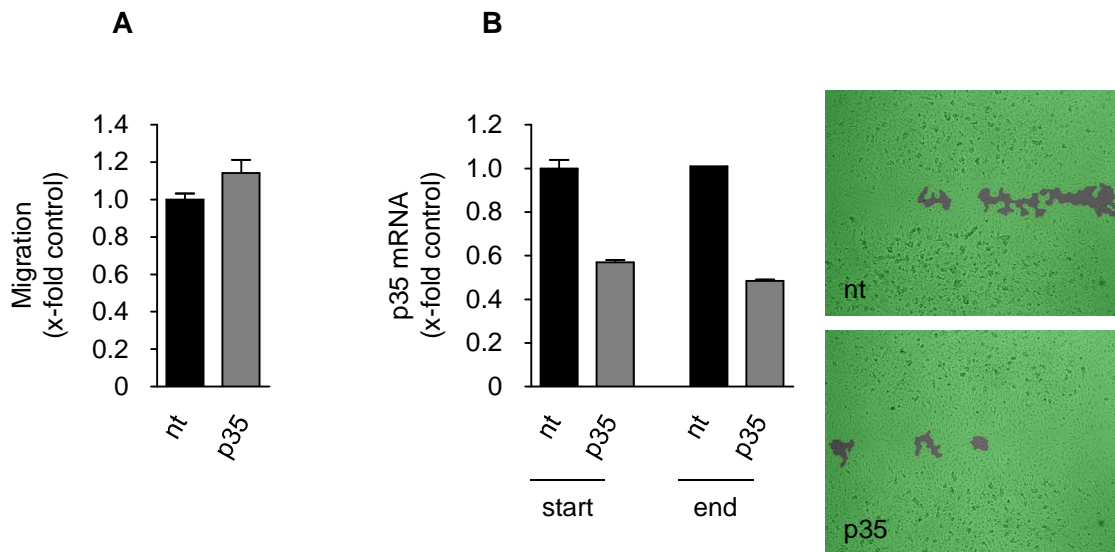


Figure 18 p35 RNAi knockdown does not affect migration of endothelial cells. HMEC-1 were transfected with p35 siRNA or non-targeting (nt) siRNA. 40h after transfection, the cells were scratched and allowed to migrate for 8-12h. Downregulation of p35 was assured by Real Time RT-PCR. **A:** The columns indicate the relative area re-covered by migrating cells. (n=3, mean \pm SEM, $p > 0.05$, t-test). **B:** Representative images of one scratch assay are shown with the corresponding downregulation control. p35 mRNA was reduced by 50-60% in the three experiments (single experiment data not shown).

On protein level, the silencing was visible only after treatment with the proteasome inhibitor MG132 (Figure 19), due to the short half life of p35.

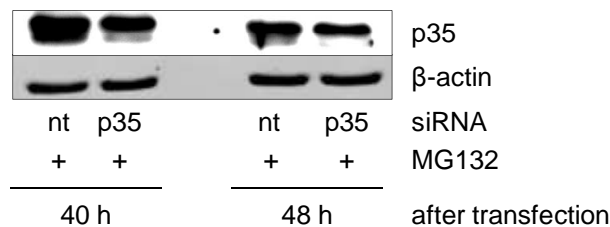


Figure 19 p35 downregulation can be detected on protein level after proteasome inhibition. HMEC-1 were transfected with p35 siRNA or non-targeting (nt) siRNA as a control and seeded. After 38 h or 46 h respectively, the cells were treated with 10 μ M of the proteasome inhibitor MG132 for two hours and then harvested (40 h or 48 h after transfection) for Western blot. β -actin served as a loading control (n=1).

As we could detect p39 in endothelial cells at a very low level (Figure 20), we hypothesized that p35 downregulation might be compensated by p39 upregulation which would mask an effect on migration.^{53, 98} Yet, no significant increase of p39 mRNA levels was found after downregulation of p35 (Figure 21). This demonstrates that p39 does not compensate p35 downregulation and is probably not crucial for endothelial cell migration.

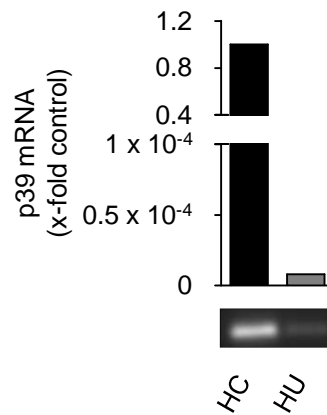


Figure 20 In endothelial cells, p39 mRNA is detectable but at an insignificant level in comparison to brain tissue. mRNA from human cortex (HC) and confluent HUVECs (HU) was isolated and the amount of p39 mRNA was determined by Real Time RT-PCR. *Lower panel:* Agarose gel bands of p39 RT-PCR product (n=1).

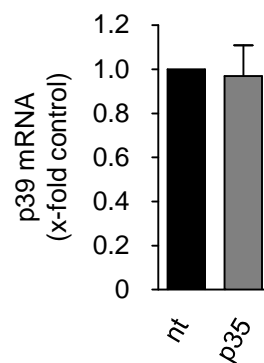


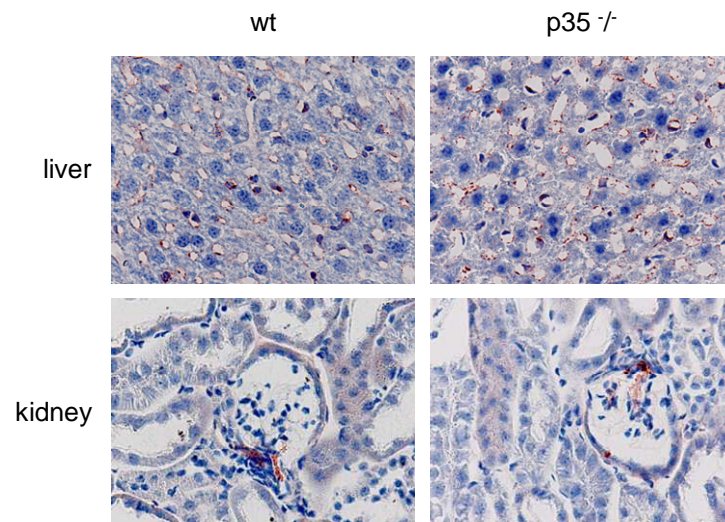
Figure 21 Downregulation of p35 does not lead to upregulation of p39. HMEC-1 were transfected with p35 siRNA or non-targeting (nt) siRNA as a control and harvested 40 h after transfection. The relative expression of p39 mRNA was determined by Real Time RT-PCR. p35 downregulation of 50-60% was assured in the p35 siRNA samples by Real Time RT-PCR (n=3, mean \pm SEM, $p > 0.05$, t-test).

3.1.3.6 p35 knockout mice do not show visible defects in their vascular phenotype

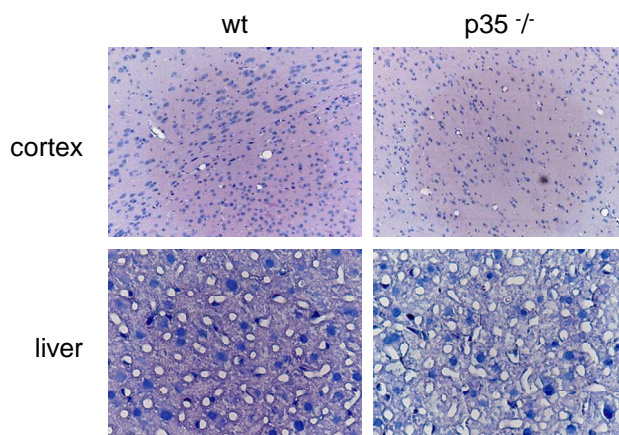
In order to finally clarify the role of p35 in endothelial cell migration and angiogenesis *in vivo*, we investigated the vascular phenotype of p35 deficient mice. p35 knockout mice are viable and show defects in the cortical layering similar to Cdk5 deficient mice.⁹⁸ To detect severe defects in vascular patterning in p35 k.o. mice, organ sections of brain, heart, lung, liver and kidney were stained for CD31 and analyzed. No obvious differences in vessel patterning were found between the wild type and p35 mice. Figure 22A displays representative images of liver and kidney sections. For quantitative

evaluation, the vessel density was determined for brain and liver sections. No significant difference in vessel density between wild type and p35 k.o. mice could be detected (Figure 22B and C). The experiments for Figure 22 were performed under my supervision by Tanja Tran for her Bachelor Thesis.

A



B



C

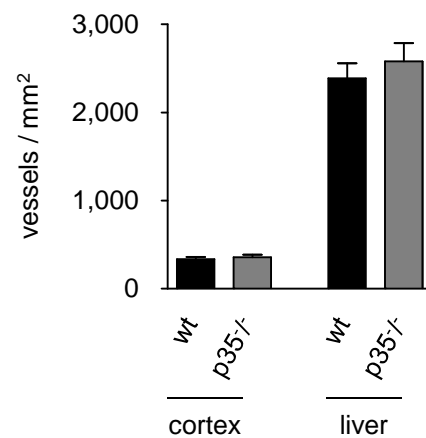


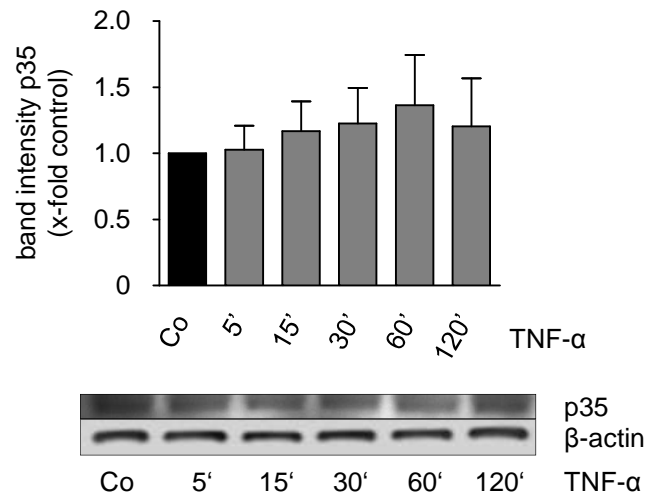
Figure 22 p35-deficient mice display a regular vascular phenotype. **A:** Representative images of liver and kidney of wild type and p35^{-/-} mice (40x magnification; red: CD31 staining; blue: nuclei). **B:** Representative images of the cortex and liver of wild type and p35^{-/-} mice (cortex: 10x magnification; liver: 40x magnification; HE staining). **C:** Vessel density of cortex and liver, determined in the HE-stained sections and expressed as vessels / mm² (wt: n=3, p35^{-/-}: n=4, mean ± SEM, p>0.05, t-test).

3.1.3.7 TNF does not affect p35 levels in endothelial cells

The previous results excluded p35 as the crucial regulator of Cdk5 in endothelial cell migration and angiogenesis. Recently, our group was able to show that Cdk5 inhibition targets the endothelium in a second central process: Cdk5 is responsible for the regulation of inflammation, where it is in control of TNF- α -induced expression of adhesion molecules in endothelial cells.⁷⁶ Therefore we hypothesized that p35 might not be central for Cdk5 regulation in endothelial cell migration but in inflammatory activated endothelial cells. For this reason we tested whether TNF- α treatment of endothelial cells leads to an increase of p35 expression, as it has been shown for PC12 cells and adipocytes.^{41, 42}

In HUVECs, TNF- α treatment for short and long periods did not cause a significant elevation of p35 protein levels (Figure 23).

A



B

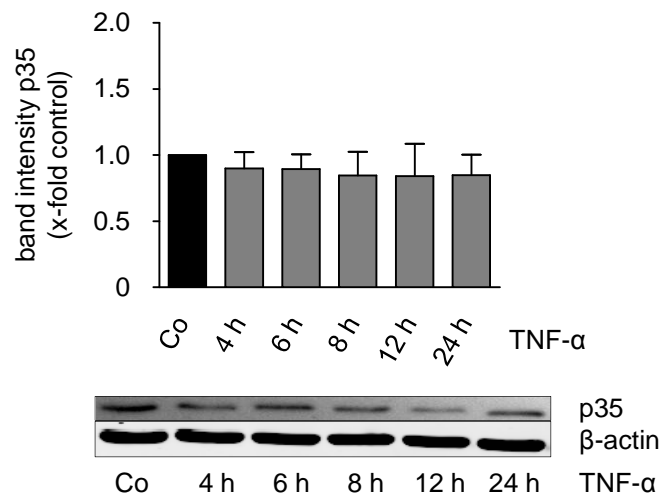


Figure 23 p35 protein levels are not significantly increased upon TNF- α treatment. HUVECs were treated with 10 ng/ml TNF- α for the indicated time periods or left untreated as control. p35 protein amount was determined by Western blot. β -actin served as a loading control and for normalization of protein amount. Relative quantification and representative image of at least three individual blots is shown (A and B: $n \geq 3$, mean \pm SEM, $p > 0.05$, One Way ANOVA, Dunnett).

3.1.4 Cdk5 kinase activity in endothelial cells

Inhibition of Cdk5 kinase activity both by roscovitine and overexpression of a dominant negative kinase dead D144N-Cdk5 mutant decreases endothelial cell migration, as well as Cdk5 downregulation by siRNA.⁷⁵ These findings point to a crucial role of Cdk5 activity during endothelial cell migration. In order to measure Cdk5 activity, we set up a

kinase assay according to the following procedural method: Immunoprecipitation of Cdk5 (or p35) – kinase reaction with [γ - 32 P]-ATP and Histone H1 as a substrate – SDS-PAGE and autoradiography, as previously described in different variations.¹⁰⁴

3.1.4.1 Cdk5 immunoprecipitation

Cdk5 was precipitated as described in the Materials and Methods section, using a Cdk5 mouse monoclonal antibody (Invitrogen, Carlsbad, CA, USA), *Kinase assay lysis buffer 1* and *Kinase buffer 1*. To assure Cdk5-specific activity, 10 μ M roscovitine were added to one probe as negative control. Successful immunoprecipitation was verified by Western blot.

In this setting, only a weak signal was obtained, and the negative control did not consistently differ from the samples (Figure 24).

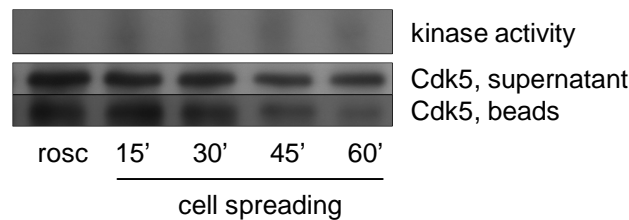


Figure 24 Kinase Assay after Cdk5 immunoprecipitation. HUVECs were freshly seeded, allowed to spread for the indicated time periods, and lysed in *Kinase assay lysis buffer 1*. Cdk5 activity was assayed after Cdk5 immunoprecipitation in *Kinase buffer 1*. 10 μ M roscovitine were added to one assay reaction as negative control. Western blot for Cdk5 served as immunoprecipitation control (n=3).

3.1.4.2 p35 immunoprecipitation

In order to obtain a higher amount of active kinase, we changed the protocol to immunoprecipitation of the putative activator p35, as we had not yet fully excluded p35 for Cdk5 activation in endothelial cell migration.

The lysis conditions were altered to avoid disruption of the Cdk5/p35 complex: detergent-free *Homogenization buffer* and sonication were used for the lysis, and the kinase reaction was carried out in *Kinase buffer 2* according to the protocol of S. Bach (Station Biologique, Roscoff, Bretagne, France, personal communication). The amount of roscovitine was increased in order to assure complete inhibition (Figure 25).

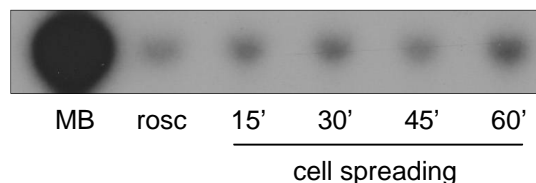


Figure 25 Kinase Assay after p35 immunoprecipitation. HUVECs were freshly seeded, allowed to spread for the indicated time periods, and lysed in *Homogenization buffer*. Cdk5 activity was assayed after p35 immunoprecipitation in *Kinase buffer 2*. p35 immunoprecipitation from mouse brain tissue lysate served as positive control. 100 μ M roscovitine were added to one assay reaction as negative control. (n=4).

The positive control from brain consistently displayed a very strong signal. This confirms the functioning of the assay. For the endothelial cell samples, the signal was consistently similar to the negative control. Densitometric quantification of the signals with the roscovitine control as zero point showed no significant differences and resulted partly in negative values (data not shown).

In order to rule out that the weak signal in endothelial cells was due to unspecific binding, we compared immunoprecipitations with p35, Cdk5, irrelevant rabbit polyclonal IgG and beads only from endothelial cells. The autoradiography (Figure 26) showed no difference in the signal.

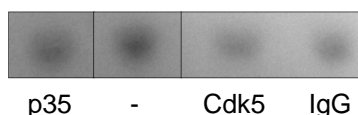


Figure 26 Kinase activity after IP. HUVECs were freshly seeded, allowed to spread for 15 min, and then lysed in *Homogenization buffer*. Cdk5 activity was assayed after p35 (p35) or Cdk5 (Cdk5) immunoprecipitation or mock IP with irrelevant IgG (IgG) or no IgG (-) in *Kinase buffer 2*. (n=1).

3.1.4.3 Cdk5 overexpression

According to our previous findings, we concluded that Cdk5 activity in endothelial cells is present, but probably very weak. In order to increase the Cdk5 amount and activity, we overexpressed Cdk5 in endothelial cells. To reduce unspecific binding, we used a HA-tagged Cdk5 together with the Pierce ProFound™ Mammalian HA-tag IP/Co-IP kit, where the anti-HA antibody is directly coupled to the beads without Protein A or G.

The kinase assay was carried out in *Kinase Buffer 3* directly on the beads. A comparable approach is used in Brinkkoetter et al.⁵⁹ Overexpression of Cdk5-HA and equal loading was assured by Western blot of the supernatants for Cdk5 and β -actin, respectively. In order to check if a “dilution effect” in the activator/Cdk5 ratio caused by

Cdk5 overexpression would decrease the signal, we also co-transfected Cdk5-HA with p35-myc. Cells transfected with the empty vector were used as negative control. Overexpression of Cdk5-HA did not lead to a stronger signal in comparison to negative control (empty vector). p35-myc co-expression with Cdk5-HA did also not result in an increased signal (Figure 27).

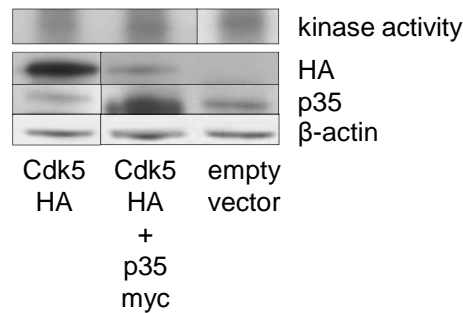


Figure 27 Kinase activity after Cdk5-HA overexpression and HA immunoprecipitation. HUVECs were transfected with Cdk5-HA only, Cdk5-HA and p35-myc or empty vector as control. Kinase activity was assayed after immunoprecipitation with the ProFound™ Mammalian HA-tag IP/Co-IP kit in *Kinase Buffer 3*. Overexpression of plasmids and equal loading was confirmed in the supernatant by Western blot for HA-tag, p35 and β-actin. (Cdk5-HA overexpression: n≥3, Cdk5-HA/p35-myc co-transfection: n=1)

3.1.4.4 Evaluation of different Cdk5 antibodies with recombinant Cdk5/p35

To finally exclude that the IP procedure and the buffers would interfere with Cdk5 activity, we first tested the used buffers with an active recombinant Cdk5/p35 complex (Millipore, Billerica, MA, USA). An additional set of a lysis and a kinase buffer was also tested, which had been used for Cdk5 kinase assay in endothelial cells by Cho *et al.*¹⁰⁵ (data not shown). *Kinase assay lysis buffer 1* and *Kinase buffer 3* were chosen for the evaluation of antibodies.

We compared the previously used mouse monoclonal Cdk5 antibody with a rabbit polyclonal Cdk5 (C-8) and a mouse monoclonal Cdk5 (J-3) antibody (both from Santa Cruz Biotechnology, Santa Cruz, CA, USA). IP with beads only served as a negative control. As a positive control, 20 ng of active recombinant Cdk5/p35 were added to one lysate before the IP. All antibodies were able to immunoprecipitate the recombinant Cdk5 activity. However no difference between Cdk5 immunoprecipitation (IP) and unspecific IP was detected in the endothelial cell lysates (Figure 28).

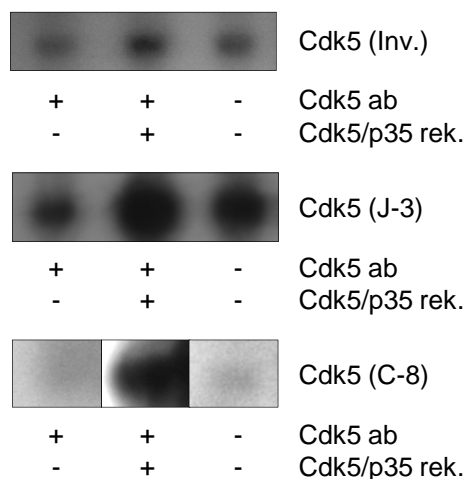


Figure 28 Evaluation of Cdk5 antibodies for Cdk5 kinase assay. For Cdk5 (Inv.) and Cdk5 (J-3) HMEC-1 lysates, and for Cdk5 (C-8), HUVEC lysates obtained with *Kinase assay lysis buffer 1* were used for immunoprecipitations with or without active recombinant Cdk5/p35 added as indicated in the figure legend. Immunoprecipitation without IgG served as negative control. Kinase activity was assayed in *Kinase buffer 3*. (n=1).

3.1.5 A proteomics approach to reveal novel Cdk5 interacting proteins

According to the experimental data up to now, Cdk5 regulation in endothelial cells seems to differ from the “canonical” pathway with p35 and p39 as central activators. For detection of significant levels of Cdk5 kinase activity, it is important to identify the endothelial specific activator(s), as immunoprecipitation of activators leads to increased Cdk5 kinase activity in the assay.

In order to find novel Cdk5 interacting proteins, we used immunoprecipitation of Cdk5 and a proteomics approach after separation of the samples in SDS-PAGE gels. For this experiment, we compared confluent and 45 min spreading HMEC-1 as well as starved and FCS treated HMEC-1. Figure 29 shows the Coomassie stained SDS-PAGE gel after Cdk5 immunoprecipitation. Cdk5 is clearly precipitated as a band at 33 kDa is visible in the precipitation samples in comparison to IgG IP. The bands marked in Figure 29B and C appear to be regulated upon spreading or stimulation with FCS.

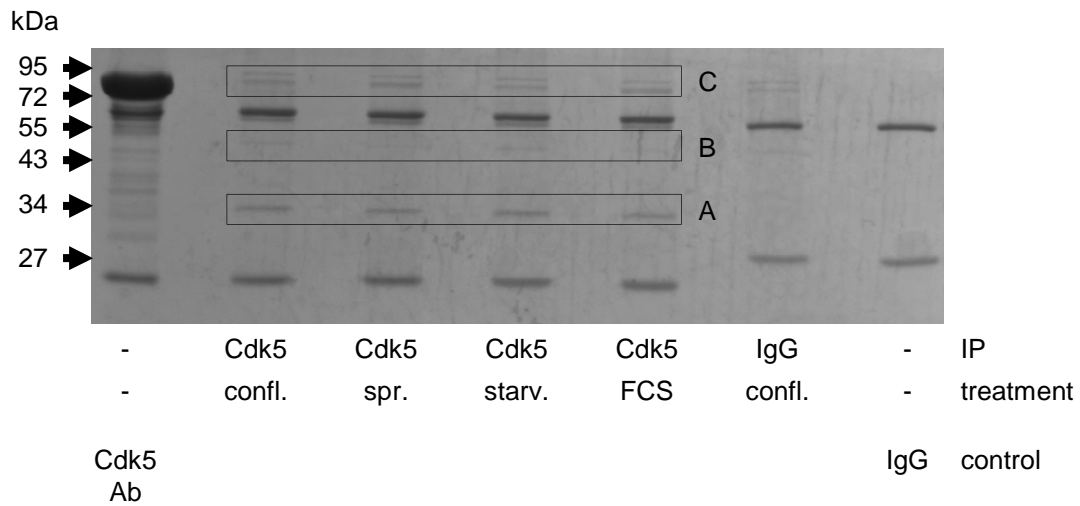


Figure 29 Coomassie stained SDS-PAGE gel after CDK5 immunoprecipitation. **A:** In comparison to negative control IP (IgG/confl., lane 6), precipitated Cdk5 is present as a 33kDa band. **B:** At 40-50 kDa, a weak negatively regulated band can be seen. **C:** At about 75 kDa a pair of bands is visible, positively regulated during spreading or FCS stimulation.

Bands A, B and C were kindly analyzed by G. Maccarrone in the laboratory of C. Turck (Max Planck Institute of Psychiatry, Munich). The results are displayed on the next page in Table 26.

Table 26 Proteins co-immunoprecipitated with Cdk5 and identified by LC-ESI-MS/MS.

Band	UniProt	Protein name	Mascot Score	M _r (Da)	No. of peptide matches	Sequence coverage (%)
A	CDK1_HUMAN	Cell division protein kinase 1	1175	34131	42	61.6
	CDK5_HUMAN	Cell division protein kinase 5	586	33739	25	38.4
	CDK2_HUMAN	Cell division protein kinase 2	245	34079	14	30.2
	GBLP_HUMAN	Guanine nucleotide-binding protein subunit beta-2-like 1	177	35511	6	11
B	ACTB_HUMAN	Actin, cytoplasmic 1	1057	42052	56	38.4
	POTEE_HUMAN	POTE ankyrin domain family member E	266	122882	17	6.7
C, upper	GRP78_HUMAN	78 kDa glucose-regulated protein	1371	72402	61	44.8
	DLG4_HUMAN	Disks large homolog 4	708	80788	36	24.6
	LMNA_HUMAN	Lamin-A/C OS=Homo sapiens	404	74380	12	17.8
C, lower	HSP7C_HUMAN	Heat shock cognate 71 kDa protein	1448	71082	57	43.8
	HSP71_HUMAN	Heat shock 70 kDa protein 1	789	70294	30	30.1
	GRP75_HUMAN	Stress-70 protein, mitochondrial	608	73920	25	32.7
	HSP72_HUMAN	Heat shock-related 70 kDa protein 2	584	70263	22	20
	HS71L_HUMAN	Heat shock 70 kDa protein 1L	480	70730	17	18.4
	DLG4_HUMAN	Disks large homolog 4	418	80788	11	17.7
DESP_HUMAN	Desmoplakin	395	334021	22	6.2	
HSP76_HUMAN	Heat shock 70 kDa protein 6	314	71440	14	15.1	

3.2 Novel Cdk inhibitors with increased Cdk5 selectivity show anti-angiogenic effects *in vitro* and *in vivo*

We identified Cdk5 as a novel target in endothelial cell migration and angiogenesis using roscovitine as a molecular tool. Roscovitine does however not only inhibit Cdk5 but also Cdk2, further Cdk1, Cdk7 and Cdk9.^{106, 107} Therefore, we tested novel roscovitine derivatives in order to identify highly potent anti-angiogenic Cdk inhibitors with an increased selectivity for Cdk5. The compounds LGR 1404, LGR 1406, LGR 1407, LGR 1492, LGR 1667, LGR 1695 and LGR 1730 were kindly provided by V. Krystof and R. Jorda (Palacký University & Institute of Experimental Botany, Olomouc, Czech Republic). For the chemical structures see the Materials and Methods section (Figure 5).

3.2.1 The LGR compounds do not show acute toxicity on endothelial cells

To rule out potential toxic effects, the impact of the novel Cdk inhibitors on cell viability was tested. No lower cell viability was found for 10 μ M of each of the inhibitors in comparison to control. By contrast, 30 μ M of LGR 1404, 1406, 1407, 1492, 1695 and 1730 displayed a weak but significant decrease of viability. Therefore, in the functional assays, the effects at 10 μ M were used as selection criterion (Figure 30).

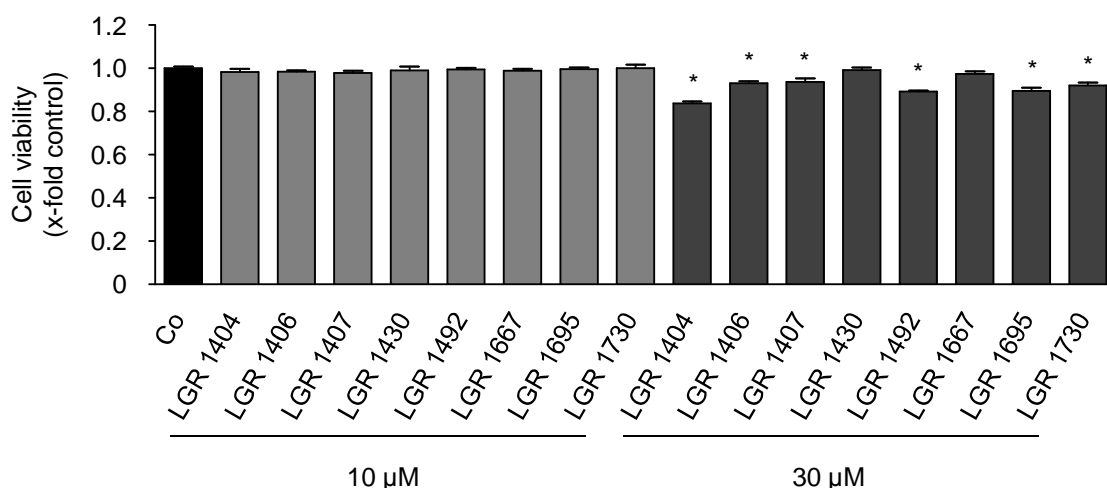


Figure 30 The tested LGR compounds do not affect cell viability of endothelial cells in the concentration range used in the functional assays. Confluent HUVECs were treated for 16 h with the indicated compounds or left untreated as control. Cell viability was determined in CellTiter-Blue™ assays (n=3, mean \pm SEM, * p<0.05, One Way ANOVA, Dunnett).

3.2.2 The LGR compounds inhibit endothelial cell proliferation

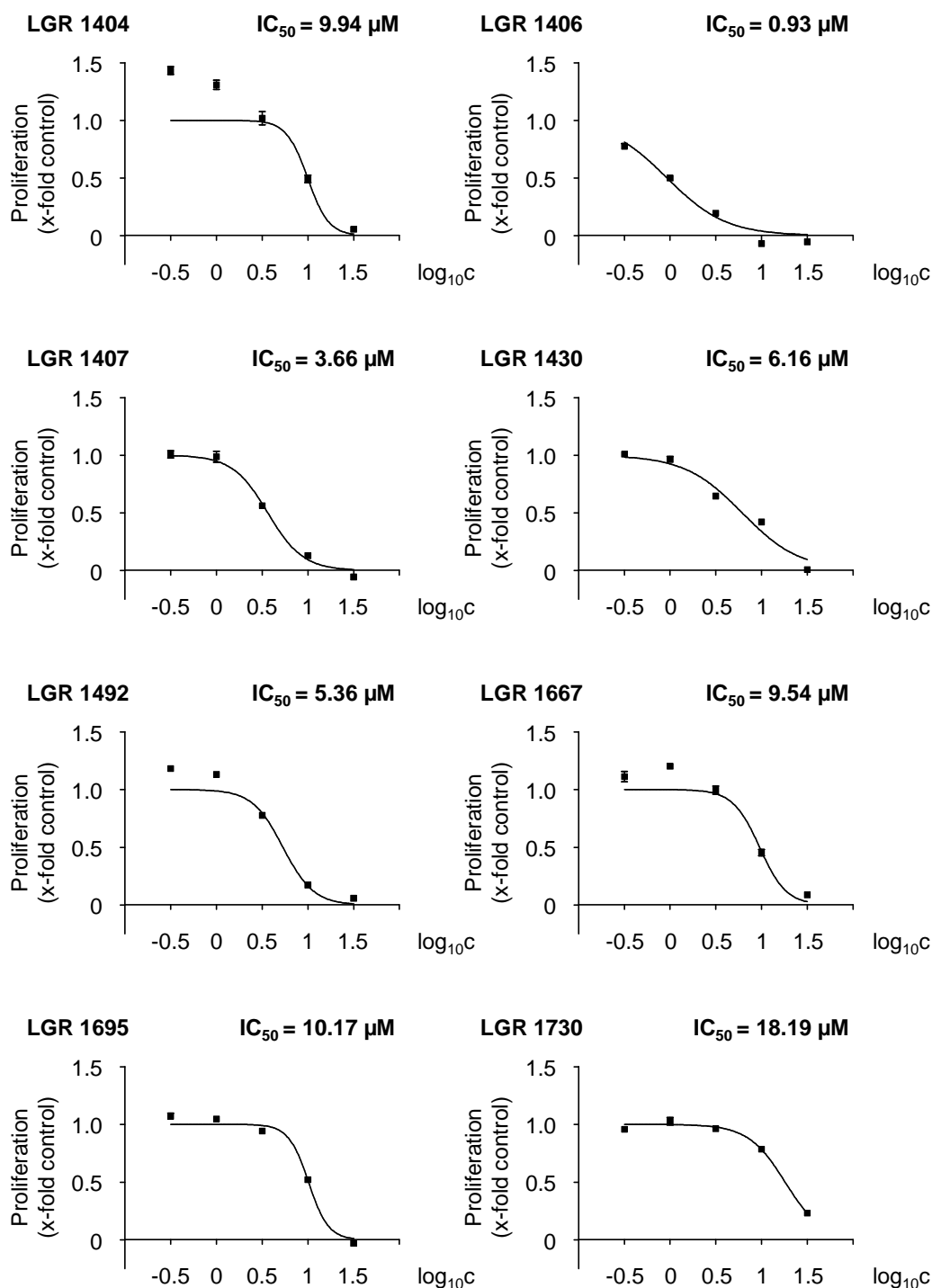


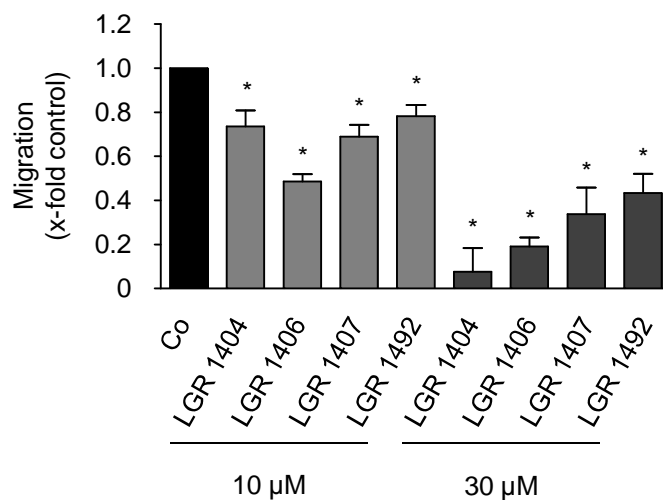
Figure 31 The LGR compounds concentration-dependently inhibit endothelial cell proliferation. HMEC-1 were left untreated as control or treated with 0.3-1-3-10-30 μM of the indicated LGR Cdk inhibitors. After 72 h, cell proliferation was determined by crystal violet staining ($n=3$, mean \pm SEM, IC_{50} values calculated with Graph Pad Prism).

As a first screening step, the novel inhibitors were tested in crystal violet proliferation assays with HMEC-1 (Figure 31). All eight compounds concentration-dependently showed an impact on endothelial cell proliferation, with an IC_{50} between approximately 1 μ M (LGR 1406) and 20 μ M (LGR 1730).

3.2.3 LGR 1404, 1406, 1407 and 1492 significantly reduce endothelial cell migration at a concentration of 10 μ M

Endothelial cell migration is the subsequent crucial step in angiogenesis after the activation of the quiescent endothelial cells to proliferate. All eight LGR compounds were tested for their effect on migration at 10 μ M and 30 μ M. LGR 1404, 1406, 1407 and 1492 were able to significantly decrease endothelial cell migration at 10 μ M. Treatment with 10 μ M of the most potent substances, LGR 1406 and 1407, reduced migration by 51 % and 31 %, respectively (Figure 32).

A



B

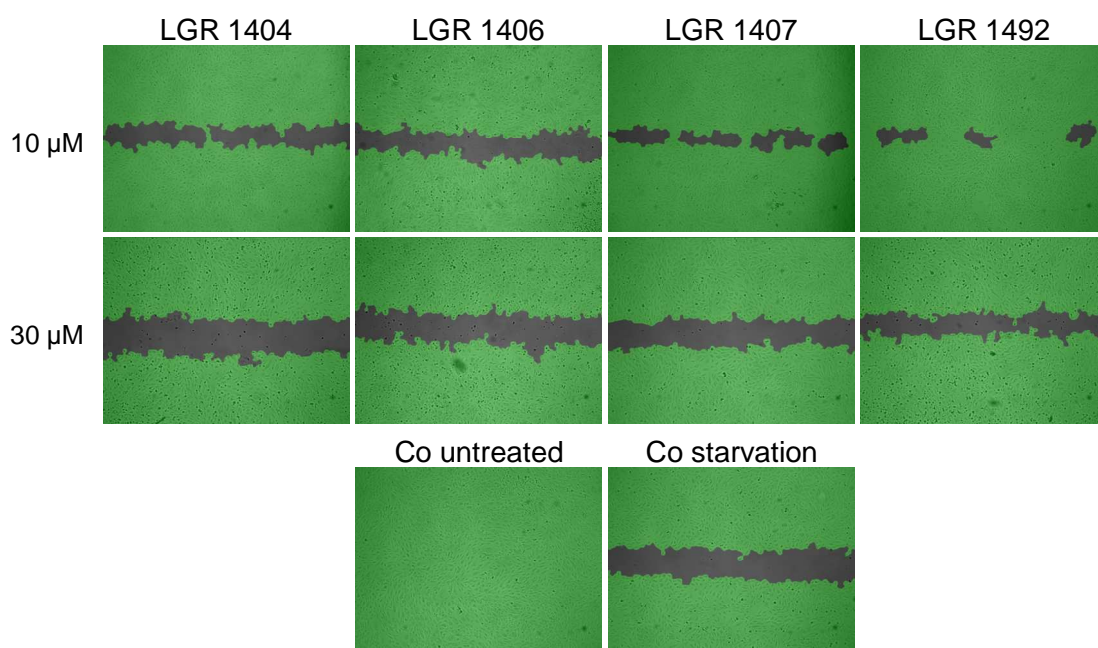
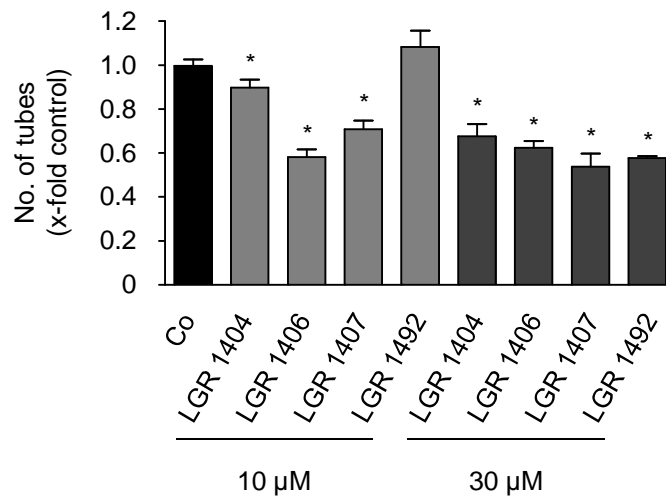


Figure 32 The four compounds LGR 1404, 1406, 1407 and 1492 significantly reduce endothelial cell migration at 10 µM. Confluent layers of HUVECs were scratched and the cells were allowed to migrate for 16 h in the presence or absence of the respective concentration of the compounds. **A:** The columns indicate the area re-covered by migrating cells. (n=3, mean ± SEM, * p<0.05, One Way ANOVA, Dunnett). **B:** Scratches at endpoint, representative images taken out of three experiments.

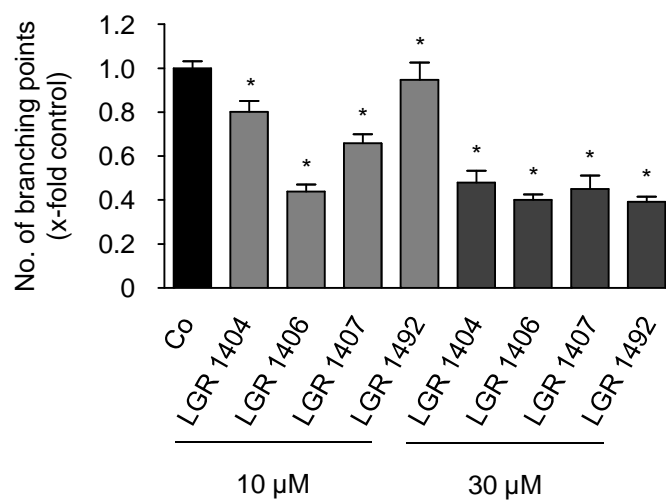
3.2.4 LGR 1404, 1406, 1407 and 1492 concentration-dependently inhibit tube formation

The most powerful compounds from the migration experiments, LGR 1404, 1406, 1407 and 1492 were chosen for tube formation assays. 10 μ M of LGR 1404, 1406 and 1407 showed a significant reduction of tube and branching point numbers as well as of total tube length. LGR 1406 and 1407 again showed the strongest effects. 10 μ M of LGR 1406 decreased tube length and number of branching points by 56 %, and the tube number by 42 %. Treatment with 10 μ M of LGR 1407 resulted in an about 30 % reduction of tube number and total tube length; and to a 35 % reduction in the number of branching points (Figure 33).

A



B



C

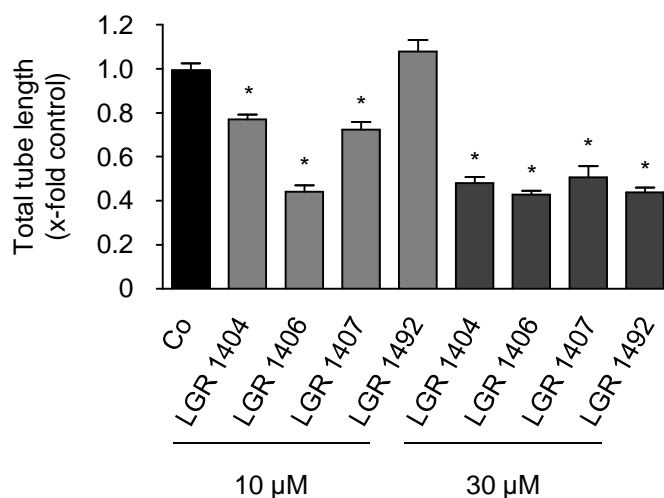


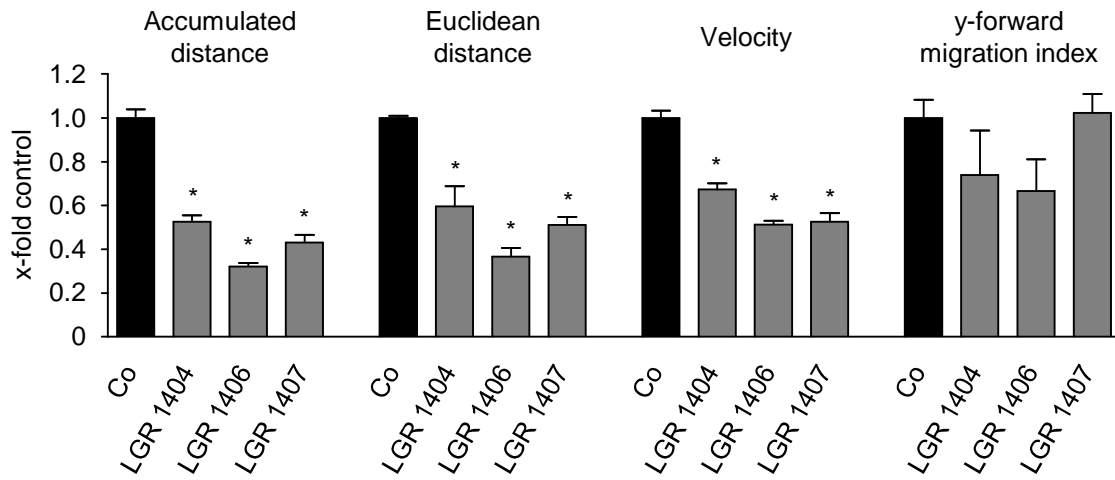
Figure 33 LGR 1404, 1406, 1407 and 1492 concentration-dependently inhibit tube formation. HUVECs were seeded onto a matrix of growth-factor reduced Matrigel™ in the presence or absence of the compounds in the respective concentration. After 16h, images were taken and tube characteristics were quantified. **A:** Number of tubes **B:** Number of branching points **C:** Tube total length (**A, B, C:** n=3, mean ± SEM, * p<0.05, One Way ANOVA, Dunnett).

3.2.5 Overall motility of HUVECs in a chemotactic gradient is affected by LGR 1404, 1406 and 1407

LGR 1404, 1406 and 1407 inhibit endothelial cell migration and also tube formation, where cytoskeletal rearrangement and migration-like processes take place as well.

In order to study the impact of LGR 1404, 1406 and 1407 on migration in more detail, chemotaxis experiments in an FCS gradient were performed with HUVECs in the presence of 10 µM of the respective compound. Cell paths were analyzed for accumulative and Euclidean distance, velocity and y-forward migration index. Accumulative distance maps the complete distance a cell migrates, whereas the Euclidean distance represents the linear distance between starting and end point of migration. The y-forward migration index describes the orientation in the chemotactic gradient. All three compounds led to a decrease in accumulative distance and velocity, which are indicators for general cell motility. Orientation did not seem to be clearly affected, as the y-forward migration index was not significantly reduced. However, the Euclidean distance, as a second indicator for orientation, was decreased (Figure 34).

A



B

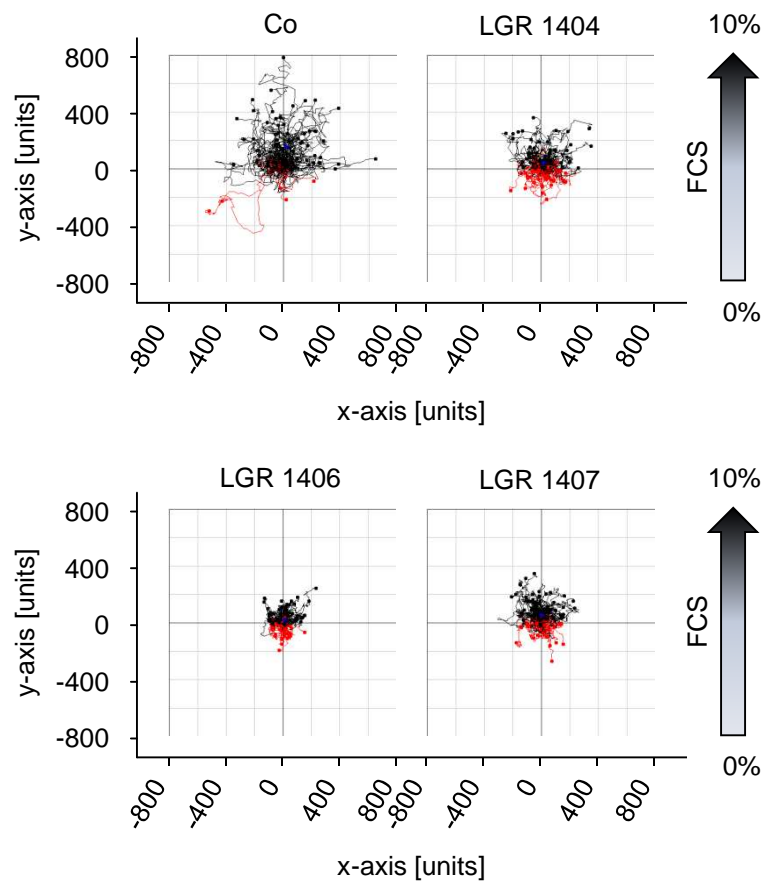


Figure 34 LGR 1404, 1406 and 1407 decrease chemotaxis of endothelial cells. Chemotaxis of HUVECs in the presence or absence of 10 μ M of the indicated compounds was determined in μ -slides Chemotaxis. **A:** Quantitative evaluation of accumulated and Euclidean distance, velocity and y-forward migration index (n=3, mean \pm SEM, * p<0.05, One Way ANOVA, Dunnett). **B:** Representative cell tracking plots of untreated and LGR treated cells.

3.2.6 LGR 1404, 1406 and 1407 completely inhibit vessel formation in the CAM assay

The anti-angiogenic potency of the three most effective compounds has been evaluated *in vitro* so far. In order to substantiate these findings, chorioallantoic membrane (CAM) assays were performed with LGR 1404, 1406 and 1407, where they completely abolished VEGF-induced vessel formation (Figure 35).

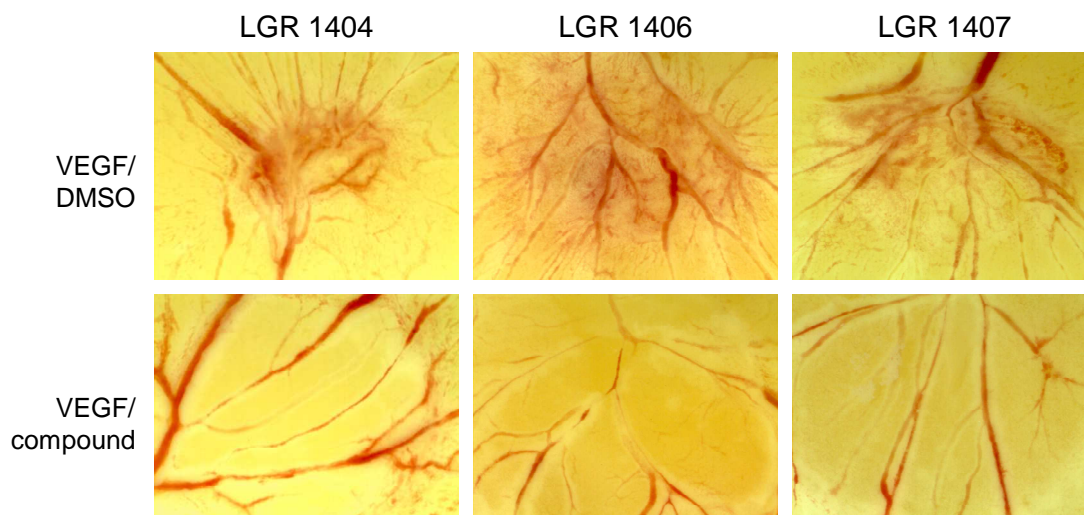


Figure 35 LGR 1404, 1406 and 1407 completely inhibit VEGF-induced vessel formation in the CAM assay. Cellulose discs with 2.5 ng VEGF / 250 nmol compound or 2.5 ng VEGF / DMSO as control were placed on the membrane for 24 h. Representative images of the stimulated areas of at least three independent experiments are shown.

3.2.7 Kinase profile of LGR 1406 and 1407 shows preferential inhibition of Cdk5 and Cdk2

We found that LGR 1406 and 1407 were the most potent compounds in the *in vitro* assays. Therefore it was of interest to see which kinases, especially Cdks, are inhibited by those compounds. The kinase profiling was performed by ProQinase (Freiburg, Germany). For LGR 1404, synthesis, kinase profiling and biological effects on cancer cells have recently been published.¹⁰⁸

LGR 1406 and 1407 were tested for their IC_{50} in a panel of 24 kinases, including the Cdk/Cyclin complexes Cdk1/Cyclin B, Cdk2/Cyclin A, Cdk2/Cyclin E, Cdk4/Cyclin D1, Cdk5/p25NCK, CDK6/Cyclin D1, CDK7/Cyclin H/MAT1 and Cdk9/Cyclin T. The other kinases tested were

- PTK6 (Protein tyrosine kinase 6, also known as breast tumor kinase, BRK)
- EGFR (Epidermal growth factor receptor)

- FAK (Focal adhesion kinase)
- FGFR1 and FGFR2 (Fibroblast growth factor receptor 1 and 2)
- NLK (Nemo-like kinase)
- PAK4 (p21 protein (Cdc42/Rac)-activated kinase 4)
- VEGFR1 and VEGFR2 (Vascular endothelial growth factor receptor 1 and 2)
- MEK1 (Mitogen-activated protein kinase kinase 1, MAP2K1)
- ROCK1 (Rho-associated, coiled-coil containing protein kinase 1)
- RAF1 (v-raf-1 murine leukemia viral oncogene homolog 1),
- ALK (Anaplastic lymphoma receptor tyrosine kinase)
- RSK3 (Ribosomal protein S6 kinase, 90kDa, polypeptide 2, RPS6KA2)
- AURKA (Aurora kinase A)
- AMPK α 1 (protein kinase, AMP-activated, alpha 1 catalytic subunit, PRKAA1)

The IC₅₀ [M] of LGR 1406 and LGR 1407 for the Cdk/Cyclin complexes are shown in Table 27.

Table 27 Cdk profile of the two most potent substances LGR 1406 and 1407. Both compounds show increased selectivity for Cdk2 and Cdk5.

	Cdk1/ CycB	Cdk2/ CycA	Cdk2/ CycE	Cdk4/ CycD1	Cdk5/ p25	Cdk6/ CycD1	Cdk7/ CycH/ MAT1	Cdk9/ CycT
LGR 1406	3,2 ·10 ⁻⁶	9,9 ·10 ⁻⁷	5,9 ·10 ⁻⁷	1,5 ·10 ⁻⁵	4,4 ·10 ⁻⁷	>10 ⁻⁴	> 10 ⁻⁴	1,0 ·10 ⁻⁶
LGR 1407	5,8 ·10 ⁻⁶	1,5 ·10 ⁻⁶	9,9 ·10 ⁻⁷	6,6 ·10 ⁻⁵	1,6 ·10 ⁻⁶	9,1 ·10 ⁻⁵	> 10 ⁻⁴	1,9 ·10 ⁻⁶

< 10⁻⁷  > 10⁻⁴ [M]

Both compounds inhibit mainly Cdk2 and Cdk5, and to some extent Cdk9 and Cdk1. Concerning the other tested kinases, FAK, PAK4, RSK3 and Aurora kinase A are inhibited by LGR 1406 with an IC₅₀ below 1 x 10⁻⁵ M. LGR 1407 only inhibits Aurora kinase A (IC₅₀ ≤ 1 x 10⁻⁵ M) in addition to the Cdks displayed in Table 27.

3.2.8 LGR 1404, 1406 and 1407 reduce lamellipodia formation and Rac1 localization to lamellipodia, indicating a Cdk5-dependent mode of action

In order to gain insight into the anti-angiogenic action of the three most potent LGR, we analyzed their effect on the lamellipodia formation in migrating endothelial cells. It is known that Cdk5 inhibition leads to impaired endothelial cell migration via a downstream inactivation of Rac1 and resulting in decreased Rac1 localization to the leading edge and breakdown of lamellipodia.⁷⁵

LGR 1404, 1406 and 1407 significantly diminished the formation of lamellipodia by 54 % (LGR 1404) to 67 % (LGR 1406) at 10 μ M. This can be seen in the corresponding images stained for f-actin. The strong decrease in lamellipodia formation was a first indication for a Cdk5-dependent mode of action (Figure 36).

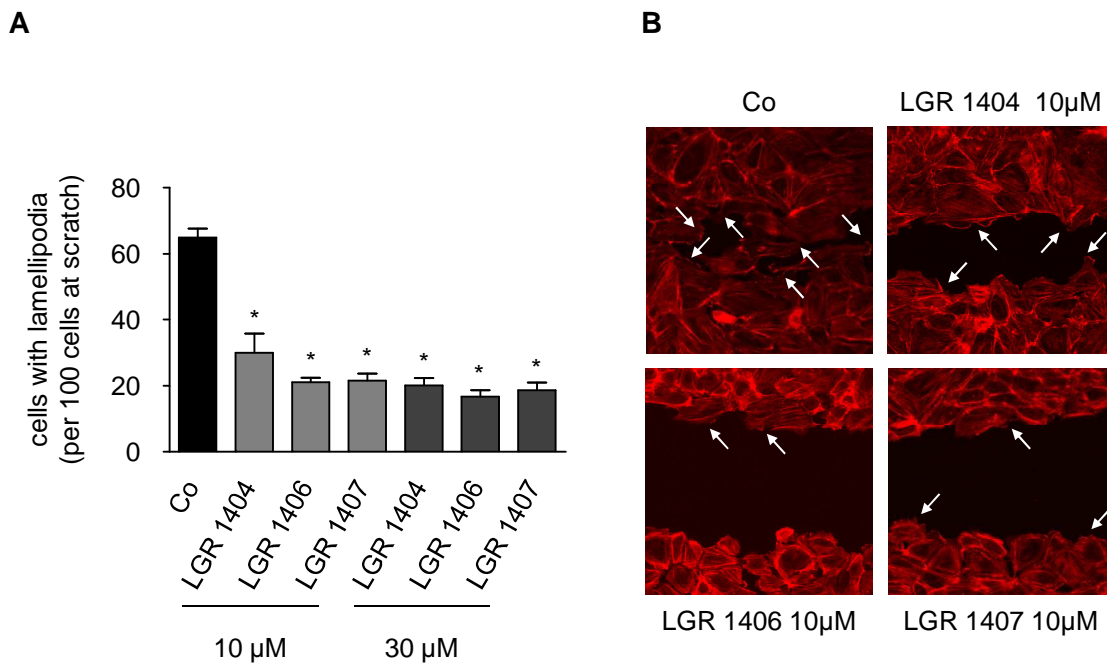


Figure 36 LGR 1404, 1406 and 1407 significantly decreased lamellipodia formation in migrating endothelial cells. Confluent HUVECs were scratched and allowed to migrate in the presence of 10 μ M or 30 μ M of the respective compounds for 8 h. The cells were fixed, stained for f-actin and the cells with prominent lamellipodia were counted at the scratch front from 10x magnification fluorescence images. **A**: The graph shows the number of cells with prominent lamellipodia per 100 cells at scratch front (n=3, mean \pm SEM, * p<0.05, One Way ANOVA, Dunnett). **B**: Representative images of the scratch front (f-actin, 10x magnification).

To substantiate this finding, we examined the localization of Rac1 to the cell front of migrating cells. In immunofluorescence stainings we found a decreased Rac1

localisation to lamellipodia as displayed in Figure 37. Cortactin served as a marker protein for lamellipodia. Again, LGR 1406 and LGR 1407 showed the strongest effects.

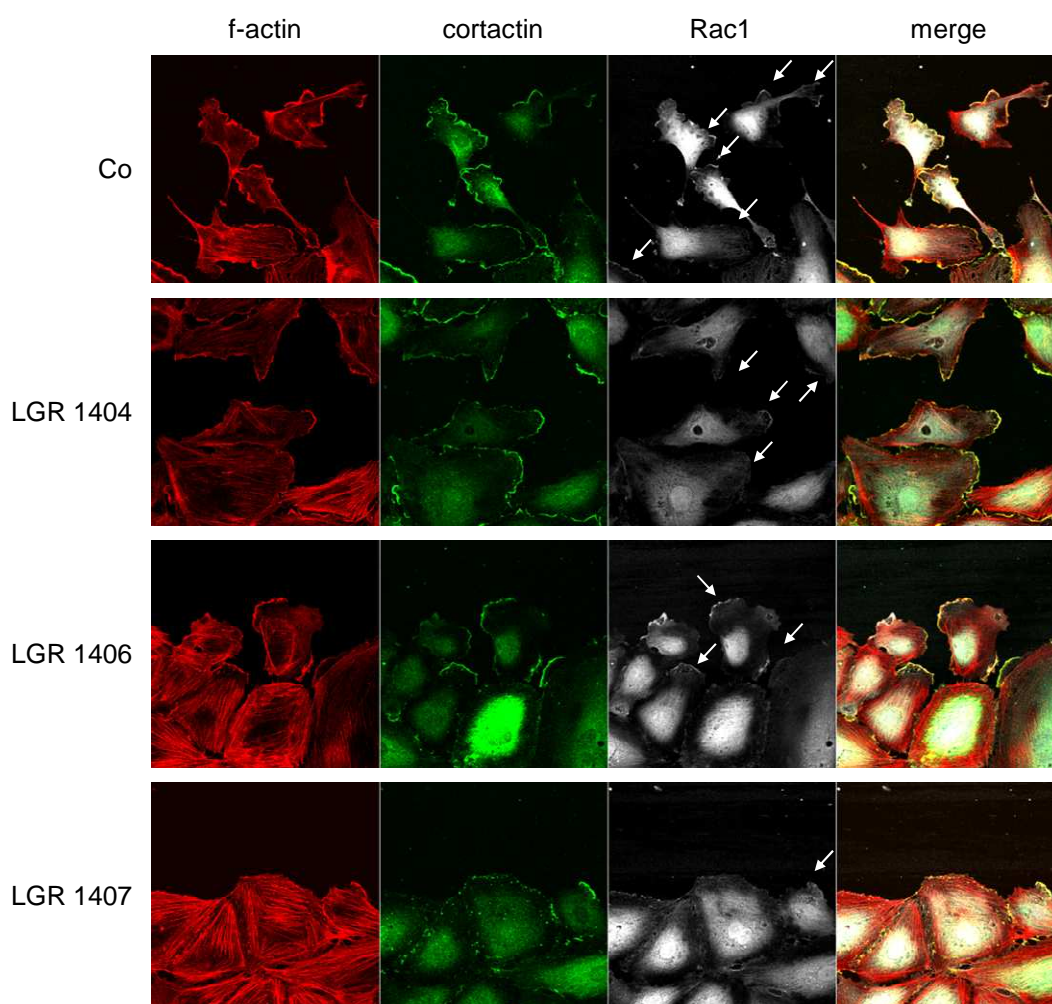


Figure 37 The LGR compounds 1404, 1406 and 1407 decreased colocalization of Rac1 and cortactin at lamellipodia. Confluent HUVECs were scratched and allowed to migrate in the presence of 10 μ M of the respective compounds for 8 h. The cells were fixed and stained for f-actin (red), cortactin (green) and Rac1 (white) and pictures were taken. Representative images out of three experiments are shown (CLSM, 40x magnification).

3.2.9 LGR 1407 significantly inhibits tumor growth and vascularization in a hepatoma xenograft mouse model

In the *in vitro* and *ex vivo* angiogenesis assays, LGR 1406 and LGR 1407 have consistently shown the strongest effects, with LGR 1406 being slightly more potent. In order to prove the anti-angiogenic and anti-tumor potential of the inhibitors, we evaluated the effects of LGR 1407 on tumor growth and vascularization in an *in vivo* tumor model of xenograft hepatocellular carcinoma in SCID mice. LGR 1407 was chosen because of its potency and higher selectivity for Cdks in the kinase panel.

LGR 1407 was able to clearly reduce tumor growth after seven days of treatment of the xenograft tumors (Figure 38).

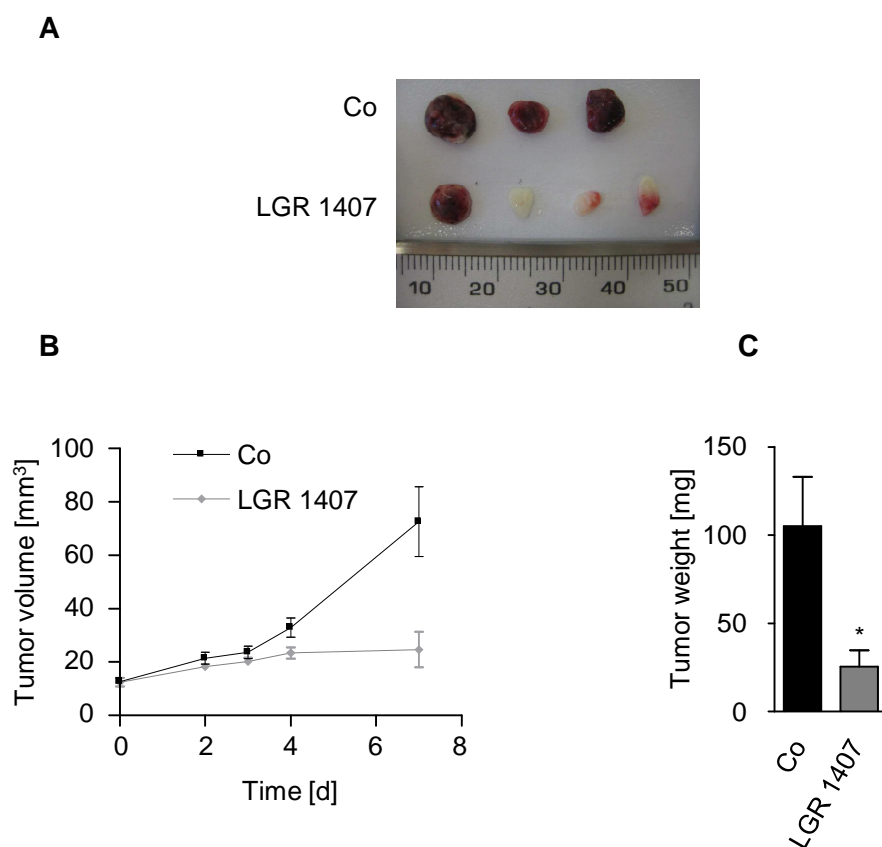


Figure 38 LGR 1407 significantly impairs tumor growth in a hepatoma xenograft mouse model. SCID mice with established subcutaneous HUH7 xenograft tumors were treated with 30 mg/kg/day LGR 1407 or vehicle for 7 days. **A:** Images of the tumors after extraction (scale: mm) **B:** Tumor volume during treatment ($l \times w \times d \times \pi/6$; Co: n=3, LGR 1407: n=4, mean \pm SEM) **C:** Tumor weight at end point (Co: n=3, LGR 1407: n=4, mean \pm SEM, * $p < 0.05$, t-test).

Figure 38A displays that the treated tumors are not only smaller, but also seem to lack sufficient vascularization and blood supply as the tissue appears in part colorless. This was further analyzed in CD31 stained tumor sections. In the treated tumors, the microvessel density was decreased by 70 % in comparison to the controls (Figure 39).

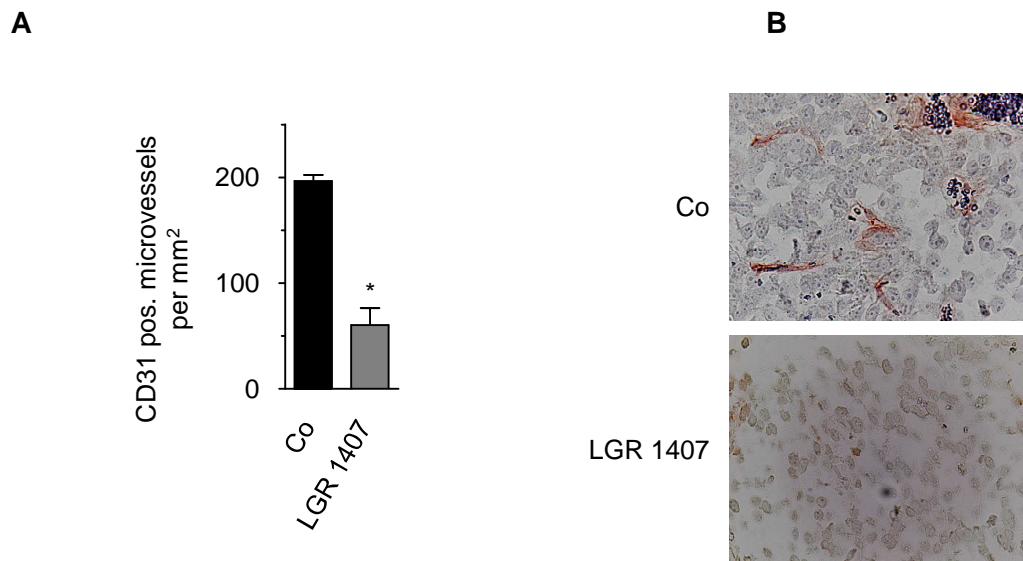


Figure 39 LGR 1407 significantly decreases microvessel density in the hepatoma xenograft tumors. Microvessel density per mm² tumor tissue was determined after CD31 staining of tumor sections. **A:** Microvessel density of Control and LGR 1407 treated tumors (Co: n=3, LGR 1407: n=4, mean \pm SEM, * p<0.05, t-test). **B:** Representative images of Control and LGR 1407 treated tumor sections (40x magnification, CD31 (red) and hematoxylin counterstaining).

4 DISCUSSION

4.1 Elucidation of novel endothelial signaling pathways as the basis for future anti-angiogenic therapy

For the first time, we have demonstrated that regulation of Cdk5 in endothelial cell migration differs from the “canonical” pathway reported in neurons and cancer cells. This finding is of importance with regard to established anti-angiogenic tumor therapy. Therapeutic agents targeting VEGF or its signaling pathways in clinical use show only transient benefits. The tumor adapts to anti-angiogenic therapy by switching to alternative pro-angiogenic pathways.⁷ Therefore it is of central interest to elucidate novel signaling pathways in tumor angiogenesis to provide the knowledge for future therapeutic exploitation. Our group has recently identified Cdk5 as a potential new target in endothelial cell migration and angiogenesis. In order to increase our understanding of the mechanisms of Cdk5 regulation and to find possible links to established angiogenesis signaling pathways, it is necessary to reveal the characteristics of Cdk5 activation in endothelial cell migration. New insight into Cdk5 regulation in endothelial cells might as well lead the way to Cdk5 specific and at the same time endothelium-specific inhibitors that target activator-kinase binding. This has been established for neurons: the p35-derived CIP¹⁰⁹ and p5¹¹⁰ are specific p25/Cdk5 interaction inhibitors without disturbing p35/Cdk5 activity.

4.2 Cdk5 regulation in endothelial cell migration exerts non-canonical characteristics

In neurons, p35 and p39, and their truncated forms p25 and p29, respectively, activate Cdk5. Additionally, Cdk5 can be regulated by phosphorylation on tyrosine 15 and serine 159 (reviewed in Dhavan & Tsai³⁹). Aim of the work was to investigate if Cdk5 regulation in endothelial cell migration follows the same principles as in neuronal migration.

4.2.1 Cdk5 phosphorylation on tyrosine 15 is dispensable in endothelial cell migration

In our work, we concentrated on tyrosine 15 phosphorylation, which is well described as activating in neuronal and in non-neuronal cells, and has also been implicated in migration and actin dynamics.^{42, 47, 96} Further phosphorylation sites of Cdk5 on serine

159 and threonine 14 have been reported, but their significance in cell signaling mechanisms is not clearly defined.⁶²⁻⁶⁶ Cdk5 inhibition in migrating endothelial cells leads to defects in the actin cytoskeleton and lamellipodia formation, so our hypothesis was that Cdk5 may be activated during endothelial cell migration via phosphorylation of tyrosine 15.

Fyn⁴⁷ and c-abl⁴⁶ reportedly phosphorylate Cdk5 at tyrosine 15. Yet, treatment of endothelial cells with fyn inhibitor SU6656 or the c-abl inhibitor imatinib did not affect migration. Moreover, phosphorylation of Cdk5 during endothelial cell spreading by so far unidentified tyrosine kinases is obviously not the case, since Cdk5 tyrosine 15 phosphorylation was not increased. Finally, a crucial function of phospho-Cdk5^{Y15} in endothelial cell migration was ruled out by overexpression of a non-phosphorylatable Cdk5 mutant.

For Cdk5, it has not conclusively been shown that phosphorylation is essential for full activation after binding to its activator. Regarding the structure of activator/Cdk5 complex, phosphorylation of serine 159 in Cdk5 is not required for reaching the fully active conformation.⁶⁵ If Cdk5 needs to be phosphorylated at tyrosine 15 for full activation has not been proven. According to our data, phosphorylation on tyrosine 15 is not essential for Cdk5 regulation in endothelial cell migration. Recently, a novel mode of Cdk5 regulation has been shown: Cdk5 can be activated by S-nitrosylation.^{111, 112} To investigate a regulation of Cdk5 by nitrosylation during endothelial cell migration may be of interest, as it has been reported that Cdk5 can inactivate eNOS by phosphorylation.¹⁰⁵ Moreover, eNOS co-localizes with actin at the cell front during HUVEC migration¹¹³, and is also connected to Rac1 signaling.^{114, 115}

4.2.2 p35 and p39 are not central for Cdk5 regulation in endothelial cell migration

Expression of p35 and activation of Cdk5 by p35 has been described in non-neuronal cells.⁵⁴⁻⁵⁸ We have shown that p35 and p39 are expressed in endothelial cells as well, but reach only a fraction of 3×10^{-3} and 1×10^{-4} of the mRNA expression in brain tissue, respectively. In comparison, the protein levels of Cdk5 in endothelial cells are by trend lower than in human brain, but not significantly. The extremely low expression level of the classical Cdk5 regulators in endothelial cells is in line with the investigations of Cho *et al.*¹⁰⁵ In contrast to their findings, we were able to identify p35 on protein level in HUVECs and also in HMEC-1.

As the expression of p39 was hardly detectable on mRNA level, we focused on the role of p35 in endothelial cells, in order to identify its function in migration and angiogenesis. To examine the role of p35 during endothelial cell migration, we used spreading cells as a model for cytoskeletal activation in comparison to confluent cells. During endothelial cell spreading, Cdk5 is targeted to the membrane and p35 expression is weakly increased after 45 min and 240 min. As p35 carries a myristoylation which targets Cdk5 to the membrane in neuronal cells⁴⁴, these findings suggested that 1) p35 might be involved in Cdk5 regulation during migration and 2) p35 may be responsible for the membrane localization of Cdk5 during spreading. However, we could not consistently detect p35 protein in membrane fractions due to its low amount.

As Cdk5 inhibition affects growth factor-induced endothelial cell migration⁷⁵, the influence of VEGF, a fundamental stimulus in angiogenesis and endothelial cell migration, was investigated. For p35, growth factor (NGF) induced increase in protein level has already been shown in neurons.⁴⁰ p35 protein expression in endothelial cells, though, is not induced upon treatment with VEGF, neither with PDGF-B and bFGF. This further indicates that p35 is not involved in Cdk5 regulation in endothelial cell migration.

However, we supposed that the degradation of p35 by the proteasome or calpain might be involved in Cdk5 activation and redistribution within the cell. Further, stabilization of unstable p35 protein by inhibiting degradation could facilitate detection. Indeed, we found that p35 protein level is controlled by the proteasome, since treatment with a proteasome inhibitor leads to increased protein levels of p35. This effect was utilized to detect the p35 siRNA downregulation on protein level. The impact of MG132 on p35 protein amount indicates a rapid cycle of p35 proteasomal degradation, as has been reported for neurons.⁴⁵ The significance of p35 stabilization for endothelial cell migration cannot be determined by MG132 treatment, as this substance strongly inhibits NF- κ B and this in itself affects endothelial cell migration.¹¹⁶

The alternative degradation pathway of p35 via the protease calpain leads to the cleavage product p25. In neurons, p25 deregulates Cdk5 activity with regard to cytosolic localization and prolonged activation. Calpain and the endogenous calpain inhibitor calpastatin are active in endothelial cells¹¹⁷ and calpain can be activated during VEGF-induced endothelial cell migration.¹¹⁸ However, p25 was not detected in endothelial cells, neither after stabilization of the p35 protein by proteasome inhibition, which should favor the second degradation pathway. Furthermore, calpain inhibition had no effect on endothelial cell migration and did not lead to increased p35 levels.

These findings demonstrate that calpain cleavage of p35 to p25 is not involved in the regulation of Cdk5 during endothelial migration.

In p35 siRNA experiments, we could finally rule out a key role of p35 in endothelial cell migration. Since it has been shown that p39 is able to counteract the loss of p35⁵³, compensation of p35 downregulation by rise of p39 was also excluded.

The conclusion drawn from the *in vitro* experiments – p35 is not crucial for endothelial cell migration – was substantiated *in vivo* by our investigations in p35 deficient mice. The vascular pattern and the vessel density in p35^{-/-} animals did not differ from those of wild type mice. If p35 knockout had affected endothelial cell migration during developmental and physiological angiogenesis, obvious defects should have been visible in organ vascularization and vessel density, and this is not the case.

Altogether, the results presented in this study exclude p35 and p39 as key regulators in endothelial cell migration. Therefore we, for the first time, have demonstrated that Cdk5 in endothelial cell migration is not dependent on p35/p25 and p39/p29 as activators.

4.2.3 p35 is not increased in Cdk5-dependent endothelial inflammatory reaction

Our group has previously proven that additional anti-inflammatory properties of the Cdk inhibitor roscovitine result from Cdk5 inhibition in the endothelium.⁷⁶ This means two central functions of the endothelium, migration/angiogenesis and inflammation, are regulated by Cdk5. Therefore, the question was, whether p35 might be crucial for Cdk5 in the endothelial inflammatory response although it has been proven to be extraneous in endothelial cell migration. It has already been shown that Cdk5 can be differentially modulated by disparate activators in the same cell type.^{59, 119}

Thus, we investigated the influence of TNF- α treatment on p35 expression in endothelial cells, as TNF- α stimulation can increase p35 levels in neuronal and non-neuronal cells.^{42, 120} TNF- α had no impact on the amount of p35 protein in endothelial cells, which may indicate that p35 has no key role for Cdk5 regulation in inflammatory activated endothelium as well. This supports the findings from our investigation of p35 and p39 in endothelial cell migration, and points out to a specific regulatory mechanism for Cdk5 in the endothelium.

4.2.4 Evaluation of Cdk5 activity in endothelial cells

The effect of Cdk5 inhibition on endothelial cell migration is derived from inhibition of the kinase activity, since the inhibitor roscovitine blocks the ATP binding-pocket of the kinase.⁷⁴ Furthermore, a dominant negative kinase dead mutant of Cdk5 exerts the same effects as Cdk5 loss after siRNA downregulation.⁷⁵ Thus, it is the activity, and not only the presence of Cdk5 that is crucial for endothelial cell migration.

Measuring the influence of stimuli on Cdk5 kinase activity is of central importance in order to explore activators and activating processes of Cdk5. To assess Cdk5 activity, we first immunoprecipitated Cdk5, p35, or overexpressed Cdk5-HA. Cdk5-specific kinase activity was evaluated by comparison to a negative control, which was obtained by addition of Cdk5 inhibitor roscovitine to the kinase reaction, by immunoprecipitation with irrelevant or no IgG, or by using HA-untransfected cell lysate, respectively. In all settings, the kinase activity in endothelial cells did not significantly differ from the negative control. This indicates that endogenous Cdk5 activity is very low in endothelial cells and difficult to distinguish from background signal. Methodical issues were ruled out by using recombinant Cdk5/p35 kinase to check buffers and antibodies for their compatibility with the assay. With p35 immunoprecipitation, it was possible to obtain a strong kinase activity from neuronal cell lysate – demonstrating that the assay worked – however the signal from the endothelial cells was not distinguishable from background. This could now be explained by the finding that p35 does not seem to be involved in Cdk5 regulation in endothelial cell migration. After Cdk5-HA overexpression and p35-myc co-transfection in order to increase Cdk5 activity and to improve the signal/background ratio the signal was still not increased over background. Cdk5 overexpression alone may lead to an inappropriate activator/kinase ratio. As this could not be overcome by p35 co-transfection, our previous findings that p35 is no central Cdk5 activator in endothelial cells are further substantiated.

As Cdk5 activity is reliant on the pairing with its activating subunit, the crucial step in the assay is the co-immunoprecipitation of the activator. According to our findings so far, Cdk5 activity in endothelial cells is presumably much lower than in neuronal cells. In order to get sufficient kinase activity, it is therefore essential to identify the endothelial activator of Cdk5 and precipitate the activator with Cdk5, as it is described for Cdk5/p35 by Nicolic & Tsai.¹⁰⁴

The challenges that remain for the evaluation of Cdk5 activity in migrating endothelial cells are 1) to identify the so far unknown endothelial Cdk5 activator and 2) to optimize the kinase assay with the precipitation of activator, in order to obtain sufficient kinase

activity, as Cdk5 activity in endothelial cells is supposedly much lower than in neuronal cells but central for migration.

4.2.5 A proteomics approach provides novel insights into endothelial Cdk5 signaling

In literature, few works have investigated the role of Cdk5 in the endothelium; and the part of the canonical activators p35/p25 and p39/p29 has not been thoroughly examined yet, except by this work. The fact that the central endothelial-related processes inflammation and angiogenesis which are regulated by Cdk5 do not depend on p35 and p39 raises the question, which up to date unknown activator is responsible for Cdk5 activity in endothelial cells.

We chose a proteomics approach with LC-ESI-MS/MS identification of protein bands after Cdk5 immunoprecipitation in order to find novel Cdk5 interacting proteins. This approach aims first to identify the activator of Cdk5 in endothelial cell migration. Second, up to now unknown Cdk5 substrates upstream from Rac1 could be determined in order to reveal the mechanism of Rac1 inactivation by Cdk5 inhibition during endothelial cell migration.⁷⁵ We used two migration-related stimulations for the investigations – 45 min spreading and starved/FCS treated cells – in comparison to confluent or starved control cells. Three bands were analyzed, as described in the results part (list of identified proteins: see Results part, Table 26). The LC-ESI-MS/MS identified also Cdk2 and Cdk1 in the band containing Cdk5. This could be either due to the about 60% sequence homology of Cdk5 with Cdk1 and Cdk2 respectively²⁷, which would lead to overlapping peptides; or owing to partly unspecific antibody binding, as the Cdk5 antibody is raised against the whole Cdk5 protein. GBLP (guanine nucleotide-binding protein subunit beta-2-like 1), also known as RACK1 (Receptor for activated protein C kinase 1) belongs to the RACK family of proteins identified as adaptor proteins in PKC signaling.¹²¹ RACK1 has been shown to regulate VEGFR1-mediated endothelial cell migration: RACK1 silencing led to impaired migration, suppressed PI3K/AKT cascade activation and inhibited Rac1 activation and membrane ruffling.¹²² However, inactivation of Rac1 by Cdk5 inhibition with roscovitine did not affect AKT phosphorylation, which suggests an AKT independent pathway. If RACK1 might be the link between Cdk5 and Rac1 in endothelial cell migration, still needs to be elucidated. RACK1 could be a novel Cdk5 substrate as it carries potential phosphorylation sites for Cdk5 (determined with GPS Version 2.1^{123, 124}).

Cdk5 plays an important role in the regulation of the actin cytoskeleton¹²⁵, and it is localized to the dense actin network of lamellipodia in endothelial cell migration⁷⁵. This could explain the presence of actin in the immunoprecipitation, although no direct interaction of Cdk5 and actin has been reported, only via its neuronal activators p35 and p39.^{126, 127}

Various HSP 70 Heat shock proteins co-immunoprecipitated with Cdk5. Heat shock proteins are molecular chaperons which guide protein folding and are involved in cellular transport. They are upregulated in response to cellular stress but some are also constitutively expressed.¹²⁸ In neurons, Heat shock cognate 71 kDa protein HSP7C can bind to, and regulate degradation of Cdk5-hyperphosphorylated tau in neurons; a direct Cdk5/HSP7C interaction is not reported.¹²⁹ The role of HSP 70 in angiogenesis has been investigated by Shiota *et al.*: They showed that global HSP 70 inhibition decreased endothelial cell migration, VEGF-induced eNOS phosphorylation and angiogenesis *in vivo*.¹³⁰ This again might allude to a connection of Cdk5 and eNOS during endothelial cell migration.

The co-IP of lamin A and disks large homolog 4 (or PSD-95), both substrates of Cdk5 in neurons, proves that our approach of Cdk5-IP and LC-ESI-MS/MS is suitable for identifying Cdk5 interacting proteins in endothelial cell migration. Lamin A is a nuclear envelope protein, and its phosphorylation by Cdk5 in neuronal cells results in nuclear envelope dispersion, which precedes cell death.¹³¹ Lamin A can be cleaved during endothelial cell apoptosis.¹³² Further, a lamin A mutant (progerin) is responsible for the vascular symptoms in Hutchinson–Gilford progeria syndrome.¹³³ Disks large homolog 4 (PSD-95) is a post-synaptic density (PSD) protein in glutamatergic synapses, and is known as a substrate of Cdk5 in hippocampal neurons.¹³⁴ Its presence as a synaptic protein in endothelial cells is striking and a function in endothelial cells is so far unknown. With neuexin and neurogilin two other synaptic proteins have been shown to play a role in the vasculature; and the parallels between signaling in nerves and vessels very likely exceed the field of guiding cues.¹³⁵

Desmoplakin is an intracellular part of desmosomes, tight intercellular junctions, and anchors intermediate filaments to these structures. Desmoplakin localizes with VE-cadherin in HUVECs at tight junctions¹³⁶ and also is involved in tube formation of endothelial cells *in vitro*.¹³⁷ In epithelial cells, Cdk5 is involved in the maintenance of cell-cell-adhesion.^{138, 139} The presence of desmoplakin may therefore indicate a role for Cdk5 in endothelial barrier function.

POTE ankyrin domain family member E (POTE-2) belongs to the primate specific POTE family¹⁴⁰, which share an ankyrin repeat domain and sequence homology with actin. POTE proteins were discovered in prostate, ovary, testis and placenta (POTE= **p**rostate **o**vary **t**estis **e**xpressed protein) but have been reported to be overexpressed in certain tumors¹⁴¹. POTE proteins are palmitoylated and located at the membrane.¹⁴² Nothing so far is known about their role in the endothelium or a link to Cdk5.

In order to find the endothelial specific activator a comparison between IPs with different antibodies needs to be carried out. It cannot be excluded that the antibody interfered with the binding of the activator to Cdk5, as it was not yet possible to precipitate a potential candidate for Cdk5 activation. The antibody used was tested in the kinase assay with recombinant Cdk5/p35 and does not disturb p35 binding, but the binding and amount of the endothelial specific activator might be weaker or lower, respectively. Besides p35/p25 and p39/p29, there are reports that Cdk5 can bind to several cyclins^{59,35-38}, of which only Cyclin I is able to activate Cdk5.⁵⁹ Cyclin I is expressed in endothelial cells (data not shown), but if it is involved in Cdk5 activation needs to be elucidated. Nevertheless, our approach identified promising novel Cdk5 interacting proteins in endothelial cells. For example RACK1, desmoplakin, lamin A and PSD-95 could be worth closer investigations, possibly revealing novel roles of Cdk5 in PKC signaling, barrier function, (endothelial cell) apoptosis, and so far unknown functions of neuronal synaptic proteins in endothelial cells.

4.3 Novel LGR inhibitors are potent anti-angiogenic compounds and validate Cdk5 as a target

4.3.1 *In vitro* potency of LGR compounds is confirmed in the CAM assay *in vivo*

Our approach to use the effect on endothelial migration as the crucial selection criterion resulted in the identification of compounds that were tested further in functional assays for their tube formation and directed migration in a chemotactic gradient. Finally, the most potent compounds LGR 1404, 1406 and 1407 proved their anti-angiogenic potency in CAM-assays, where they completely inhibited VEGF-induced vessel formation. We have identified three potent novel roscovitine derivatives that display increased anti-angiogenic activity in comparison to their mother substance.

4.3.2 Kinase data and Cdk5-dependent mode of action of LGR 1404, 1406 and 1407

Roscovitin inhibits several Cdks, mainly Cdk1, Cdk2, Cdk5, Cdk7 and Cdk9. The selectivity data depend on the kinase panel referred to.^{74, 108, 143, 144} LGR 1407 is equally potent in inhibition of Cdk2 and Cdk5, and inhibits Cdk1 and Cdk9 to some extent. LGR 1406 is by one order of magnitude more selective towards Cdk5 and Cdk2 in comparison to Cdk1 and Cdk9. Both compounds inhibited preferably Cdks in our kinase panel, with LGR 1407 showing a higher Cdk selectivity. Comparing the two most powerful compounds LGR 1406 and 1407, the lower IC₅₀ for Cdk5 and the higher selectivity for Cdk5 (and Cdk2) of LGR 1406 mirror the effect in the angiogenesis assays. LGR 1407 is more selective towards Cdk5 in comparison to LGR 1404, which mainly inhibits Cdk2 (IC₅₀ for Cdk2 0.22 μM, for Cdk5 0.94 μM according to Jorda *et al.*¹⁰⁸). This is probably the reason why LGR 1404 is the least potent anti-angiogenic compound of the three with regard to the *in vitro* data. Determining the effect of LGR 1404, 1406 and 1407 on lamellipodia formation and Rac1 localization, we suggest that their mode of action is the potent inhibition of Cdk5 and not Cdk2. The lower selectivity of LGR 1404 for Cdk5 becomes also apparent in the lamellipodia quantification and the Rac1/lamellipodia immunofluorescence images: the disruption of lamellipodia and the effect on Rac1 is not that prominent as with LGR 1406 and LGR 1407.

4.3.3 Structure and anti-angiogenic potency of the LGR

In order to optimize the structure of the Cdk inhibitors for optimal anti-angiogenic potential, the relation of structure changes and anti-angiogenic effect is of interest. For the LGR compounds as roscovitin derivatives, the structure was modified in three points:

1 - Changing the purine scaffold to a pyrazolo[4,3-d]pyrimidine

In general, the change of the scaffold led to a higher anti-angiogenic potency of the substances. All substances chosen for further evaluation after the migration assay share the pyrazolo[4,3-d]pyrimidine scaffold. Direct comparison of the potency of roscovitin and its pyrazolo[4,3-d]pyrimidine bioisoster, LGR 1404, substantiates this observation. The only compound tested with a purine scaffold, LGR 1730, showed the weakest effect on proliferation and only a minor impact on migration.

2 - *ortho*-amino function in the aminobenzyl group at C6 (purine) or C7 (pyrazolo[4,3-*d*]pyrimidine)

The presence of an amino group rather seems to decrease the anti-angiogenic potential of the compounds. The compounds LGR 1430 and LGR 1492 differ from LGR 1406 and LGR 1404, respectively, only in the presence of the amino function, and show both weaker effects. This is especially obvious in the comparison of LGR 1406 and LGR 1430 as LGR 1406 was the most potent compound in the assays, whereas LGR 1430 showed no detectable effect on migration at 30 μ M (data not shown).

3 - Variation of the side chain at C2 (purine) or C5 (pyrazolo[4,3-*d*]pyrimidine)

Evaluating the impact of different side chains on the anti-angiogenic effect is difficult as the compounds differ from roscovitine in more than one structural property and no direct comparison is possible. By trend, a bulky side chain like the substituted sec-butyl- (e.g. LGR 1404) or cyclohexyl- (e.g. LGR 1406) groups seem to increase anti-angiogenic potency.

4.3.4 Novel Cdk5 inhibitors validate Cdk5 as an anti-angiogenic target *in vitro* and in the LGR 1407 tumor xenograft

For further evaluation of Cdk5 as a target in angiogenesis, novel inhibitors with increased Cdk5 selectivity need to be synthesized and examined for their anti-angiogenic potential. We have demonstrated that LGR 1404, 1406 and 1407 are able to potently inhibit angiogenesis *in vitro* via a Cdk5-dependent mechanism and show a higher potency and selectivity for Cdk5 in comparison to the established Cdk5 inhibitor roscovitine. Additionally, LGR 1407 was well tolerated in the *in vivo* mouse model and led to a clear decrease in tumor vascularization and tumor growth. The conclusions we can draw from this experiment are clear: On the one hand, with LGR 1407 we have a potent anti-tumor agent displaying low toxicity *in vivo*. On the other hand, for the first time we have shown the efficacy of a Cdk5 inhibitor on tumor angiogenesis *in vivo*. This further validates Cdk5 as a promising target in angiogenesis and the therapeutic potential of Cdk5 inhibitors.

4.4 Conclusion and future aspects

4.4.1 Cdk5 upstream regulation in endothelial cells

This work provides first insight into Cdk5 upstream regulation in endothelial cells, which we have for the first time proven to substantially differ from the “canonical” pathway via p35/p25 and p39/p29 and tyrosine 15 phosphorylation. A goal for future research is the identification of the so far unknown endothelial specific Cdk5 activator(s). A possible candidate for further investigations is Cyclin I, which is expressed in HUVECs and HMEC-1, and has been shown to activate Cdk5. A useful approach for further research is provided by the Cdk5 immunoprecipitation and LC-ESI-MS/MS: on the one hand it showed that neuronal substrates of Cdk5 are probably also involved in endothelial cell signaling, and on the other hand revealed potential novel Cdk5 interacting partners, with RACK1 as a possible link to Rac1 activation.

4.4.2 Cdk inhibitors with higher potency and selectivity to Cdk5

The concept of Cdk5 inhibition to target angiogenesis has recently been introduced by our group. In this study, novel roscovitine derivatives were tested in order to find effective and non-toxic small molecule inhibitors for a possible therapeutic application. Three potent compounds were identified: LGR 1404, 1406 and 1407 strongly inhibit angiogenesis in vitro and in vivo. Their impact on Cdk5 parallels the efficacy in the angiogenesis assays which supports the strategy of Cdk5 inhibition as a powerful new approach in anti-angiogenic therapy. Moreover, for the first time the efficacy of a Cdk5 inhibitor on tumor angiogenesis in a HCC xenograft mouse model has been demonstrated with the compound LGR 1407. For the further development of anti-angiogenic roscovitine derivatives, comparison of the structures of the tested LGR inhibitors shows a positive correlation to anti-angiogenic potency for the pyrazolo[4,3-d]pyrimidine scaffold and a negative correlation for an additional amino function in the benzyl group.

5 SUMMARY

The discovery, characterization and validation of novel targets in angiogenesis is of central interest, as clinical use of anti-angiogenic drugs in anticancer therapy has shown that in many cases resistance and sustained tumor growth occur in response to blockade of VEGF-induced angiogenesis by a shift towards alternative angiogenic pathways.

Cyclin-dependent kinase inhibitors, which were actually designed as anti-proliferative drugs affecting the cell cycle of the limitless proliferating tumor cells, exert anti-angiogenic properties as well. The atypical cyclin-dependent kinase Cdk5 has recently been identified as a potential target protein for the anti-angiogenic effects. Cdk5 inhibition leads – via Rac1 inactivation – to actin disorganization, lamellipodia breakdown and consequently to a decrease of endothelial cell migration.⁷⁵

In the first part of the presented study, the question was addressed if Cdk5 is regulated during endothelial cell migration by the known mechanisms: via its neuronal non-cyclin activators p35 or p39, or by tyrosine 15 phosphorylation.

The activating tyrosine 15 phosphorylation of Cdk5 was found to be dispensable for Cdk5 regulation in endothelial cell migration.

A low amount of p35 is expressed in endothelial cells on mRNA and protein level, whereas p39 mRNA is at the limit of detection. p25, the calpain cleavage product of p35 and alternative Cdk5 activator, though, is not present in endothelial cells. Downregulation of p35 does not affect endothelial cell migration and does not lead to a compensatory upregulation of p39. *In vivo*, p35 deficient mice do not display vascular aberrations. These findings exclude p35 as a central regulator of endothelial cell migration during angiogenesis. Cdk5 kinase activity in endothelial cells is very likely independent of p35 as well. There was also no strong hint for a prominent role of p35 in TNF- α induced inflammatory reaction of endothelial cells, a second major process in the endothelium under the control of Cdk5. Mass spectrometric identification of proteins co-immunoprecipitated with Cdk5 revealed novel potential Cdk5 interactants in endothelial cells. If Cyclin I, an alternative Cdk5 activator which is also expressed in endothelial cells, is involved in Cdk5 regulation in endothelial cells still needs to be elucidated.

The second part of the study dealt with the evaluation of prospective anti-angiogenic Cdk inhibitors, paying particular consideration on their potency to inhibit Cdk5. Eight novel roscovitine derivatives were assessed *in vitro* for their impact on endothelial proliferation, migration, chemotaxis and tube formation. The three most potent compounds LGR 1404, 1406 and 1407 were selected and proved their anti-angiogenic

potency in chorioallantoic membrane assays *in vivo*. LGR 1406 and LGR 1407 showed preferred inhibition of Cdk5 (and Cdk2), whereas the slightly less effective LGR 1404 inhibited Cdk2 rather than Cdk5. Immunostainings demonstrated that the three LGR compounds affect endothelial cell migration by lamellipodia breakdown and cortactin and Rac1 mislocalization, which suggests a Cdk5-dependent mode of action. LGR 1407 decreased tumor growth and angiogenesis in a hepatocellular carcinoma xenograft in SCID mice. For the future development of anti-angiogenic compounds, comparison of the structures of the tested LGR inhibitors shows a positive correlation to anti-angiogenic potency for the pyrazolo[4,3-d]pyrimidine scaffold and a negative correlation for an additional amino function in the benzyl group.

From these findings, we conclude that regulation of Cdk5 in endothelial cells follows an alternative mechanism different from the canonical pathway via p35 and p39 described in neurons. Moreover, we present a promising approach to identify novel Cdk5 interacting proteins and suggest Cyclin I as a candidate for upcoming investigations. Using novel potent Cdk inhibitors, our results further support the idea of Cdk5 inhibition as a future approach for anti-angiogenic therapy, highlighting the compound LGR 1407 as a potent inhibitor of tumor growth and vascularization.

6 REFERENCES

1. Lamalice L, Le Boeuf F, Huot J. Endothelial cell migration during angiogenesis. *Circ Res*. Mar 30 2007;100(6):782-794.
2. Hanahan D, Weinberg RA. The hallmarks of cancer. *Cell*. Jan 7 2000;100(1):57-70.
3. Tonini T, Rossi F, Claudio PP. Molecular basis of angiogenesis and cancer. *Oncogene*. Sep 29 2003;22(42):6549-6556.
4. Hanahan D, Folkman J. Patterns and emerging mechanisms of the angiogenic switch during tumorigenesis. *Cell*. Aug 9 1996;86(3):353-364.
5. Zeneca A. AstraZeneca announces trade name CAPRELSA® for vandetanib. 2011; <http://www.astrazeneca-us.com/about-astrazeneca-us/newsroom/all/12379191?itemId=12379191>. Accessed September 20, 2011, 2011.
6. Carmeliet P, Jain RK. Molecular mechanisms and clinical applications of angiogenesis. *Nature*. May 19 2011;473(7347):298-307.
7. Bergers G, Hanahan D. Modes of resistance to anti-angiogenic therapy. *Nat Rev Cancer*. Aug 2008;8(8):592-603.
8. Loges S, Mazzone M, Hohensinner P, Carmeliet P. Silencing or fueling metastasis with VEGF inhibitors: antiangiogenesis revisited. *Cancer Cell*. Mar 3 2009;15(3):167-170.
9. Paez-Ribes M, Allen E, Hudock J, et al. Antiangiogenic therapy elicits malignant progression of tumors to increased local invasion and distant metastasis. *Cancer Cell*. Mar 3 2009;15(3):220-231.
10. Herbert SP, Stainier DY. Molecular control of endothelial cell behaviour during blood vessel morphogenesis. *Nat Rev Mol Cell Biol*. 2011;12(9):551-564.
11. Fischer C SM, Carmeliet P. Principles and Therapeutic Implications of Angiogenesis, Vasculogenesis and Arteriogenesis. In: Moncada S HA, ed. *The Vascular Endothelium II*. Berlin Heidelberg: Springer-Verlag; 2006.
12. Malumbres M, Barbacid M. Mammalian cyclin-dependent kinases. *Trends Biochem Sci*. Nov 2005;30(11):630-641.
13. Malumbres M, Barbacid M. Cell cycle, CDKs and cancer: a changing paradigm. *Nat Rev Cancer*. Mar 2009;9(3):153-166.
14. Ren S, Rollins BJ. Cyclin C/cdk3 promotes Rb-dependent G0 exit. *Cell*. Apr 16 2004;117(2):239-251.
15. Fisher RP. Secrets of a double agent: CDK7 in cell-cycle control and transcription. *J Cell Sci*. Nov 15 2005;118(Pt 22):5171-5180.
16. Pinhero R, Liaw P, Bertens K, Yankulov K. Three cyclin-dependent kinases preferentially phosphorylate different parts of the C-terminal domain of the large subunit of RNA polymerase II. *Eur J Biochem*. Mar 2004;271(5):1004-1014.

17. Akoulitchev S, Chuikov S, Reinberg D. TFIID is negatively regulated by cdk8-containing mediator complexes. *Nature*. Sep 7 2000;407(6800):102-106.
18. Fu TJ, Peng J, Lee G, Price DH, Flores O. Cyclin K functions as a CDK9 regulatory subunit and participates in RNA polymerase II transcription. *J Biol Chem*. Dec 3 1999;274(49):34527-34530.
19. Garriga J, Grana X. Cellular control of gene expression by T-type cyclin/CDK9 complexes. *Gene*. Aug 4 2004;337:15-23.
20. Yokoyama H, Gruss OJ, Rybina S, et al. Cdk11 is a RanGTP-dependent microtubule stabilization factor that regulates spindle assembly rate. *J Cell Biol*. Mar 10 2008;180(5):867-875.
21. Wilker EW, van Vugt MA, Artim SA, et al. 14-3-3sigma controls mitotic translation to facilitate cytokinesis. *Nature*. Mar 15 2007;446(7133):329-332.
22. Petretti C, Savoian M, Montembault E, Glover DM, Prigent C, Giet R. The PITSLRE/CDK11p58 protein kinase promotes centrosome maturation and bipolar spindle formation. *EMBO Rep*. Apr 2006;7(4):418-424.
23. Chen HH, Wong YH, Genevriere AM, Fann MJ. CDK13/CDC2L5 interacts with L-type cyclins and regulates alternative splicing. *Biochem Biophys Res Commun*. Mar 16 2007;354(3):735-740.
24. Chen HH, Wang YC, Fann MJ. Identification and characterization of the CDK12/cyclin L1 complex involved in alternative splicing regulation. *Mol Cell Biol*. Apr 2006;26(7):2736-2745.
25. Tassan JP, Jaquenoud M, Fry AM, Frutiger S, Hughes GJ, Nigg EA. In vitro assembly of a functional human CDK7-cyclin H complex requires MAT1, a novel 36 kDa RING finger protein. *EMBO J*. Nov 15 1995;14(22):5608-5617.
26. Larochelle S, Merrick KA, Terret ME, et al. Requirements for Cdk7 in the assembly of Cdk1/cyclin B and activation of Cdk2 revealed by chemical genetics in human cells. *Mol Cell*. Mar 23 2007;25(6):839-850.
27. Hellmich MR, Pant HC, Wada E, Battey JF. Neuronal cdc2-like kinase: a cdc2-related protein kinase with predominantly neuronal expression. *Proc Natl Acad Sci U S A*. Nov 15 1992;89(22):10867-10871.
28. Songyang Z, Lu KP, Kwon YT, et al. A structural basis for substrate specificities of protein Ser/Thr kinases: primary sequence preference of casein kinases I and II, NIMA, phosphorylase kinase, calmodulin-dependent kinase II, CDK5, and Erk1. *Mol Cell Biol*. Nov 1996;16(11):6486-6493.
29. Ohshima T, Ward JM, Huh CG, et al. Targeted disruption of the cyclin-dependent kinase 5 gene results in abnormal corticogenesis, neuronal pathology and perinatal death. *Proc Natl Acad Sci U S A*. Oct 1 1996;93(20):11173-11178.
30. Smith DS, Tsai LH. Cdk5 behind the wheel: a role in trafficking and transport? *Trends Cell Biol*. Jan 2002;12(1):28-36.

31. Su SC, Tsai LH. Cyclin-Dependent Kinases in Brain Development and Disease. *Annu Rev Cell Dev Biol.* Oct 29 2010.
32. Patrick GN, Zukerberg L, Nikolic M, de la Monte S, Dikkes P, Tsai LH. Conversion of p35 to p25 deregulates Cdk5 activity and promotes neurodegeneration. *Nature.* Dec 9 1999;402(6762):615-622.
33. Liebl J, Furst R, Vollmar AM, Zahler S. Twice switched at birth: Cell cycle-independent roles of the "neuron-specific" cyclin-dependent kinase 5 (Cdk5) in non-neuronal cells. *Cell Signal.* Nov 2011;23(11):1698-1707.
34. Rosales JL, Lee KY. Extraneuronal roles of cyclin-dependent kinase 5. *Bioessays.* Oct 2006;28(10):1023-1034.
35. Xiong Y, Zhang H, Beach D. D type cyclins associate with multiple protein kinases and the DNA replication and repair factor PCNA. *Cell.* Oct 30 1992;71(3):505-514.
36. Guidato S, McLoughlin DM, Grierson AJ, Miller CC. Cyclin D2 interacts with cdk-5 and modulates cellular cdk-5/p35 activity. *J Neurochem.* Jan 1998;70(1):335-340.
37. Miyajima M, Nornes HO, Neuman T. Cyclin E is expressed in neurons and forms complexes with cdk5. *Neuroreport.* May 30 1995;6(8):1130-1132.
38. Kanaoka Y, Kimura SH, Okazaki I, Ikeda M, Nojima H. GAK: a cyclin G associated kinase contains a tensin/auxilin-like domain. *FEBS Lett.* Jan 27 1997;402(1):73-80.
39. Dhavan R, Tsai LH. A decade of CDK5. *Nat Rev Mol Cell Biol.* Oct 2001;2(10):749-759.
40. Harada T, Morooka T, Ogawa S, Nishida E. ERK induces p35, a neuron-specific activator of Cdk5, through induction of Egr1. *Nat Cell Biol.* May 2001;3(5):453-459.
41. Utreras E, Futatsugi A, Rudrabhatla P, et al. Tumor necrosis factor-alpha regulates cyclin-dependent kinase 5 activity during pain signaling through transcriptional activation of p35. *J Biol Chem.* Jan 23 2009;284(4):2275-2284.
42. Nohara A, Okada S, Ohshima K, Pessin JE, Mori M. CDK5 is a key molecule in TNF- α induced insulin resistance. *J Biol Chem.* Aug 3 2011.
43. Song JH, Wang CX, Song DK, Wang P, Shuaib A, Hao C. Interferon gamma induces neurite outgrowth by up-regulation of p35 neuron-specific cyclin-dependent kinase 5 activator via activation of ERK1/2 pathway. *J Biol Chem.* Apr 1 2005;280(13):12896-12901.
44. Asada A, Yamamoto N, Gohda M, Saito T, Hayashi N, Hisanaga S. Myristoylation of p39 and p35 is a determinant of cytoplasmic or nuclear localization of active cyclin-dependent kinase 5 complexes. *J Neurochem.* Aug 2008;106(3):1325-1336.

45. Patrick GN, Zhou P, Kwon YT, Howley PM, Tsai LH. p35, the neuronal-specific activator of cyclin-dependent kinase 5 (Cdk5) is degraded by the ubiquitin-proteasome pathway. *J Biol Chem*. Sep 11 1998;273(37):24057-24064.
46. Zukerberg LR, Patrick GN, Nikolic M, et al. Cables links Cdk5 and c-Abl and facilitates Cdk5 tyrosine phosphorylation, kinase upregulation, and neurite outgrowth. *Neuron*. Jun 2000;26(3):633-646.
47. Miyamoto Y, Yamauchi J, Tanoue A. Cdk5 phosphorylation of WAVE2 regulates oligodendrocyte precursor cell migration through nonreceptor tyrosine kinase Fyn. *J Neurosci*. Aug 13 2008;28(33):8326-8337.
48. Kusakawa G, Saito T, Onuki R, Ishiguro K, Kishimoto T, Hisanaga S. Calpain-dependent proteolytic cleavage of the p35 cyclin-dependent kinase 5 activator to p25. *J Biol Chem*. Jun 2 2000;275(22):17166-17172.
49. Lee MS, Kwon YT, Li M, Peng J, Friedlander RM, Tsai LH. Neurotoxicity induces cleavage of p35 to p25 by calpain. *Nature*. May 18 2000;405(6784):360-364.
50. Patzke H, Tsai LH. Calpain-mediated cleavage of the cyclin-dependent kinase-5 activator p39 to p29. *J Biol Chem*. Mar 8 2002;277(10):8054-8060.
51. Yamada M, Saito T, Sato Y, et al. Cdk5--p39 is a labile complex with the similar substrate specificity to Cdk5--p35. *J Neurochem*. Sep 2007;102(5):1477-1487.
52. Hisanaga S, Saito T. The regulation of cyclin-dependent kinase 5 activity through the metabolism of p35 or p39 Cdk5 activator. *Neurosignals*. Sep-Oct 2003;12(4-5):221-229.
53. Ko J, Humbert S, Bronson RT, et al. p35 and p39 are essential for cyclin-dependent kinase 5 function during neurodevelopment. *J Neurosci*. Sep 1 2001;21(17):6758-6771.
54. Griffin SV, Hiromura K, Pippin J, et al. Cyclin-dependent kinase 5 is a regulator of podocyte differentiation, proliferation, and morphology. *Am J Pathol*. Oct 2004;165(4):1175-1185.
55. Okada S, Yamada E, Saito T, et al. CDK5-dependent phosphorylation of the Rho family GTPase TC10(alpha) regulates insulin-stimulated GLUT4 translocation. *J Biol Chem*. Dec 19 2008;283(51):35455-35463.
56. Lin H, Juang JL, Wang PS. Involvement of Cdk5/p25 in digoxin-triggered prostate cancer cell apoptosis. *J Biol Chem*. Jul 9 2004;279(28):29302-29307.
57. Feldmann G, Mishra A, Hong SM, et al. Inhibiting the cyclin-dependent kinase CDK5 blocks pancreatic cancer formation and progression through the suppression of Ras-Ral signaling. *Cancer Res*. Jun 1 2010;70(11):4460-4469.
58. Ubeda M, Kemp DM, Habener JF. Glucose-induced expression of the cyclin-dependent protein kinase 5 activator p35 involved in Alzheimer's disease regulates insulin gene transcription in pancreatic beta-cells. *Endocrinology*. Jun 2004;145(6):3023-3031.

59. Brinkkoetter PT, Olivier P, Wu JS, et al. Cyclin I activates Cdk5 and regulates expression of Bcl-2 and Bcl-XL in postmitotic mouse cells. *J Clin Invest.* Sep 1 2009.
60. Kawauchi T, Chihama K, Nabeshima Y, Hoshino M. Cdk5 phosphorylates and stabilizes p27kip1 contributing to actin organization and cortical neuronal migration. *Nat Cell Biol.* Jan 2006;8(1):17-26.
61. Besson A, Gurian-West M, Schmidt A, Hall A, Roberts JM. p27Kip1 modulates cell migration through the regulation of RhoA activation. *Genes Dev.* Apr 15 2004;18(8):862-876.
62. Sharma P, Sharma M, Amin ND, Albers RW, Pant HC. Regulation of cyclin-dependent kinase 5 catalytic activity by phosphorylation. *Proc Natl Acad Sci U S A.* Sep 28 1999;96(20):11156-11160.
63. Rosales J, Han B, Lee KY. Cdk7 functions as a cdk5 activating kinase in brain. *Cell Physiol Biochem.* 2003;13(5):285-296.
64. Poon RY, Lew J, Hunter T. Identification of functional domains in the neuronal Cdk5 activator protein. *J Biol Chem.* Feb 28 1997;272(9):5703-5708.
65. Tarricone C, Dhavan R, Peng J, Areces LB, Tsai LH, Musacchio A. Structure and regulation of the CDK5-p25(ncck5a) complex. *Mol Cell.* Sep 2001;8(3):657-669.
66. Matsuura I, Wang JH. Demonstration of cyclin-dependent kinase inhibitory serine/threonine kinase in bovine thymus. *J Biol Chem.* Mar 8 1996;271(10):5443-5450.
67. Hall M, Peters G. Genetic alterations of cyclins, cyclin-dependent kinases, and Cdk inhibitors in human cancer. *Adv Cancer Res.* 1996;68:67-108.
68. Malumbres M, Barbacid M. To cycle or not to cycle: a critical decision in cancer. *Nat Rev Cancer.* Dec 2001;1(3):222-231.
69. Senderowicz AM. Small-molecule cyclin-dependent kinase modulators. *Oncogene.* Sep 29 2003;22(42):6609-6620.
70. Malumbres M, Pevarello P, Barbacid M, Bischoff JR. CDK inhibitors in cancer therapy: what is next? *Trends Pharmacol Sci.* Jan 2008;29(1):16-21.
71. Meijer L, Raymond E. Roscovitine and other purines as kinase inhibitors. From starfish oocytes to clinical trials. *Acc Chem Res.* Jun 2003;36(6):417-425.
72. Guzi T. CYC-202 Cyclacel. *Curr Opin Investig Drugs.* Dec 2004;5(12):1311-1318.
73. Aldoss IT, Tashi T, Ganti AK. Seliciclib in malignancies. *Expert Opin Investig Drugs.* Dec 2009;18(12):1957-1965.
74. Meijer L, Bettayeb K, Galons H. (R)-Roscovitine (CYC202, Seliciclib). In: Smith PJ, Yue EW, eds. *Inhibitors of cyclin dependent kinases as anti-tumor agents*: CRC Press Taylor & Francis Group; 2006.

75. Liebl J, Weitensteiner SB, Vereb G, et al. Cyclin-dependent kinase 5 regulates endothelial cell migration and angiogenesis. *J Biol Chem*. Nov 12 2010;285(46):35932-35943.
76. Berberich N, Uhl B, Joore J, et al. Roscovitine blocks leukocyte extravasation by inhibition of cyclin-dependent kinases 5 and 9. *Br J Pharmacol*. Jul 2011;163(5):1086-1098.
77. Strock CJ, Park JI, Nakakura EK, et al. Cyclin-dependent kinase 5 activity controls cell motility and metastatic potential of prostate cancer cells. *Cancer Res*. Aug 1 2006;66(15):7509-7515.
78. Tanaka T, Serneo FF, Tseng HC, Kulkarni AB, Tsai LH, Gleeson JG. Cdk5 phosphorylation of doublecortin ser297 regulates its effect on neuronal migration. *Neuron*. Jan 22 2004;41(2):215-227.
79. Lilja L, Yang SN, Webb DL, Juntti-Berggren L, Berggren PO, Bark C. Cyclin-dependent kinase 5 promotes insulin exocytosis. *J Biol Chem*. Sep 7 2001;276(36):34199-34205.
80. Kerr JS, Wexler RS, Mousa SA, et al. Novel small molecule alpha v integrin antagonists: comparative anti-cancer efficacy with known angiogenesis inhibitors. *Anticancer Res*. Mar-Apr 1999;19(2A):959-968.
81. Zahler S, Liebl J, Furst R, Vollmar AM. Anti-angiogenic potential of small molecular inhibitors of cyclin dependent kinases in vitro. *Angiogenesis*. Sep 2010;13(3):239-249.
82. Krystof V, Rarova L, Liebl J, et al. The selective P-TEFb inhibitor CAN508 targets angiogenesis. *Eur J Med Chem*. Sep 2011;46(9):4289-4294.
83. Neuhof C, Fabiunke V, Deibele K, et al. Reduction of myocardial infarction by calpain inhibitors A-705239 and A-705253 in isolated perfused rabbit hearts. *Biol Chem*. Nov 2004;385(11):1077-1082.
84. Blake RA, Broome MA, Liu X, et al. SU6656, a selective src family kinase inhibitor, used to probe growth factor signaling. *Mol Cell Biol*. Dec 2000;20(23):9018-9027.
85. Ades EW, Candal FJ, Swerlick RA, et al. HMEC-1: establishment of an immortalized human microvascular endothelial cell line. *J Invest Dermatol*. Dec 1992;99(6):683-690.
86. Bouis D, Hospers GA, Meijer C, Molema G, Mulder NH. Endothelium in vitro: a review of human vascular endothelial cell lines for blood vessel-related research. *Angiogenesis*. 2001;4(2):91-102.
87. Li H, Oehrlin SA, Wallerath T, et al. Activation of protein kinase C alpha and/or epsilon enhances transcription of the human endothelial nitric oxide synthase gene. *Mol Pharmacol*. Apr 1998;53(4):630-637.

88. Menn B, Bach S, Blevins TL, Campbell M, Meijer L, Timsit S. Delayed treatment with systemic (S)-roscovitine provides neuroprotection and inhibits in vivo CDK5 activity increase in animal stroke models. *PLoS One*. 2010;5(8):e12117.
89. Tsai LH, Takahashi T, Caviness VS, Jr., Harlow E. Activity and expression pattern of cyclin-dependent kinase 5 in the embryonic mouse nervous system. *Development*. Dec 1993;119(4):1029-1040.
90. Smith PK, Krohn RI, Hermanson GT, et al. Measurement of protein using bicinchoninic acid. *Anal Biochem*. Oct 1985;150(1):76-85.
91. Bradford MM. A rapid and sensitive method for the quantitation of microgram quantities of protein utilizing the principle of protein-dye binding. *Anal Biochem*. May 7 1976;72:248-254.
92. Laemmli UK. Cleavage of structural proteins during the assembly of the head of bacteriophage T4. *Nature*. Aug 15 1970;227(5259):680-685.
93. Towbin H, Staehelin T, Gordon J. Electrophoretic transfer of proteins from polyacrylamide gels to nitrocellulose sheets: procedure and some applications. *Proc Natl Acad Sci U S A*. Sep 1979;76(9):4350-4354.
94. Kurien BT, Scofield RH. Protein blotting: a review. *J Immunol Methods*. Mar 1 2003;274(1-2):1-15.
95. Pfaffl MW. A new mathematical model for relative quantification in real-time RT-PCR. *Nucleic Acids Res*. May 1 2001;29(9):e45.
96. Qiao F, Gao CY, Tripathi BK, Zelenka PS. Distinct functions of Cdk5(Y15) phosphorylation and Cdk5 activity in stress fiber formation and organization. *Exp Cell Res*. Nov 15 2008;314(19):3542-3550.
97. van den Heuvel S, Harlow E. Distinct roles for cyclin-dependent kinases in cell cycle control. *Science*. Dec 24 1993;262(5142):2050-2054.
98. Chae T, Kwon YT, Bronson R, Dikkes P, Li E, Tsai LH. Mice lacking p35, a neuronal specific activator of Cdk5, display cortical lamination defects, seizures, and adult lethality. *Neuron*. Jan 1997;18(1):29-42.
99. Zengel P, Nguyen-Hoang A, Schildhammer C, Zantl R, Kahl V, Horn E. mu-Slide Chemotaxis: A new chamber for long-term chemotaxis studies. *BMC Cell Biol*. 2011;12(1):21.
100. Gao CY, Zakeri Z, Zhu Y, He H, Zelenka PS. Expression of Cdk5, p35, and Cdk5-associated kinase activity in the developing rat lens. *Dev Genet*. 1997;20(3):267-275.
101. Sharma MR, Tuszynski GP, Sharma MC. Angiostatin-induced inhibition of endothelial cell proliferation/apoptosis is associated with the down-regulation of cell cycle regulatory protein cdk5. *J Cell Biochem*. Feb 1 2004;91(2):398-409.
102. Altucci L, Addeo R, Cicatiello L, et al. 17beta-Estradiol induces cyclin D1 gene transcription, p36D1-p34cdk4 complex activation and p105Rb phosphorylation

- during mitogenic stimulation of G(1)-arrested human breast cancer cells. *Oncogene*. Jun 6 1996;12(11):2315-2324.
103. Saito T, Onuki R, Fujita Y, et al. Developmental regulation of the proteolysis of the p35 cyclin-dependent kinase 5 activator by phosphorylation. *J Neurosci*. Feb 15 2003;23(4):1189-1197.
 104. Nikolic M, Tsai LH. Activity and regulation of p35/Cdk5 kinase complex. *Methods Enzymol*. 2000;325:200-213.
 105. Cho DH, Seo J, Park JH, et al. Cyclin-dependent kinase 5 phosphorylates endothelial nitric oxide synthase at serine 116. *Hypertension*. Feb 2010;55(2):345-352.
 106. Meijer L, Borgne A, Mulner O, et al. Biochemical and cellular effects of roscovitine, a potent and selective inhibitor of the cyclin-dependent kinases cdc2, cdk2 and cdk5. *Eur J Biochem*. Jan 15 1997;243(1-2):527-536.
 107. Wang D, de la Fuente C, Deng L, et al. Inhibition of human immunodeficiency virus type 1 transcription by chemical cyclin-dependent kinase inhibitors. *J Virol*. Aug 2001;75(16):7266-7279.
 108. Jorda R, Havlicek L, McNae IW, et al. Pyrazolo[4,3-d]pyrimidine bioisostere of roscovitine: evaluation of a novel selective inhibitor of cyclin-dependent kinases with antiproliferative activity. *J Med Chem*. Apr 28 2011;54(8):2980-2993.
 109. Zheng YL, Li BS, Amin ND, Albers W, Pant HC. A peptide derived from cyclin-dependent kinase activator (p35) specifically inhibits Cdk5 activity and phosphorylation of tau protein in transfected cells. *Eur J Biochem*. Sep 2002;269(18):4427-4434.
 110. Zheng YL, Amin ND, Hu YF, et al. A 24-residue peptide (p5), derived from p35, the Cdk5 neuronal activator, specifically inhibits Cdk5-p25 hyperactivity and tau hyperphosphorylation. *J Biol Chem*. Oct 29 2010;285(44):34202-34212.
 111. Zhang P, Yu PC, Tsang AH, et al. S-nitrosylation of cyclin-dependent kinase 5 (cdk5) regulates its kinase activity and dendrite growth during neuronal development. *J Neurosci*. Oct 27 2010;30(43):14366-14370.
 112. Qu J, Nakamura T, Cao G, Holland EA, McKercher SR, Lipton SA. S-Nitrosylation activates Cdk5 and contributes to synaptic spine loss induced by {beta}-amyloid peptide. *Proc Natl Acad Sci U S A*. Aug 15 2011.
 113. Bulotta S, Cerullo A, Barsacchi R, et al. Endothelial nitric oxide synthase is segregated from caveolin-1 and localizes to the leading edge of migrating cells. *Exp Cell Res*. Apr 1 2006;312(6):877-889.
 114. Rao GK, Bender JR. Rac, PAK, and eNOS ACTION. *Circ Res*. Aug 15 2008;103(4):328-330.
 115. Sawada N, Salomone S, Kim HH, Kwiatkowski DJ, Liao JK. Regulation of endothelial nitric oxide synthase and postnatal angiogenesis by Rac1. *Circ Res*. Aug 15 2008;103(4):360-368.

116. Park SY, Yi EY, Jung M, Lee YM, Kim YJ. Ethyl pyruvate, an anti-inflammatory agent, inhibits tumor angiogenesis through inhibition of the NF-kappaB signaling pathway. *Cancer Lett.* Apr 28 2011;303(2):150-154.
117. Fujitani K, Kambayashi J, Sakon M, et al. Identification of mu-, m-calpains and calpastatin and capture of mu-calpain activation in endothelial cells. *J Cell Biochem.* Aug 1 1997;66(2):197-209.
118. Su Y, Cui Z, Li Z, Block ER. Calpain-2 regulation of VEGF-mediated angiogenesis. *FASEB J.* Jul 2006;20(9):1443-1451.
119. Brinkkoetter PT, Wu JS, Ohse T, et al. p35, the non-cyclin activator of Cdk5, protects podocytes against apoptosis in vitro and in vivo. *Kidney Int.* Apr 2010;77(8):690-699.
120. Utreras E, Futatsugi A, Pareek TK, Kulkarni AB. Molecular Roles of Cdk5 in Pain Signaling. *Drug Discov Today Ther Strateg.* Sep 2009;6(3):105-111.
121. Schechtman D, Mochly-Rosen D. Adaptor proteins in protein kinase C-mediated signal transduction. *Oncogene.* Oct 1 2001;20(44):6339-6347.
122. Wang F, Yamauchi M, Muramatsu M, Osawa T, Tsuchida R, Shibuya M. RACK1 regulates VEGF/Flt1-mediated cell migration via activation of a PI3K/Akt pathway. *J Biol Chem.* Mar 18 2011;286(11):9097-9106.
123. *GPS 2.1* [computer program]: CUCKOO Workgroup, Hefei National Laboratory for Physical Sciences at Microscale and School of Life Sciences, University of Science & Technology of China, Hefei, Anhui 230027, China; 2011.
124. Xue Y, Ren J, Gao X, Jin C, Wen L, Yao X. GPS 2.0, a tool to predict kinase-specific phosphorylation sites in hierarchy. *Mol Cell Proteomics.* Sep 2008;7(9):1598-1608.
125. Smith D. Cdk5 in neuroskeletal dynamics. *Neurosignals.* Sep-Oct 2003;12(4-5):239-251.
126. He L, Zhang Z, Yu Y, Ahmed S, Cheung NS, Qi RZ. The neuronal p35 activator of Cdk5 is a novel F-actin binding and bundling protein. *Cell Mol Life Sci.* May 2011;68(9):1633-1643.
127. Humbert S, Dhavan R, Tsai L. p39 activates cdk5 in neurons, and is associated with the actin cytoskeleton. *J Cell Sci.* Mar 2000;113 (Pt 6):975-983.
128. Meimaridou E, Gooljar SB, Chapple JP. From hatching to dispatching: the multiple cellular roles of the Hsp70 molecular chaperone machinery. *J Mol Endocrinol.* Jan 2009;42(1):1-9.
129. Shimura H, Schwartz D, Gygi SP, Kosik KS. CHIP-Hsc70 complex ubiquitinates phosphorylated tau and enhances cell survival. *J Biol Chem.* Feb 6 2004;279(6):4869-4876.

130. Shiota M, Kusakabe H, Izumi Y, et al. Heat shock cognate protein 70 is essential for Akt signaling in endothelial function. *Arterioscler Thromb Vasc Biol.* Mar 2010;30(3):491-497.
131. Chang KH, Multani PS, Sun KH, et al. Nuclear envelope dispersion triggered by deregulated Cdk5 precedes neuronal death. *Mol Biol Cell.* May 2011;22(9):1452-1462.
132. Ohta T, Eguchi R, Suzuki A, Miyakaze S, Ayuzawa R, Kaji K. Hypoxia-induced apoptosis and tube breakdown are regulated by p38 MAPK but not by caspase cascade in an in vitro capillary model composed of human endothelial cells. *J Cell Physiol.* Jun 2007;211(3):673-681.
133. McClintock D, Gordon LB, Djabali K. Hutchinson-Gilford progeria mutant lamin A primarily targets human vascular cells as detected by an anti-Lamin A G608G antibody. *Proc Natl Acad Sci U S A.* Feb 14 2006;103(7):2154-2159.
134. Morabito MA, Sheng M, Tsai LH. Cyclin-dependent kinase 5 phosphorylates the N-terminal domain of the postsynaptic density protein PSD-95 in neurons. *J Neurosci.* Jan 28 2004;24(4):865-876.
135. Bottos A, Rissone A, Bussolino F, Arese M. Neurexins and neuroligins: synapses look out of the nervous system. *Cell Mol Life Sci.* Aug 2011;68(16):2655-2666.
136. Valiron O, Chevrier V, Usson Y, Breviario F, Job D, Dejana E. Desmoplakin expression and organization at human umbilical vein endothelial cell-to-cell junctions. *J Cell Sci.* Aug 1996;109 (Pt 8):2141-2149.
137. Zhou X, Stuart A, Dettin LE, Rodriguez G, Hoel B, Gallicano GI. Desmoplakin is required for microvascular tube formation in culture. *J Cell Sci.* Jul 1 2004;117(Pt 15):3129-3140.
138. Negash S, Wang HS, Gao C, Ledee D, Zelenka P. Cdk5 regulates cell-matrix and cell-cell adhesion in lens epithelial cells. *J Cell Sci.* May 15 2002;115(Pt 10):2109-2117.
139. Nakano N, Nakao A, Ishidoh K, et al. CDK5 regulates cell-cell and cell-matrix adhesion in human keratinocytes. *Br J Dermatol.* Jul 2005;153(1):37-45.
140. Bera TK, Zimonjic DB, Popescu NC, et al. POTE, a highly homologous gene family located on numerous chromosomes and expressed in prostate, ovary, testis, placenta, and prostate cancer. *Proc Natl Acad Sci U S A.* Dec 24 2002;99(26):16975-16980.
141. Bera TK, Saint Fleur A, Lee Y, et al. POTE paralogs are induced and differentially expressed in many cancers. *Cancer Res.* Jan 1 2006;66(1):52-56.
142. Das S, Ise T, Nagata S, Maeda H, Bera TK, Pastan I. Palmitoylation of POTE family proteins for plasma membrane targeting. *Biochem Biophys Res Commun.* Nov 23 2007;363(3):751-756.

143. De Azevedo WF, Leclerc S, Meijer L, Havlicek L, Strnad M, Kim SH. Inhibition of cyclin-dependent kinases by purine analogues: crystal structure of human cdk2 complexed with roscovitine. *Eur J Biochem.* Jan 15 1997;243(1-2):518-526.
144. McClue SJ, Blake D, Clarke R, et al. In vitro and in vivo antitumor properties of the cyclin dependent kinase inhibitor CYC202 (R-roscovitine). *Int J Cancer.* Dec 10 2002;102(5):463-468.

7 APPENDIX

7.1 Publications

7.1.1 Original publications

Weitensteiner SB, Liebl J, Krystof V, Günther, M, Pechan P, Strnad M, Fürst R, Vollmar AM, Zahler S

Novel Cdk inhibitors as potent anti-angiogenic compounds in vitro and in vivo.
in preparation

Liebl J, Weitensteiner SB, Vereb G, Takács L, Fürst R, Vollmar AM, Zahler S

Cyclin-dependent kinase 5 regulates endothelial cell migration and angiogenesis.

J Biol Chem 2010 Nov 12;285(46):35932-43. Epub 2010 Sep 7.

7.1.2 Poster presentations

Weitensteiner SB, Liebl J, Krystof V, Günther, M, Pechan P, Strnad M, Fürst R, Vollmar AM, Zahler S

Novel Cdk inhibitors as potent anti-angiogenic compounds.

8th International Symposium on the Biology of Endothelial Cells (EC8),
Zürich, June 15 - 18, 2011

Weitensteiner SB, Liebl J, Krystof V, Günther, M, Pechan P, Strnad M, Fürst R, Vollmar AM, Zahler S

Novel Cdk inhibitors as potent anti-angiogenic compounds.

77. Jahrestagung der Deutschen Gesellschaft für Pharmakologie und Toxikologie
(DGPT)

Frankfurt/Main, March 30 - April 01, 2010

Weitensteiner SB, Heiskanen S, Liebl J, Vollmar AM, Zahler S

Cyclin-dependent kinase 5 (Cdk5) upstream regulation in HUVECs.

51. Jahrestagung der Deutschen Gesellschaft für Pharmakologie und Toxikologie
(DGPT)

Mainz, March 23-25, 2009

7.2 Curriculum Vitae

Personal data

Name	Sabine Bianca Monika Weitensteiner
Date of birth	September 22, 1982
Place of birth	Tirschenreuth

Education

July 2008-October 2011	PhD thesis at the department of pharmacy, pharmaceutical biology, LMU Munich, Prof. Dr. S. Zahler, Prof. Dr. A.M. Vollmar
July 2008	Licensure as a pharmacist (Approbation)
Mai 2007-April 2008	Compulsory Internship (Pharmaziepraktikum) Zweibrückenapotheke, München (November 2007-April 2008) HEXAL AG, Holzkirchen (Mai 2007-October 2007)
October 2002-April 2007	Study of Pharmacy, Universität Regensburg
August 2005	Internship, University Hospital Pharmacy, Universidade de Coimbra, Portugal
1993-2002	Stiftland-Gymnasium Tirschenreuth

Working experience

September 2008 – present	Pharmacist, Löwen-Apotheke, München
--------------------------	-------------------------------------

7.3 Acknowledgements

Diese Arbeit wurde im Department Pharmazie der LMU am Lehrstuhl für Pharmazeutische Biologie von Frau Professor Dr. Angelika M. Vollmar unter Betreuung von Herrn Professor Dr. Stefan Zahler angefertigt. Ihnen möchte ich an allererster Stelle danken für die Möglichkeit in Ihrer Arbeitsgruppe zu promovieren. Die hervorragende fachliche und persönliche Betreuung, viele anregende Diskussionen und die Bereitschaft, sich immer die Zeit für Ihre Mitarbeiter zu nehmen hat großen Anteil am Gelingen dieser Doktorarbeit – dafür ein großes Dankeschön. Vielen Dank an dieser Stelle auch Frau Dr. Johanna Liebl und Herrn PD Dr. Robert Fürst für wertvolle Hilfestellungen und viele fachliche Anregungen.

Herzlicher Dank gilt auch allen weiteren Mitgliedern meines Prüfungskomitees für Ihre Zeit und Mühe: Prof. Dr. Christoph W. Turck, Prof. Dr. Franz Bracher, Prof. Dr. Christian Wahl-Schott und Prof. Dr. Ernst Wagner.

Besonderer Dank geht auch an die an dieser Arbeit beteiligten Kooperationspartner: Herrn Professor Dr. Turck und Frau Dr. Giuseppina Maccarrone vom Max-Planck-Institut für Psychiatrie, München, für die Durchführung der LC-ESI-MS/MS-Analysen, Dr. Vladimir Krystof und Dr. Radek Jorda vom Laboratory of Growth Receptors, Institute of Experimental Botany, Palacky University, Olomouc, CZ, für die Bereitstellung der Cdk-Inhibitoren, und Dr. Michael Günther vom Lehrstuhl für Pharmazeutische Biologie und Biotechnologie, Department Pharmazie der LMU München, für die Durchführung der Tierversuche.

Vielen Dank Bettina, Hanna und Elisabeth für das Korrekturlesen.

Ein ganz besonders großes Dankeschön geht an alle ehemaligen und derzeitigen Mitglieder der Arbeitsgruppe: für die herzliche Aufnahme, die großartige Arbeitsatmosphäre für und die Tatsache, dass man hier jeden (fast) immer um Rat und Hilfe bitten kann – und natürlich auch für den Spaß in- und außerhalb des Labors. Im Besonderen: Meinem „Gegenüber-Boxenluder“ Elisabeth – Großes Danke für viel Spaß und konstanten moralischen Beistand in allen Lebenslagen. Meinem „Ex-Boxenluder“ Bettina vielen Dank für die geduldige Beantwortung aller Fragen zu Westernblot, Word-Formatierung und weiterem. Jana, Bianca, Kerstin, Frau Schnegg und Rita: Danke für große Hilfe im Labor! Romina – Danke für die angenehme Zeit im D-Zimmer. Sebastian – Danke fürs Aufpassen! Allen früheren und jetzigen „Bewohnern“ im Endothel-Labor: Lena, Martin, Michi – Danke, hat Spaß gemacht! Suvi, Katharina und Tanja – Danke für fleißige Mitarbeit am Projekt!

Zuletzt gibt es noch ein riesiges Dankeschön an meine Eltern und meine Schwester Julia. Danke für eure stetige und bedingungslose Unterstützung, ohne Euch wär ich nicht so weit gekommen.